Kilonova Lightcurve Modeling and Implications to the Recent GW Events

Kyohei Kawaguchi
ICRR, The University of Tokyo

Collaborator: Sho Fujibayashi (AEI), Kota Hayashi (Kyoto U.),
Kenta Kiuchi (AEI), Koutarou Kyutoku (Kyoto U.),
Masaru Shibata (AEI/Kyoto U.), Masaomi Tanaka (Tohoku U.),

2020.3.28

Contents

- Overview
- Kilonova Lightcurve prediction
- Application to the recent GW events
  - GW190425 (the 2nd BNS event)
  - S190814bv (a BHNS event candidate)

Background/Motivation

- Various transient electromagnetic (EM) counterparts are proposed for NS binary mergers
- for example,
  - short-hard gamma-ray-burst
  - Afterglow
  - cocoon emission
  - **kilonovae/macronovae**
  - radio flare, etc.
- Host galaxy identification
  , remnant properties, environment
- Possible synthesis site of r-process nuclei

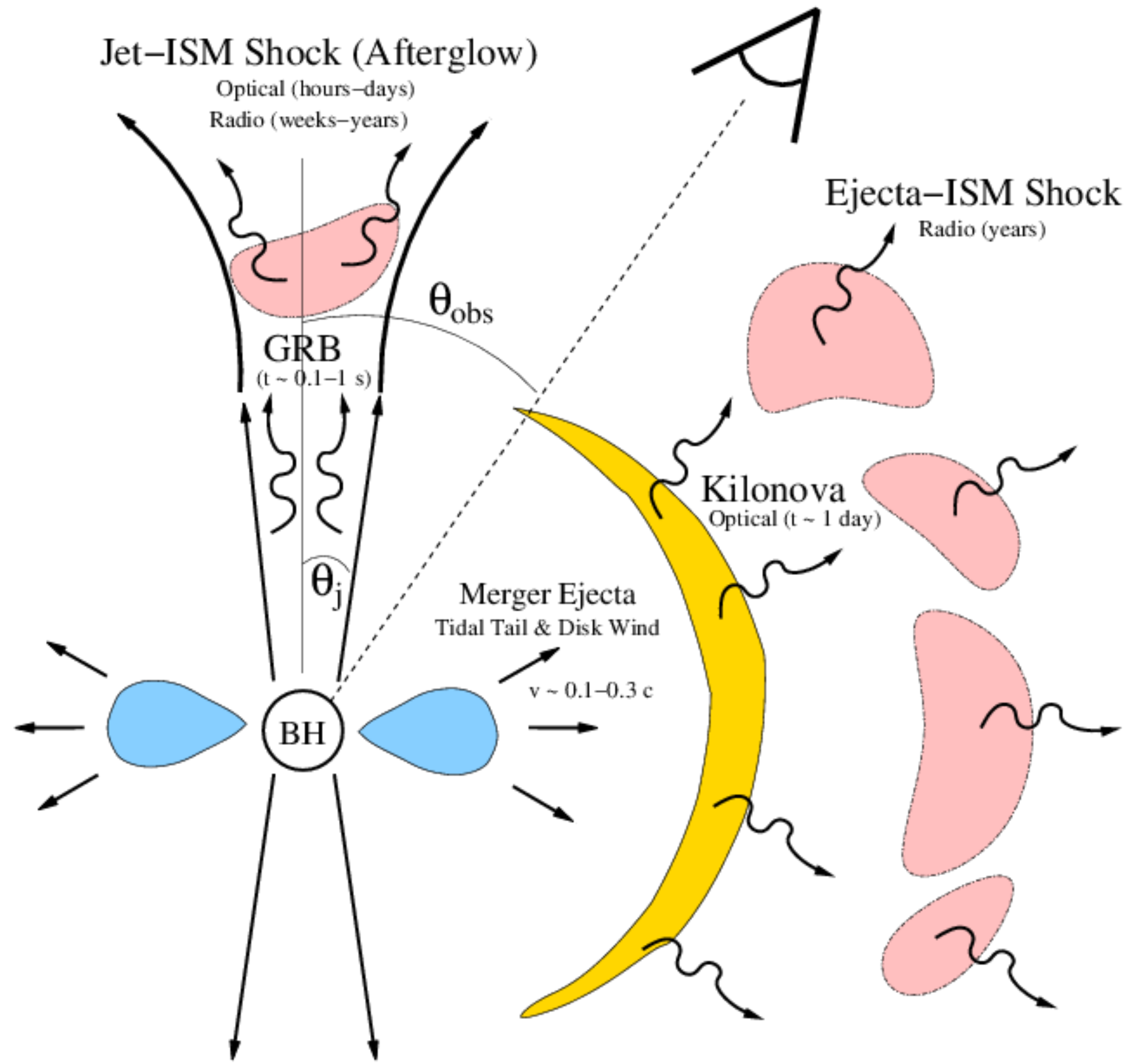

Ref: B. Metzger and E. Berger 2012

Kilonova/Macronova

- **A Kilonova/macronova** is a electromagnetic (EM) emission which expected to be associate with a NS binary merger.
- Ejected material is neutron-rich
  →heavy radioactive nuclei would be synthesized in the ejecta by the so-called **r-process nucleosynthesis**

  →EM emission in optical and infrared wavelengths could occur by radioactive decays of heavy elements : **kilonova/macronova**

  Li & Paczyński 1998, Kulkarni 2005,
  Metzger et al. 2010 …

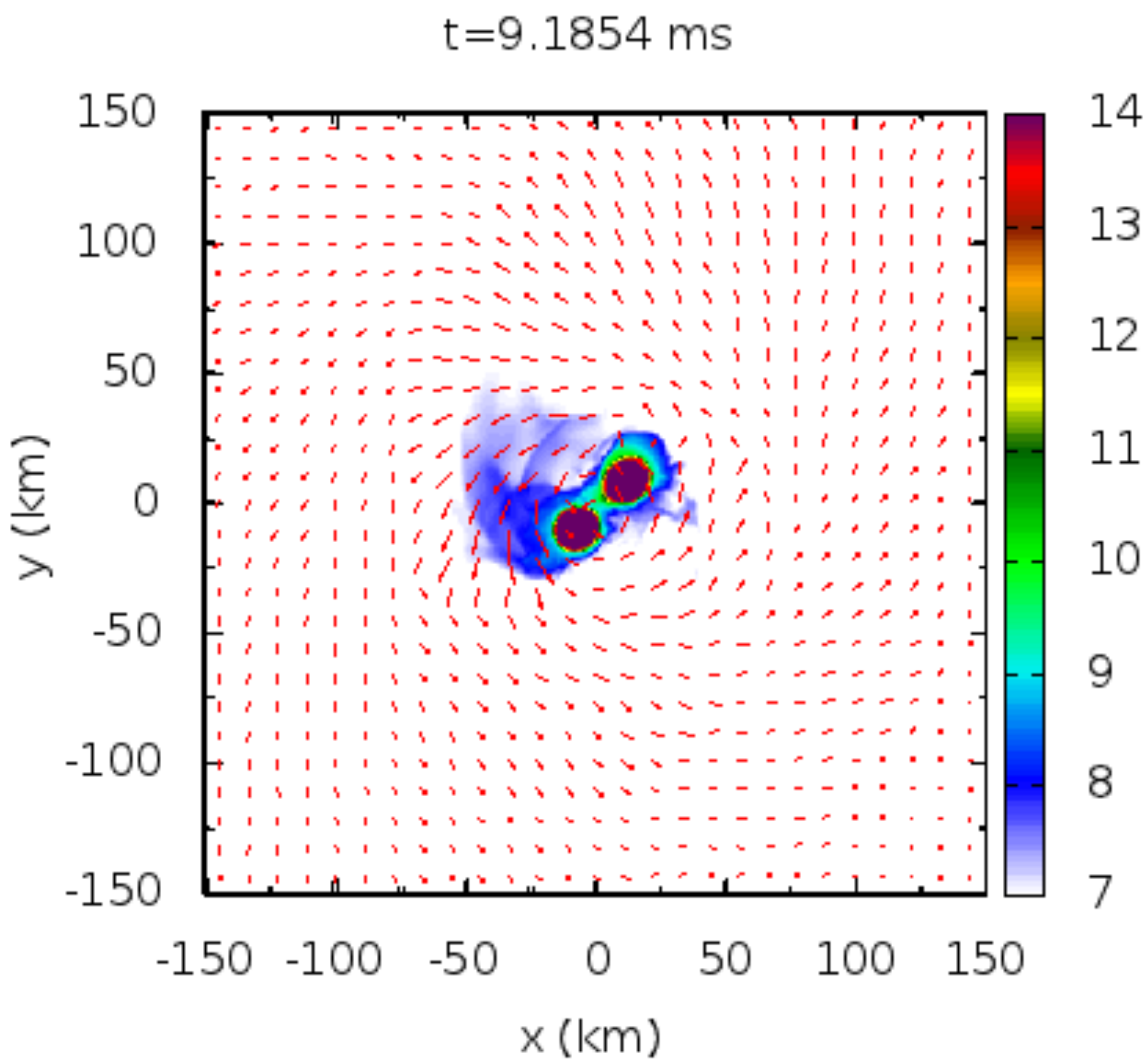

Ref: K. Hotokezaka et al. 2013

Overview

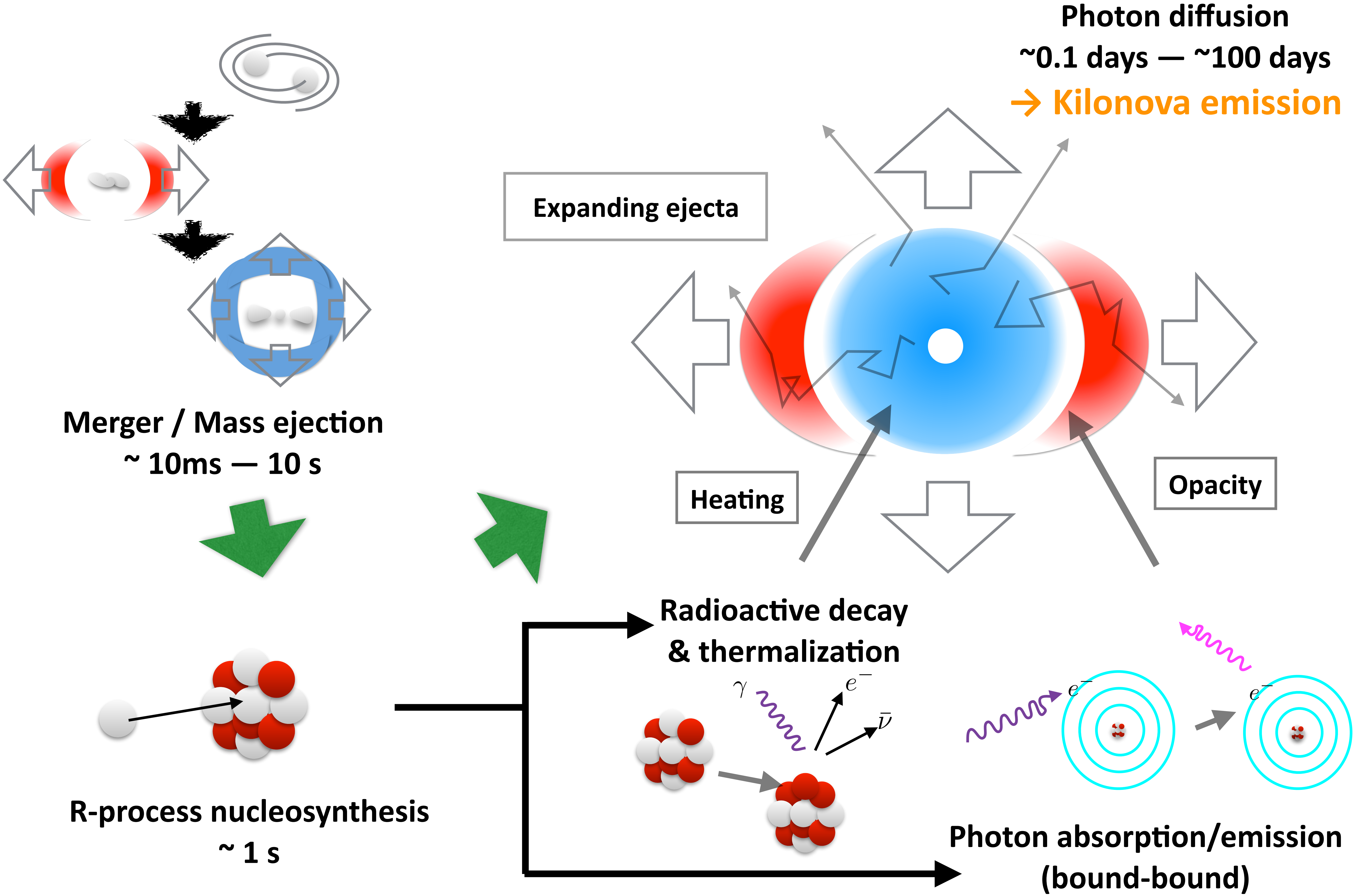

Photon diffusion
~0.1 days — ~100 days
→ Kilonova emission
Expanding ejecta
Merger / Mass ejection
~ 10ms — 10 s
Heating
Opacity
R-process nucleosynthesis
~ 1 s
Radioactive decay
& thermalization
γ
e^-
$\bar{\nu}$
e^-
e^-
Photon absorption/emission
(bound-bound)

Overview

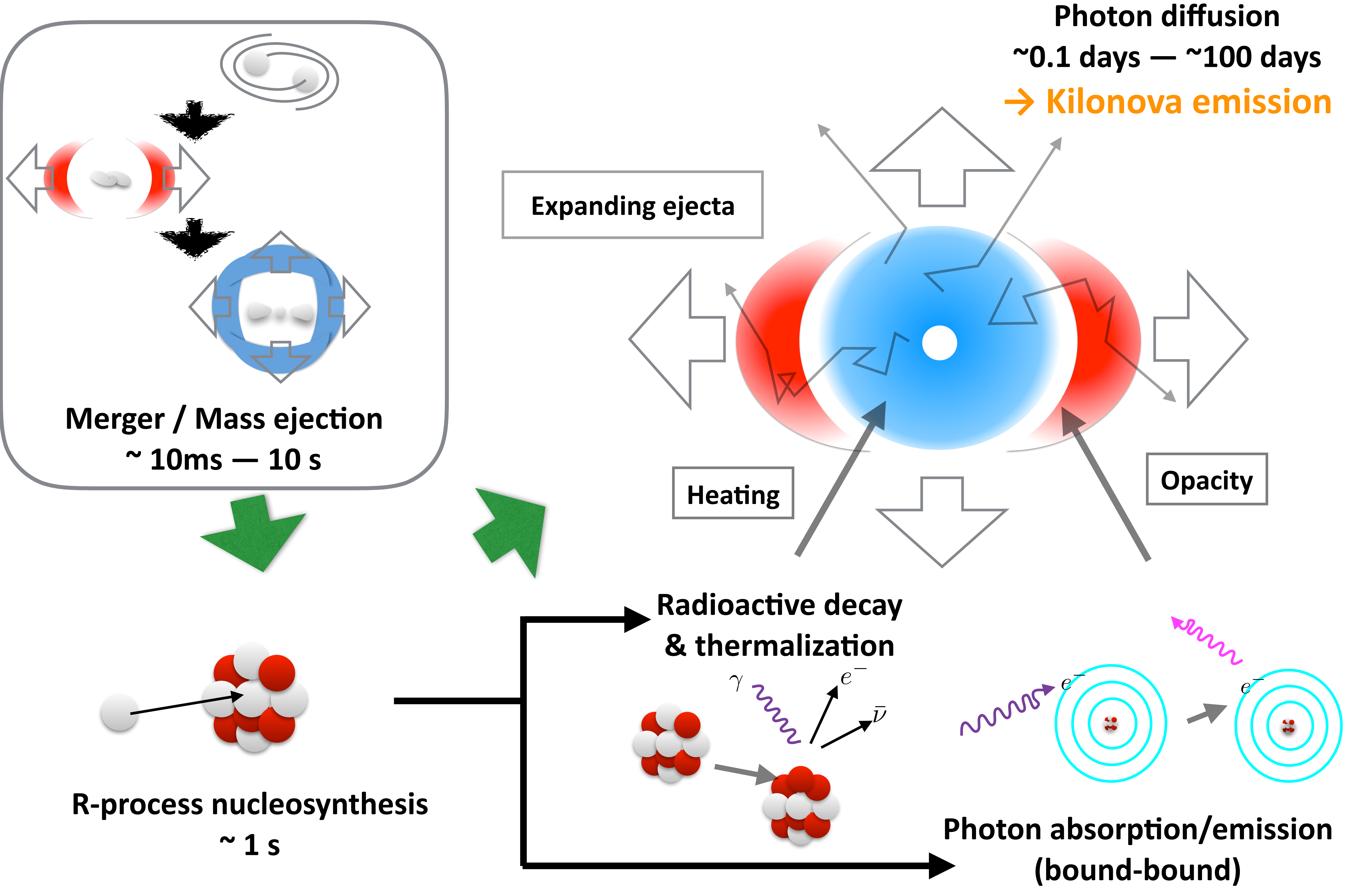

Photon diffusion
~0.1 days — ~100 days
→ Kilonova emission
Expanding ejecta
Merger / Mass ejection
~ 10ms — 10 s
Heating
Opacity
R-process nucleosynthesis
~ 1 s
Radioactive decay
& thermalization
γ
e^-
$\bar{\nu}$
e^-
e^-
Photon absorption/emission
(bound-bound)

Mass Ejection Mechanisms

- In the last decades, many efforts have been made to study the mass ejection process and evolution of the merger remnant performing numerical-relativity simulations

- **Dynamical mass ejection**
  mass ejection driven by tidal interaction
  or
  shock heating during the collision
  (e.g., Hotokezaka et al. 2013; Bauswein et al. 2013; Sekiguchi et al. 2016; Radice et al. 2016; Dietrich et al. 2017; Bovard et al. 2017)

- **Post-merger mass ejection**
  mass ejection from the merger remnant driven by magnetic fields / effective viscosity / neutrino heating
  (e.g., Dessart et al. 2009; Metzger & Fernández 2014; Perego et al. 2014; Just et al. 2015; Shibata et al. 2017; Lippuner et al. 2017; Fujibayashi et al. 2018, Siegel et al. 2018, Fernandez et al.2018,Christie et al. 2019,Fujibayashi et al. 2020)

Dynamical mass ejection
@merger

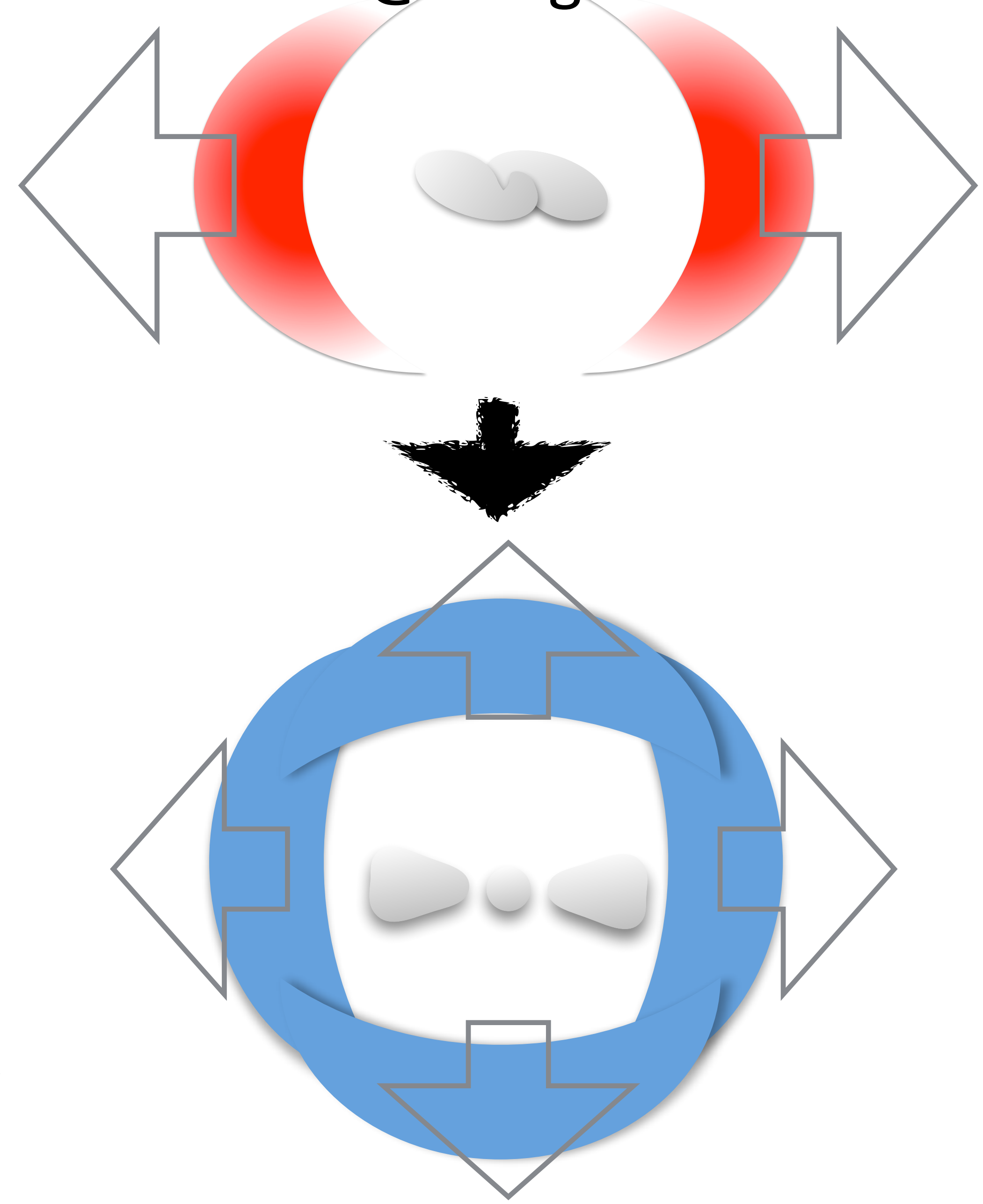

Post-merger mass ejection
@after merger

Ejecta property

$$Y_e = \frac{[e]}{[p]+[n]}$$

Type	Remnant	M_{dyn}	$Y_{e,dyn}$	M_{pm}	$Y_{e,pm}$
BNS	MNS/ SMNS	~0.001 Msun*	0.1-0.5**	~0.01-0.1 Msun	0.3-0.5
	HMNS	~0.001-0.01 Msun*	0.1-0.5**	~>0.01 Msun	0.3-0.5 (t_{life}~>1 s) 0.1-0.3? (t_{life}<<1 s)
	BH (prompt collapse)	<0.001 Msun*	<0.1?	<0.001 Msun (~0.01 Msun for asym. case)	0.1-0.3?
BHNS	Tidal disruption	~0.001-0.05 Msun	<0.1	~0.001-0.1 Msun	0.1-0.3?
	No tidal disruption	0	-	0	-

$$< v_{\rm dyn} > \approx 0.2 - 0.3\, c$$

$$< v_{\rm pm} > \lesssim 0.1\, c$$

*Dynamical ejecta ~0.01 Msun can be formed for asymmetric cases

** Ye of dynamical ejecta is high (>0.3) in the polar region

Overview

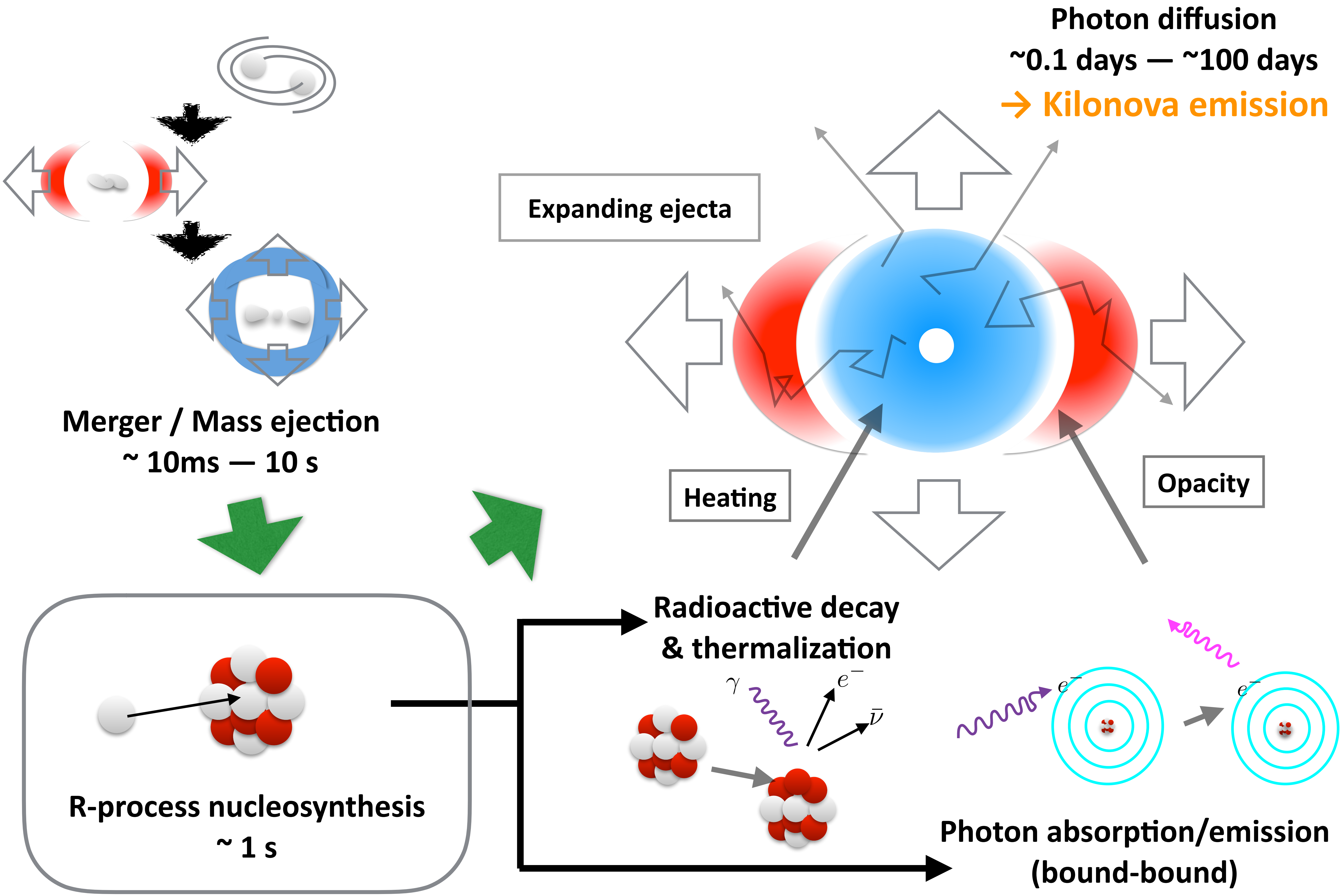

Photon diffusion
~0.1 days — ~100 days
→ Kilonova emission
Expanding ejecta
Merger / Mass ejection
~ 10ms — 10 s
Heating
Opacity
R-process nucleosynthesis
~ 1 s
Radioactive decay
& thermalization
γ
e^-
$\bar{\nu}$
e^-
e^-
Photon absorption/emission
(bound-bound)

R-process nucleosynthesis

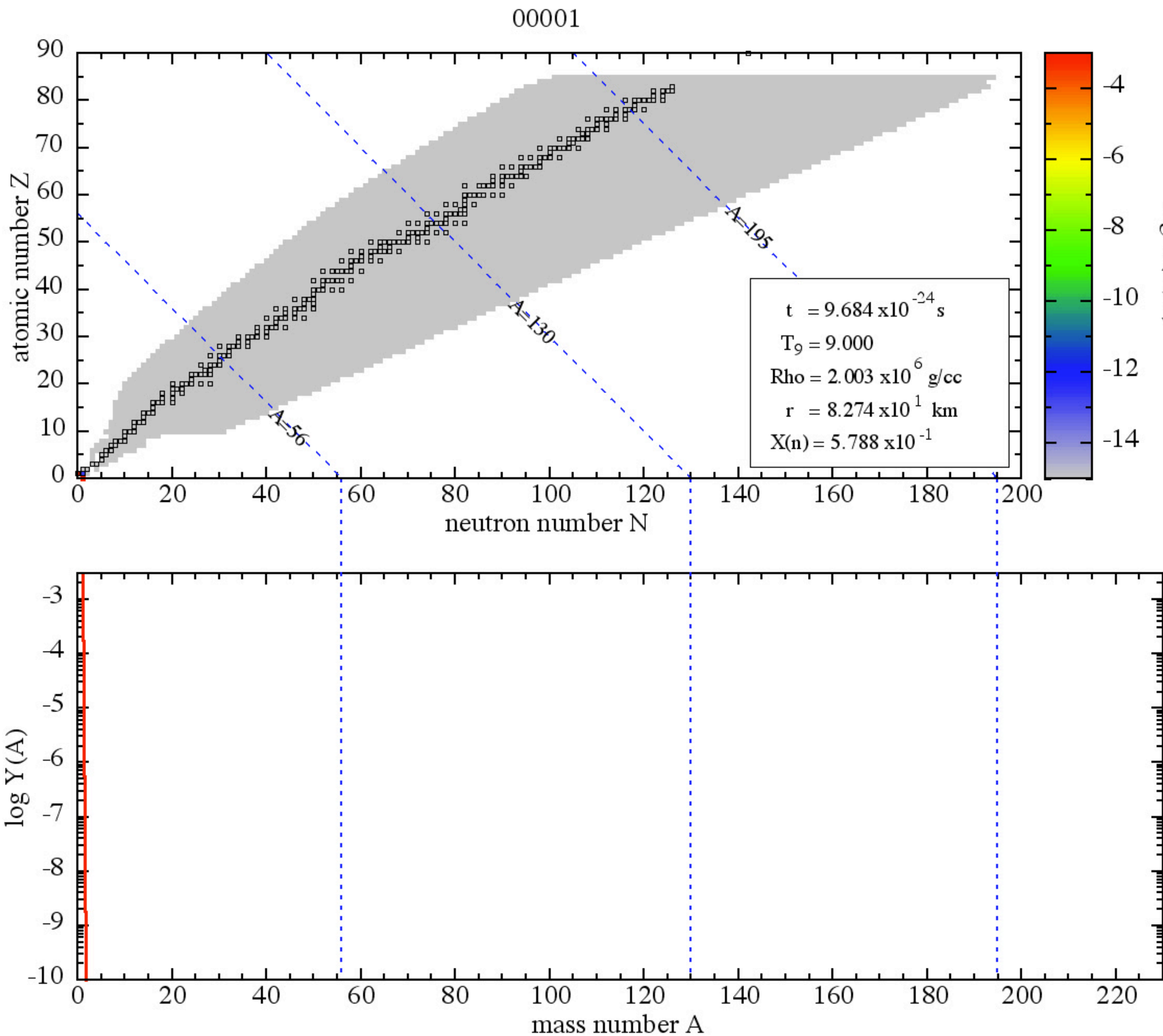

Credit) Sho Fujibayashi

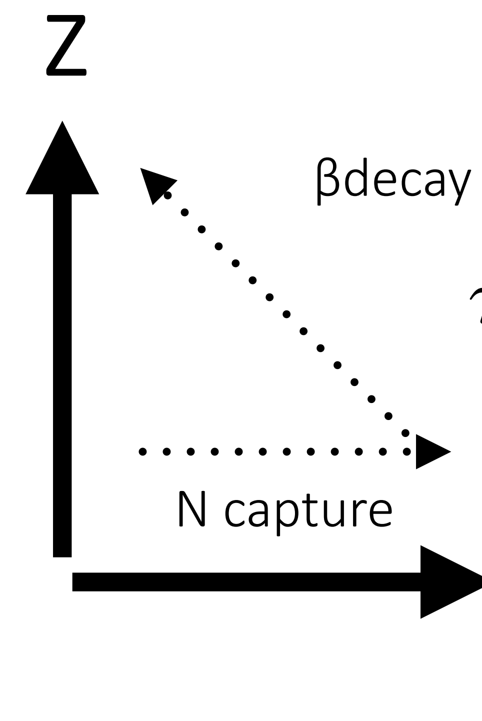

$$\tau_{\mathrm{Ncap}} \ll \tau_{\beta\mathrm{dec}}$$

$$Y_e = \frac{[e]}{[p]+[n]}$$

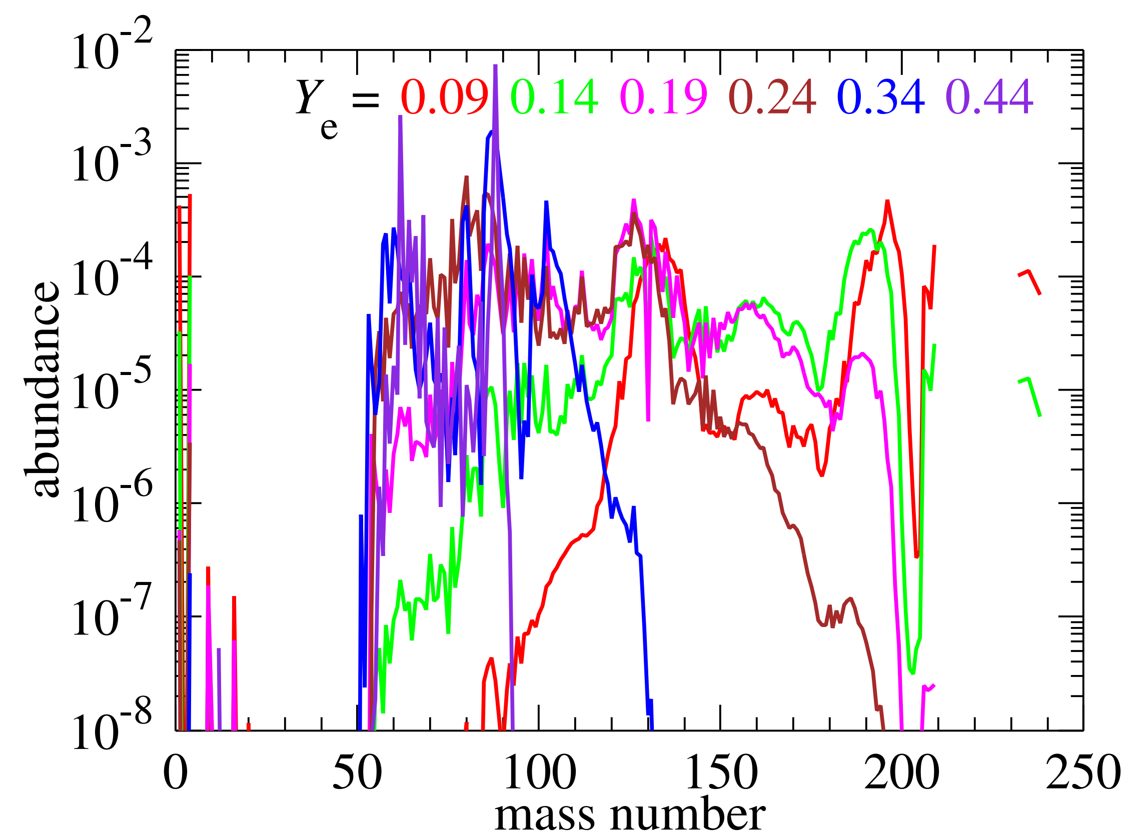

ref) Wanajo et al. 2014

Overview

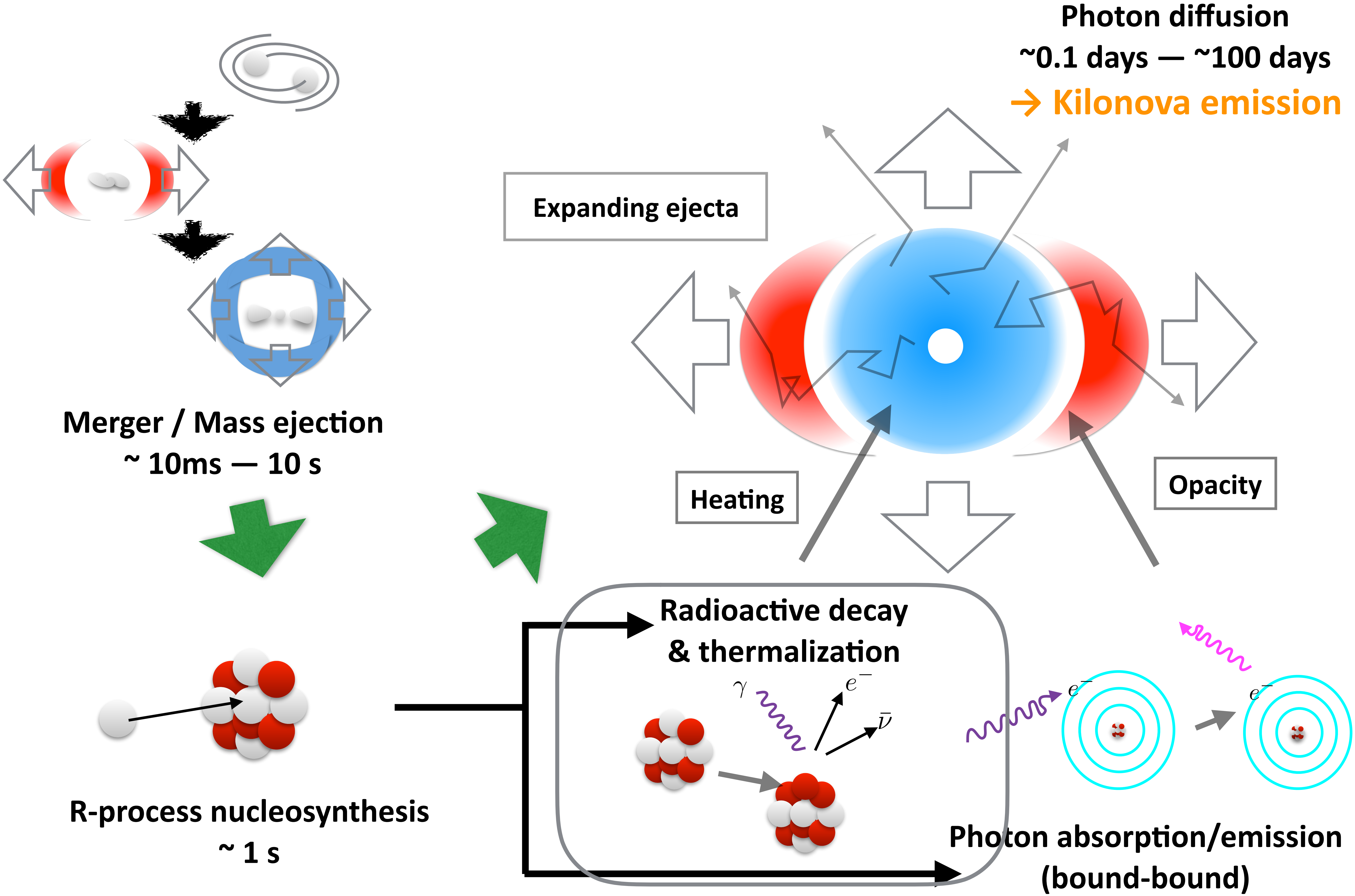

Photon diffusion
~0.1 days — ~100 days
→ Kilonova emission
Expanding ejecta
Merger / Mass ejection
~ 10ms — 10 s
Heating
Opacity
Radioactive decay
& thermalization
γ
e^-
$\bar{\nu}$
e^-
e^-
R-process nucleosynthesis
~ 1 s
Photon absorption/emission
(bound-bound)

Radioactive heating

β decay

$$(A, Z) \to (A, Z+1) + e^- + \bar{\nu}_e + \gamma$$

α decay

$$(A, Z) \to (A-4, Z-2) + {}^4_2\mathrm{He}$$

Spontaneous fission

$$(A, Z) \to (A', Z') + (A'', Z'')$$
$$(A' + A'' = A,\ Z' + Z'' = Z)$$

ref) Wanajo et al. 2014

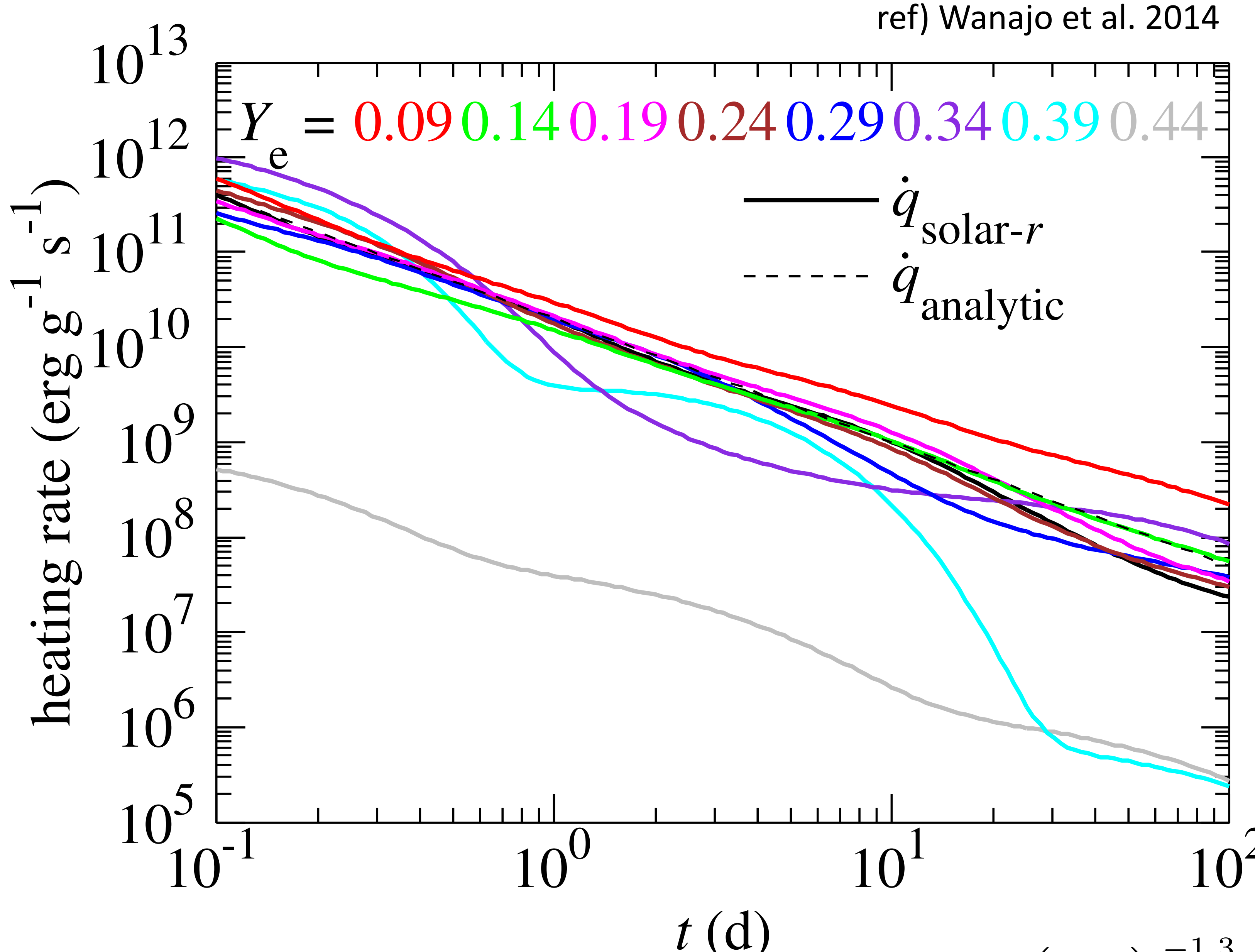

$$\dot{q}_{\text{analytic}} = 2 \times 10^{10}\text{erg/s/g}\left(\frac{t}{\text{day}}\right)^{-1.3}$$

*The contribution of the spontaneous fissions to the heating rate is highly uncertain due to the uncertainty in the β-decay and spontaneous fission lifetimes of the parents nuclide (e.g., Wanajo et al. 2014; Zhu et al. 2018; Wanajo 2018)

Thermalization

ref) Barnes et al. 2016

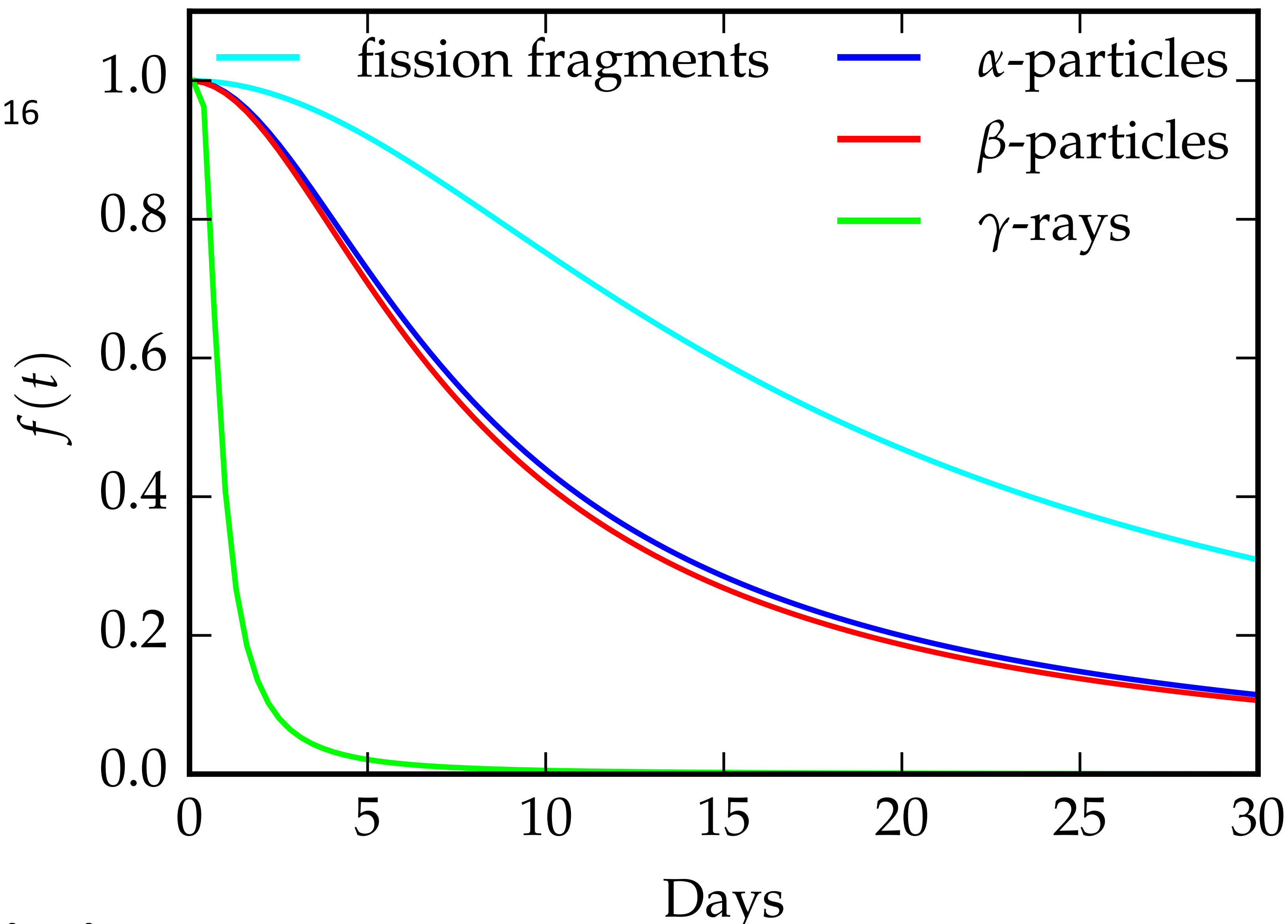

γ: photo-ionization

β, α, fission fragments: collisional ionization /excitation

- Conversion efficiency of gamma ray energy and the kinetic energy of charged particles to the ejecta thermal energy evolves with time through the evolution of density. (Barnes et al. 2016, Kasen & Barnes 2019, Waxman et al. 2019. Hotokezaka & Nakar 2019)

Overview

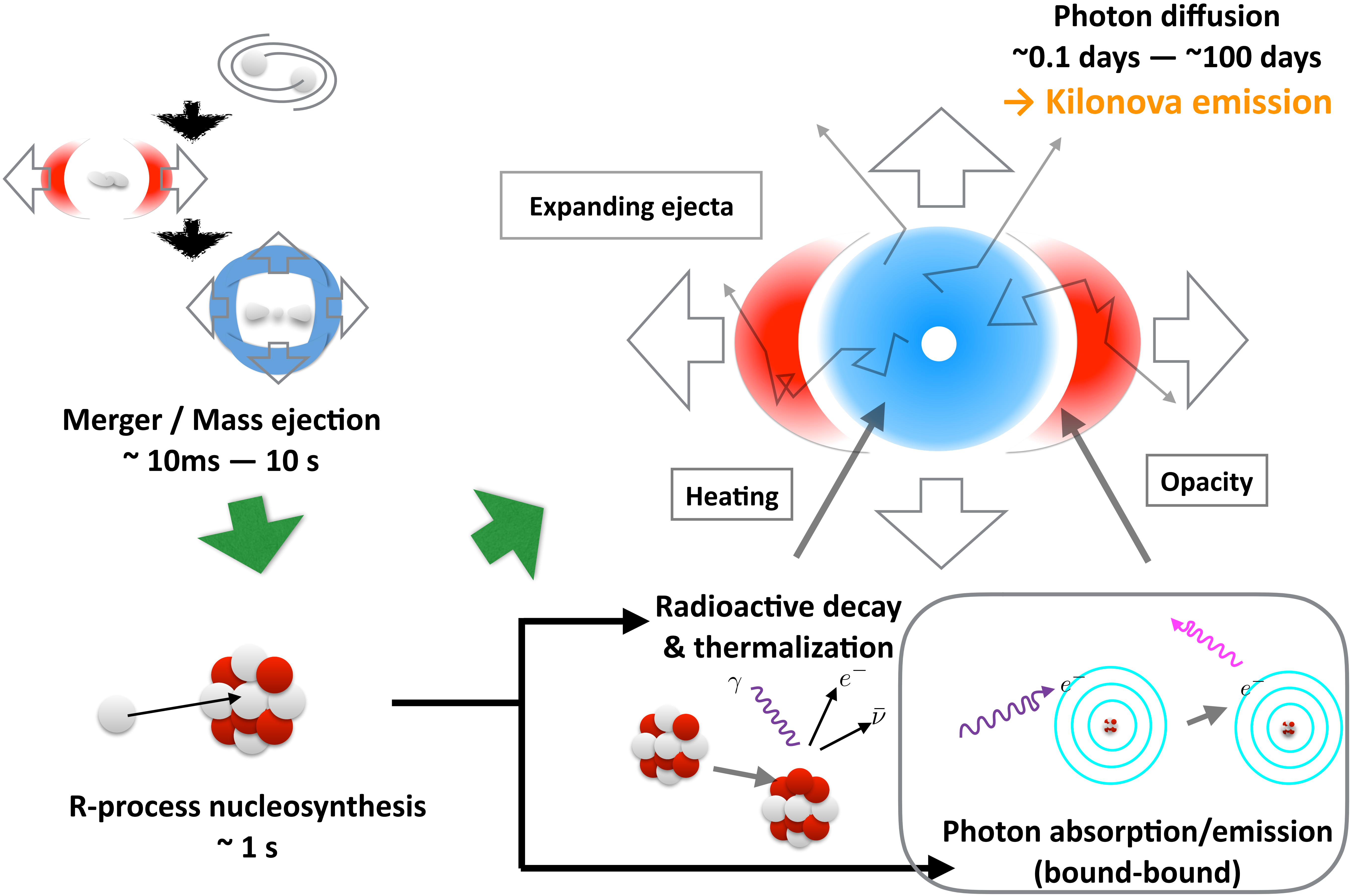
Photon diffusion
~0.1 days — ~100 days
→ Kilonova emission
Expanding ejecta
Merger / Mass ejection
~ 10ms — 10 s
Heating
Opacity
Radioactive decay
& thermalization
γ
e^-
$\bar{\nu}$
e^-
e^-
R-process nucleosynthesis
~ 1 s
Photon absorption/emission
(bound-bound)

Ejecta opacity

$$T_{\rm peak} \propto M_{\rm ej}^{-1/8} v_{\rm ej}^{-1/8} \kappa^{-3/8}$$

ref) Tanaka et al. 2018, 2019

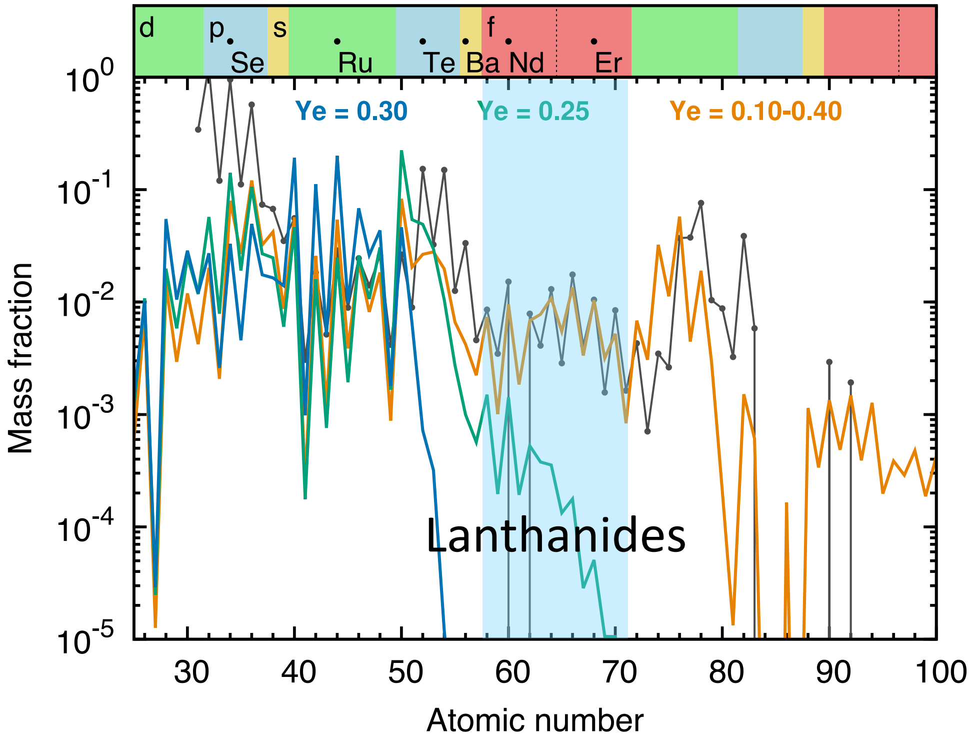

Lanthanide-poor case

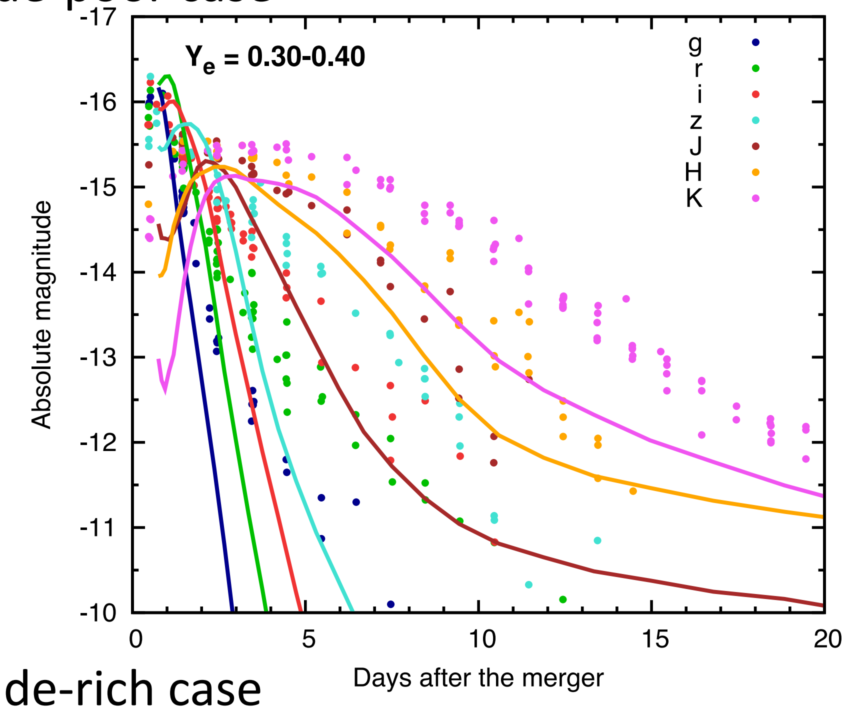

$$Y_e = \frac{[e]}{[p]+[n]}$$

Lanthanide-rich case

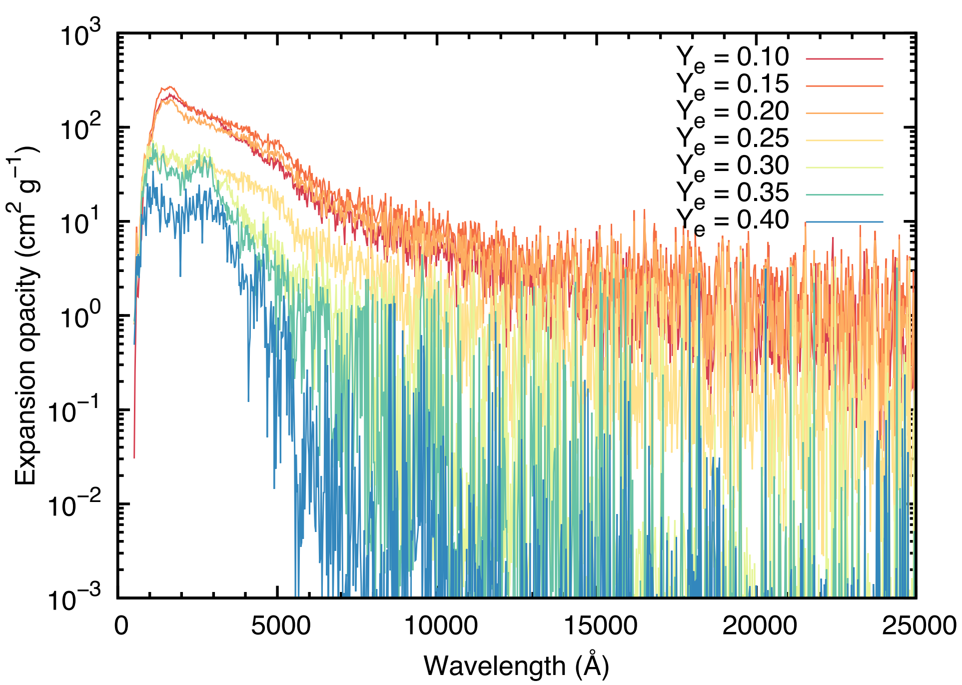

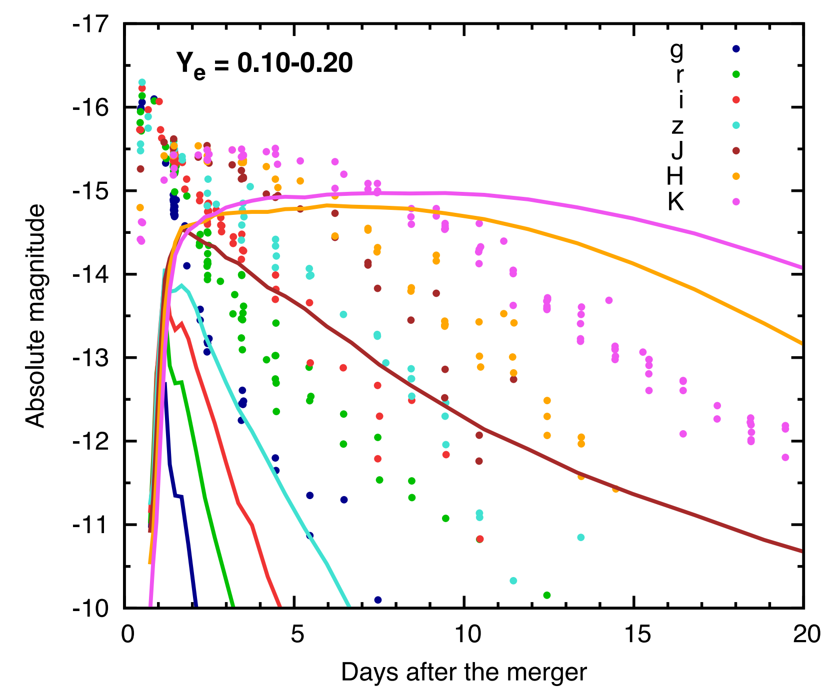

The ejecta opacity varies significantly (0.1—10 cm^2/g) depending particularly on whether **lanthanide elements** are synthesized or not, which reflects the electron fraction, Ye, of ejecta. (Kasen et al. 2013, Barnes et al. 2013, Tanaka et al. 2013)

Dependence on ρ and T

ref) Tanaka et al. 2018, 2019

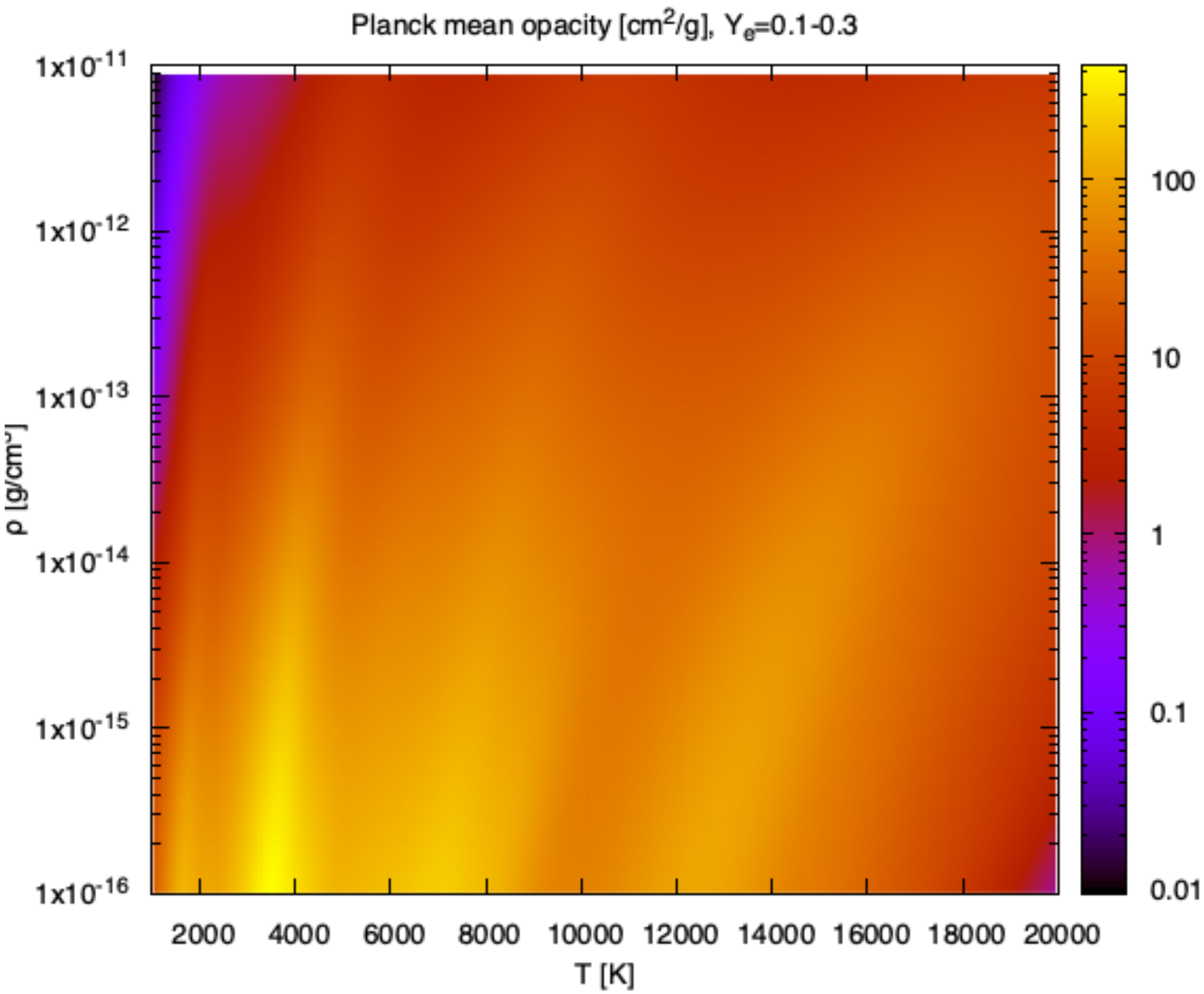

$$\dot{\epsilon}(t) = 10^{10} \mathrm{erg\,s^{-1}g^{-1}} \left(\frac{t}{\mathrm{day}}\right)^{-1.3}$$

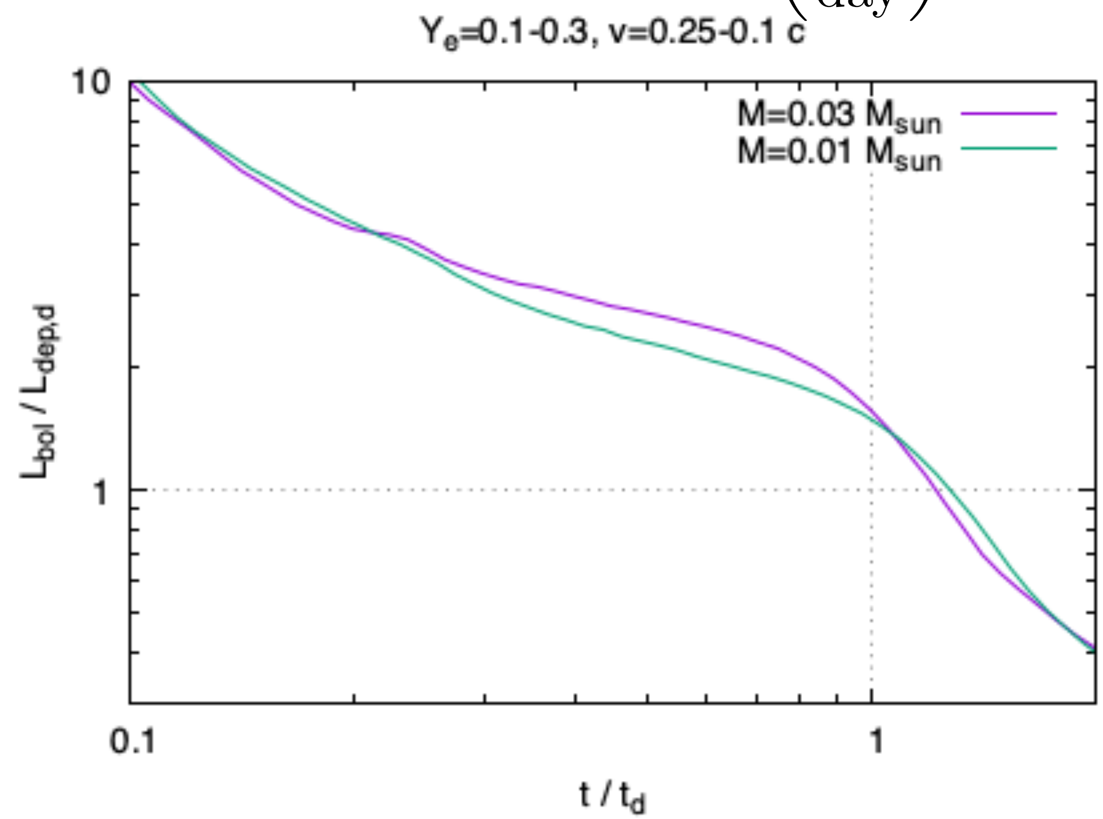

$$t_{\mathrm{d}} = \sqrt{\frac{3\kappa_{\mathrm{fid}} M}{4\pi v c}} \qquad L_{\mathrm{dep,d}} = M\dot{\epsilon}(t_{\mathrm{d}})$$

- Opacity depends on the temperature and density of ejecta through the change in the ionization levels and the saturation of line absorption.

*The Planck mean value can overestimate the effect of opacity in the expanding media (c.f. expansion opacity)

Overview

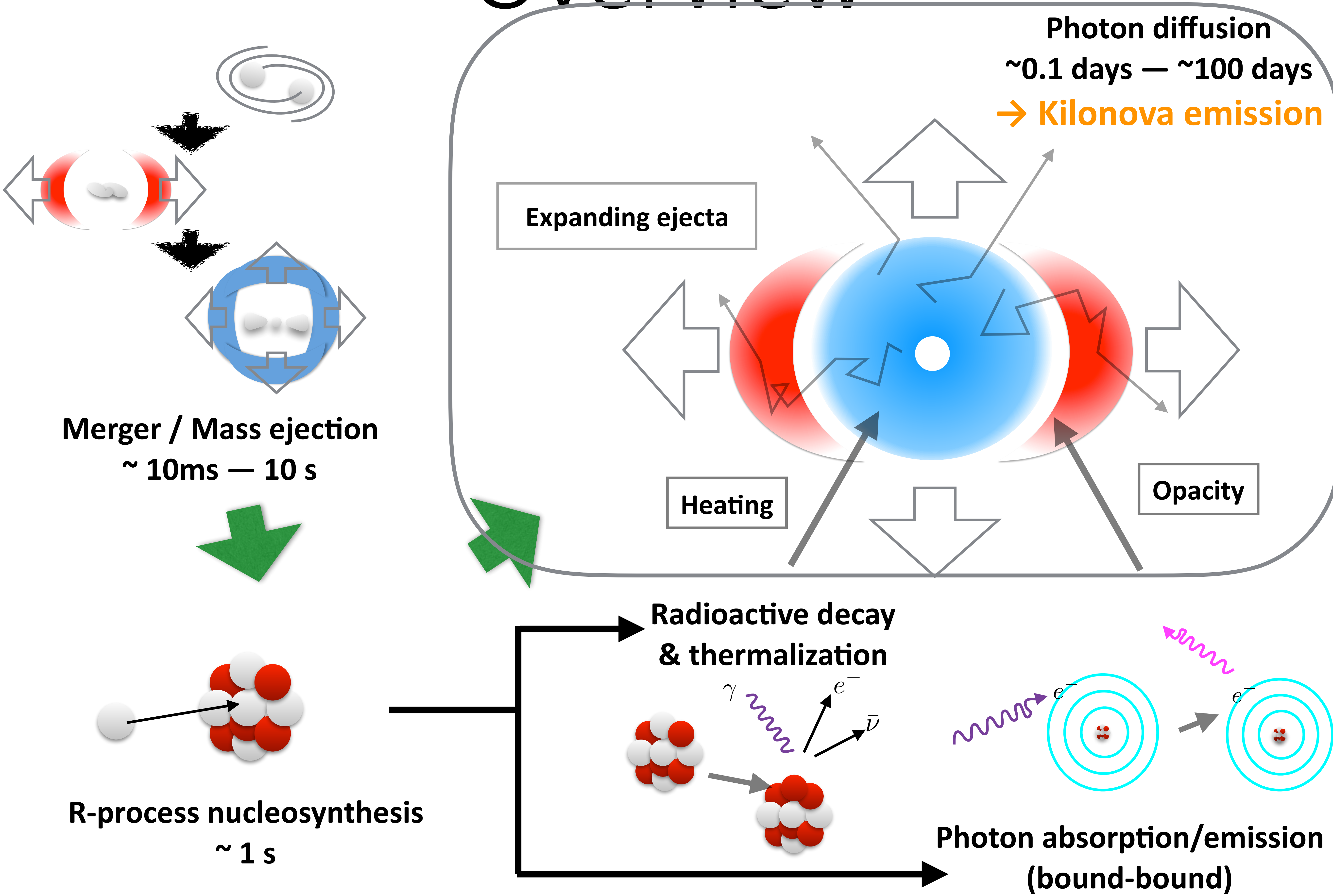
Photon diffusion
~0.1 days — ~100 days
→ Kilonova emission
Expanding ejecta
Heating
Opacity
Merger / Mass ejection
~ 10ms — 10 s
R-process nucleosynthesis
~ 1 s
Radioactive decay
& thermalization
γ
e^-
$\bar{\nu}$
e^-
e^-
Photon absorption/emission
(bound-bound)

Kilonova lightcurve prediction

GW170817:
Kilonova/macronova with multiple components

Data: Summarized in Villar et al. 2017

D=40 Mpc

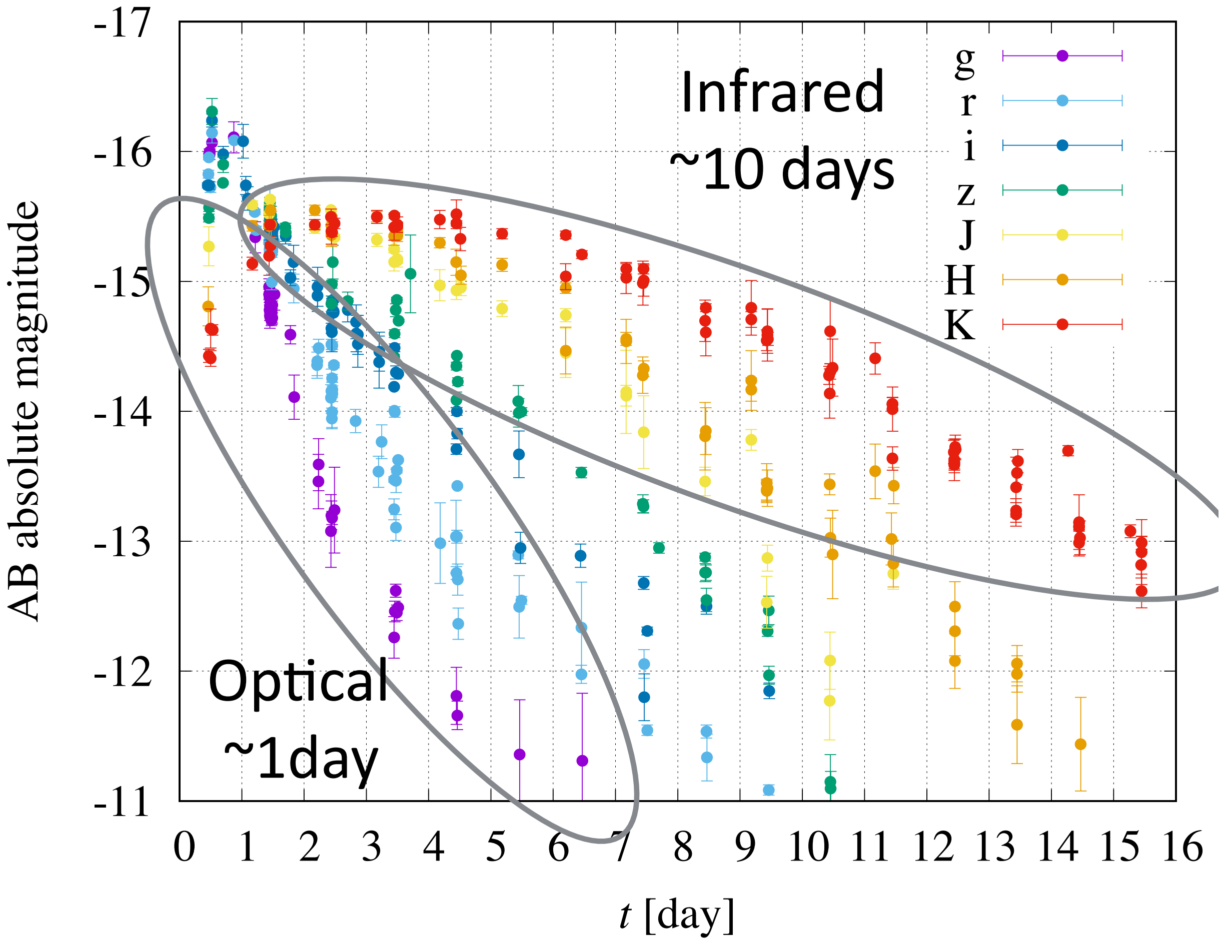

ref) Tanaka-san's slide

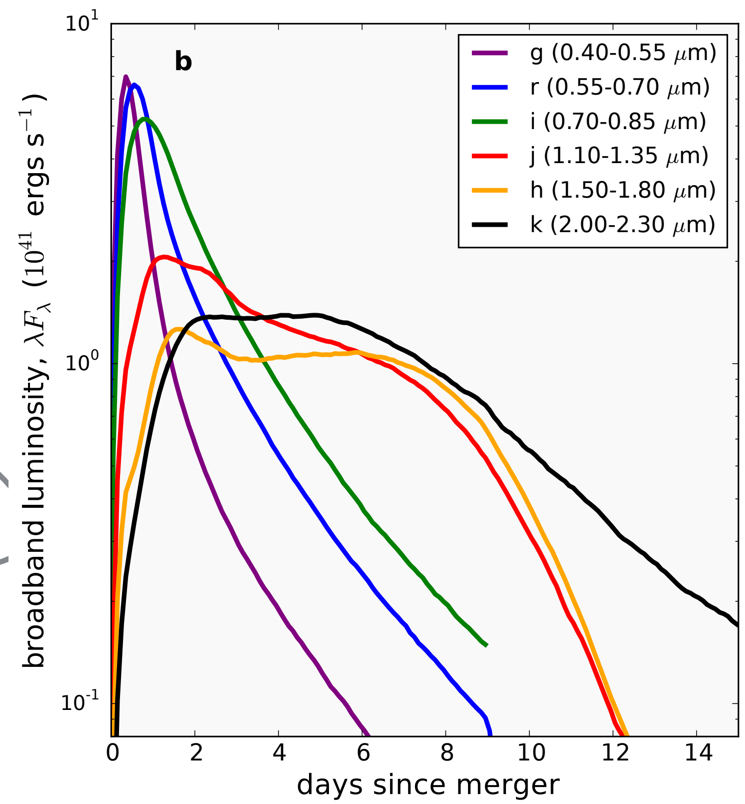

Blue (lanthanide-free)

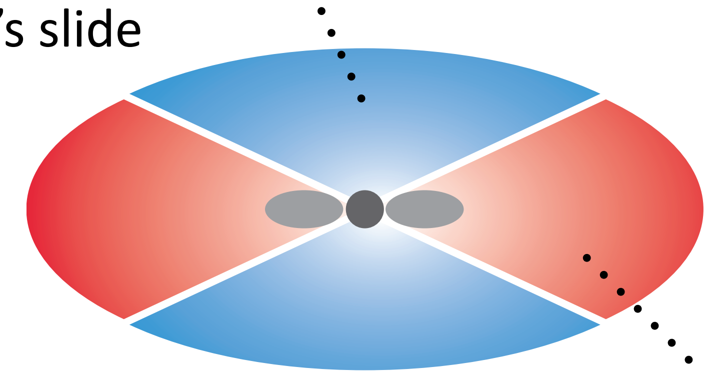

Red (lanthanide-rich)

Ref: D. Kasen et al. 2017

- **A Kilonova/macronova** model with multiple components well interprets the optical-Infrared observation (see e.g., Kasliwal et al. 2017, Cowperthwaite et al. 2017, Kasen et al. 2017, Villar et al. 2017)

- ... ^2/g)

The contribution from each ejecta component to the lightcurves is separately calculated and composited for most of the kilonova models employed for the parameter estimation

Photon interaction between different ejecta components

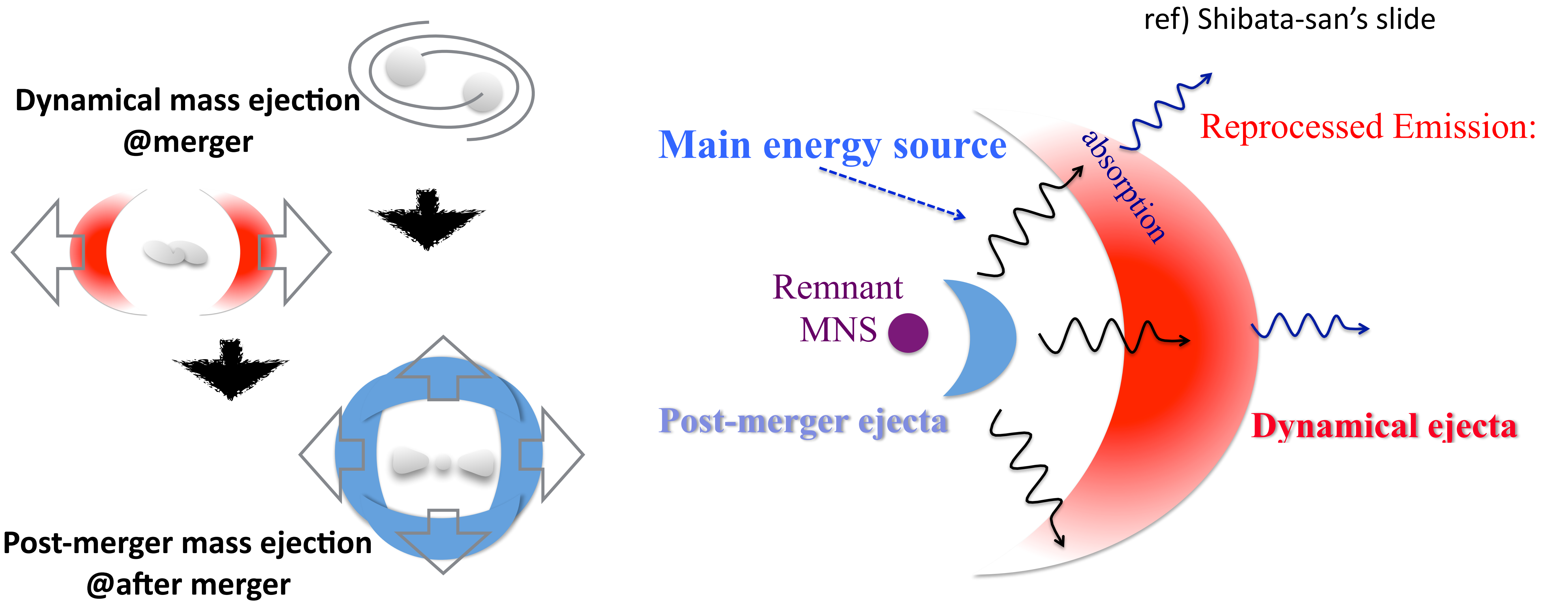

Radiative transfer of photons in multiple ejecta components
has a large impact on the lightcurve predictions
(see Perego et al. 2017, Wollaeger et al. 2017, Bulla 2019 for studies with similar setups
and also Matsumoto et al. 2018 for reprocessing models in different context)

Radiative transfer simulation

- A wavelength-dependent Monte-Carlo radiative transfer simulation code (M. Tanaka et al. 2013, 2014, 2017)
- Temperature, ionization level, and opacity are calculated consistently with the radiative filed
- The abundance pattern and nuclear heating rate are given based on r-process nucleosynthesis calculations by (Wanajo et al. 2014)
- New line list derived by systematic atomic structure calculations for all the r-process elements from Z=26 to 92 (up to 3rd ionization states, Tanaka et al. 2019)
- The density, velocity, and Ye profiles of ejecta based on predictions of numerical-relativity simulations.

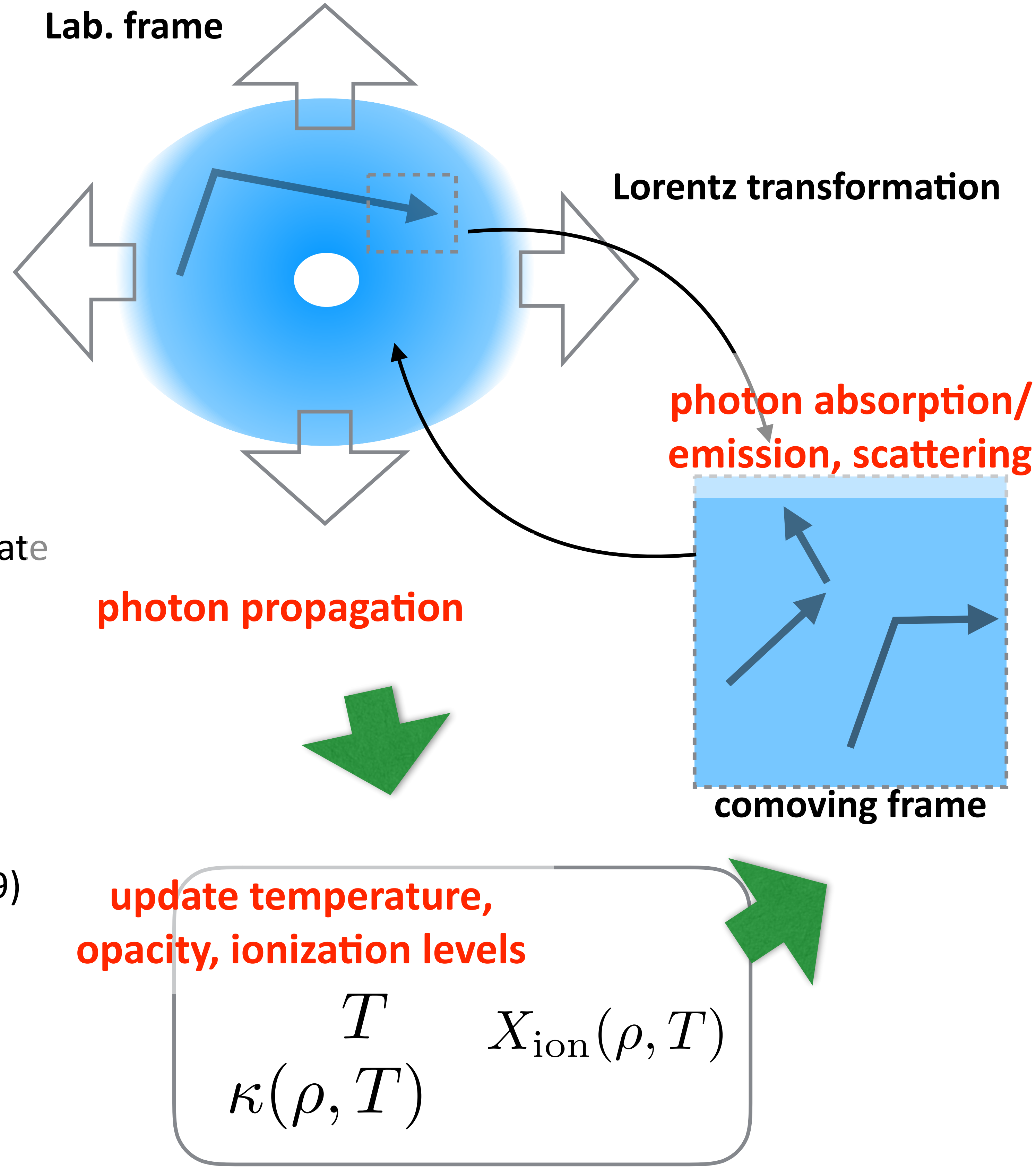

Ejecta profile

- Axisymmetric & homologous expanding ejecta

Post-merger ejecta: $v = 0.025\,c - 0.1\,c$

$$\rho \propto r^{-3} \quad < v > \approx 0.05\,c$$

Dynamical ejecta: $v = 0.12\,c - 0.9\,c$

$$\rho \propto r^{-4}\,(\leq 0.4\,c), r^{-8}\,(v > 0.4\,c) \quad < v > \approx 0.25\,c$$

- Angular dependence of density and Ye distribution is taken into account for dynamical ejecta

Density profile

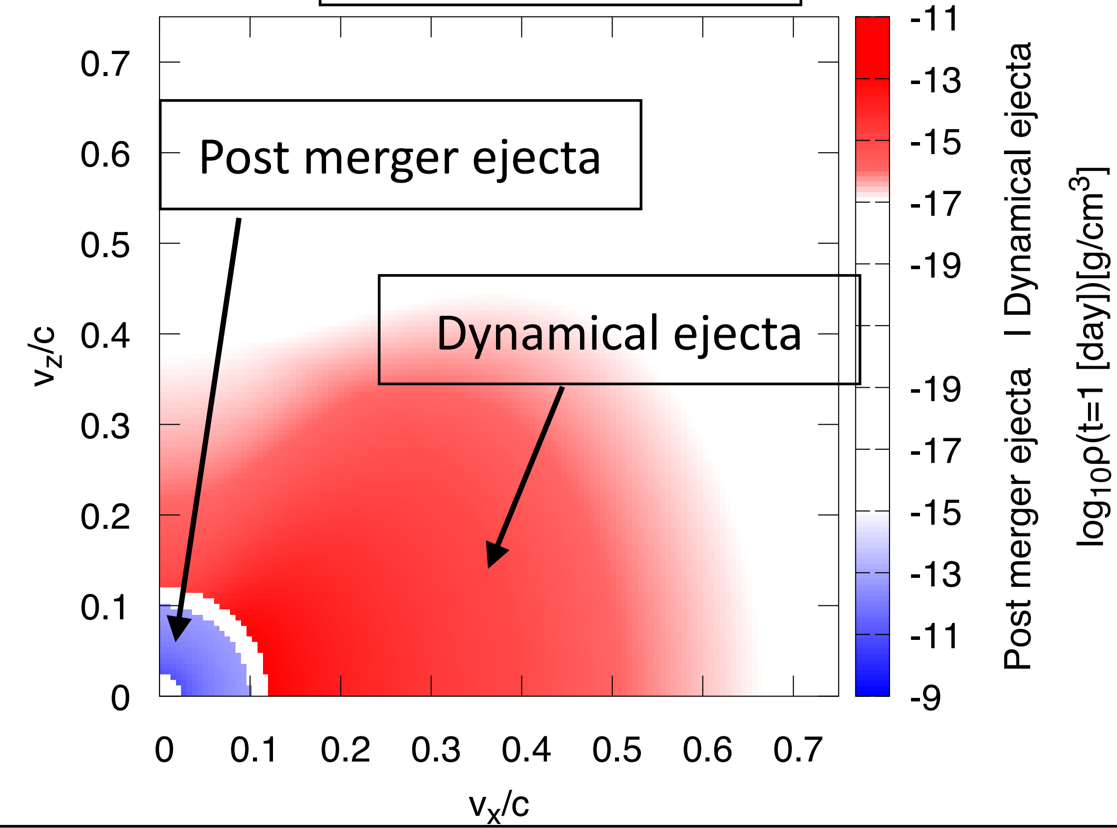

Radial density profile of dynamical ejecta

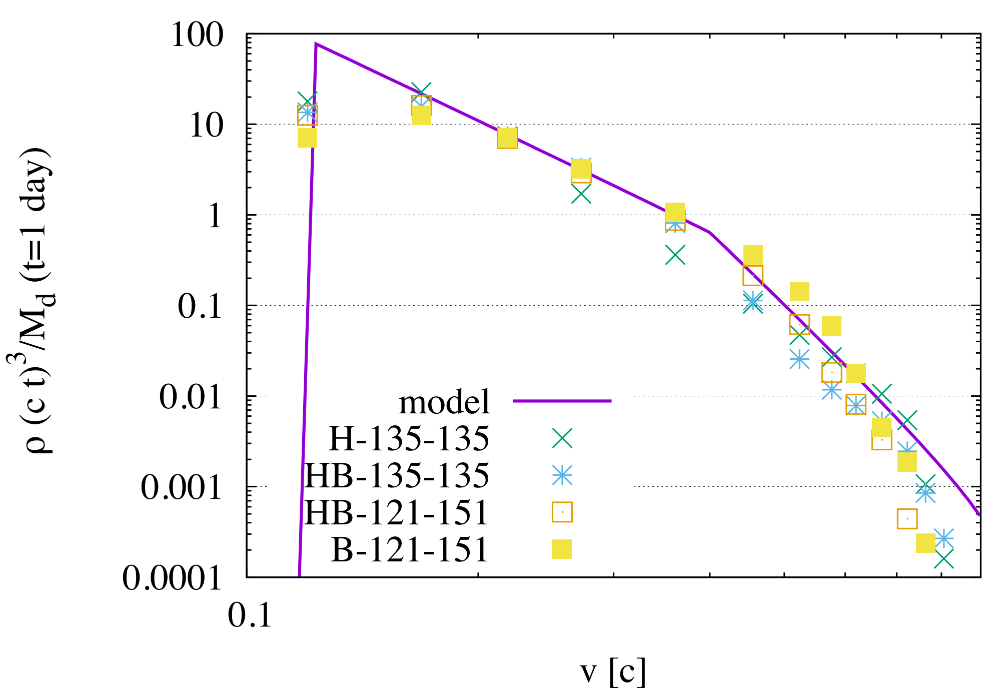

Lanthanide fraction (Hi-Ye post merger ejecta)

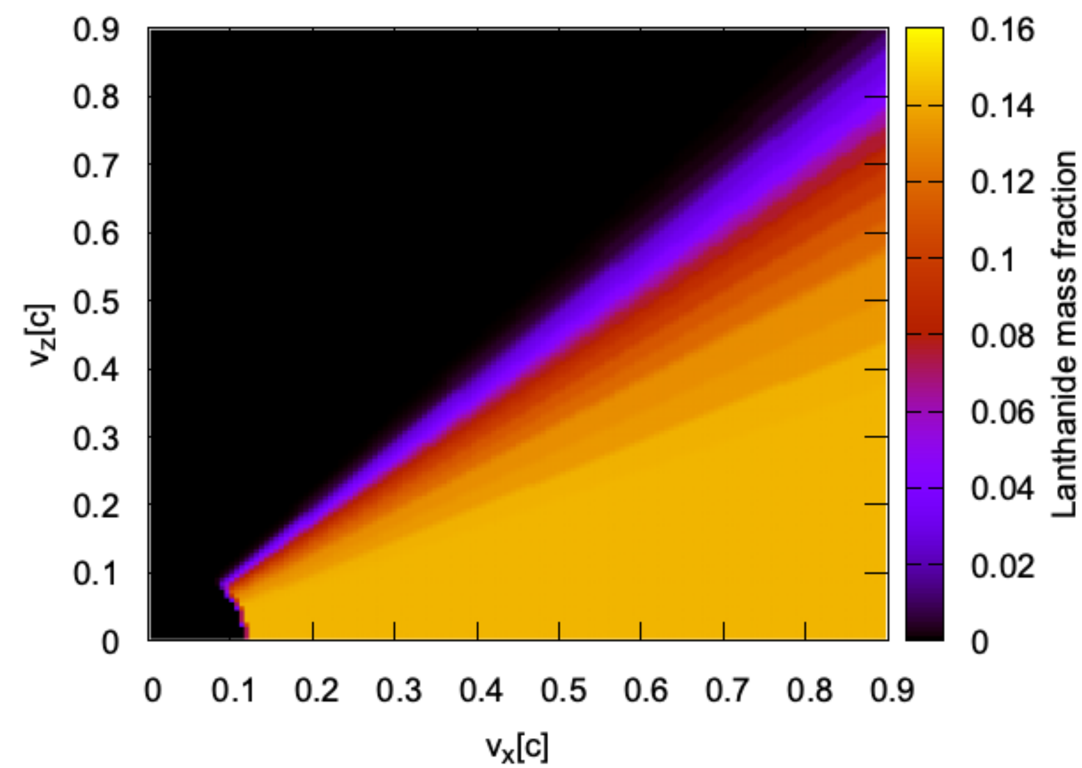

Ref: Kiuchi et al. 2017, Hotokezaka et al. 2018

Effect of radiative transfer of photons in multiple ejecta components

- **Enhancement of luminosity in polar direction**

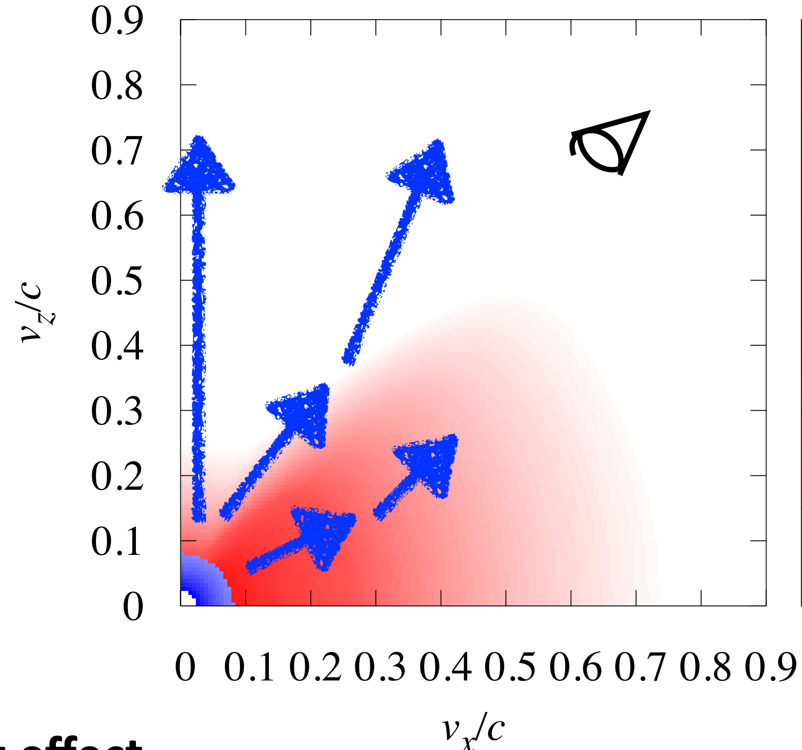

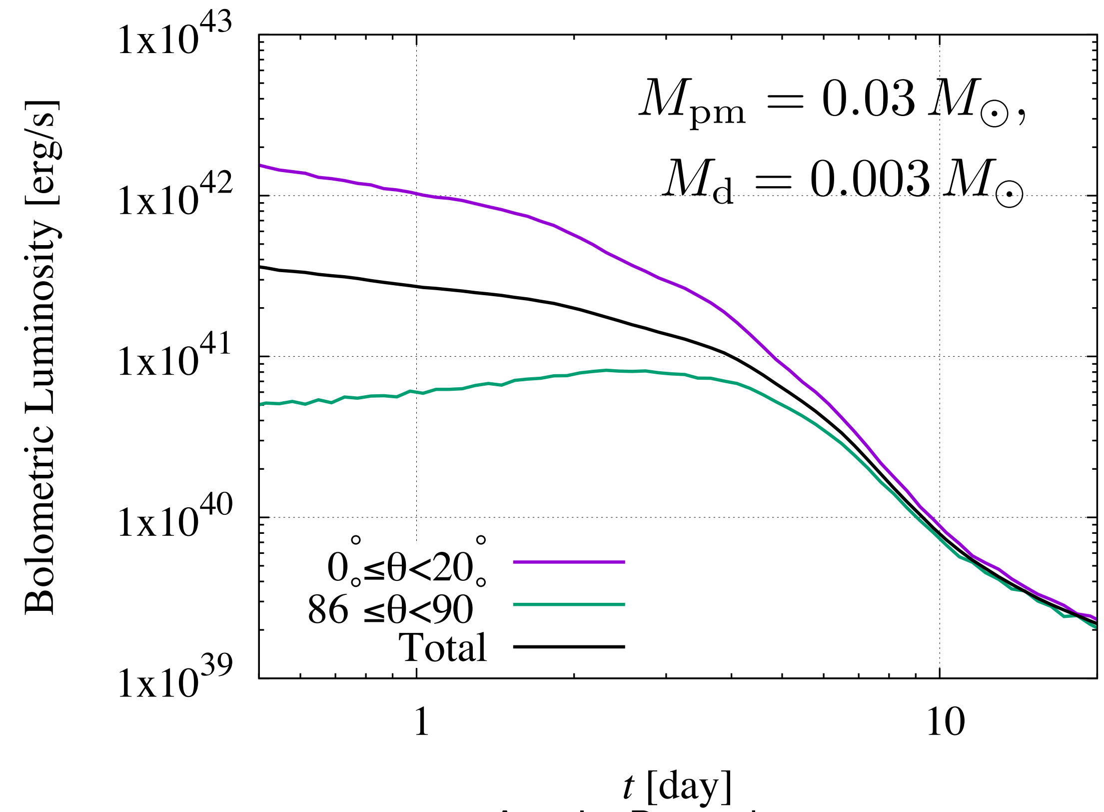

- **Blocking effect**

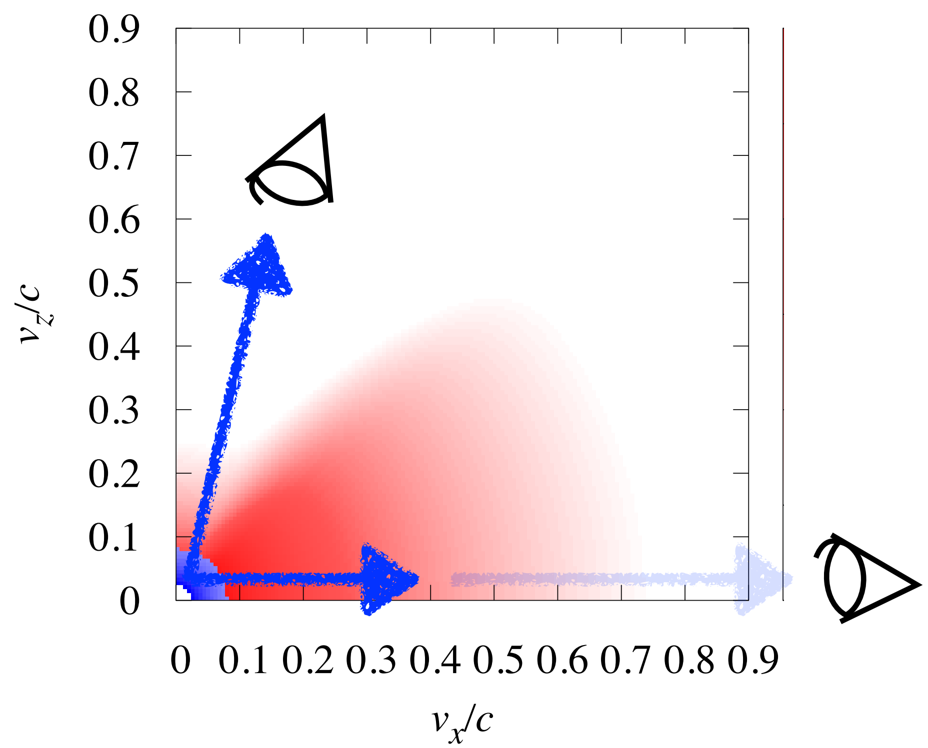

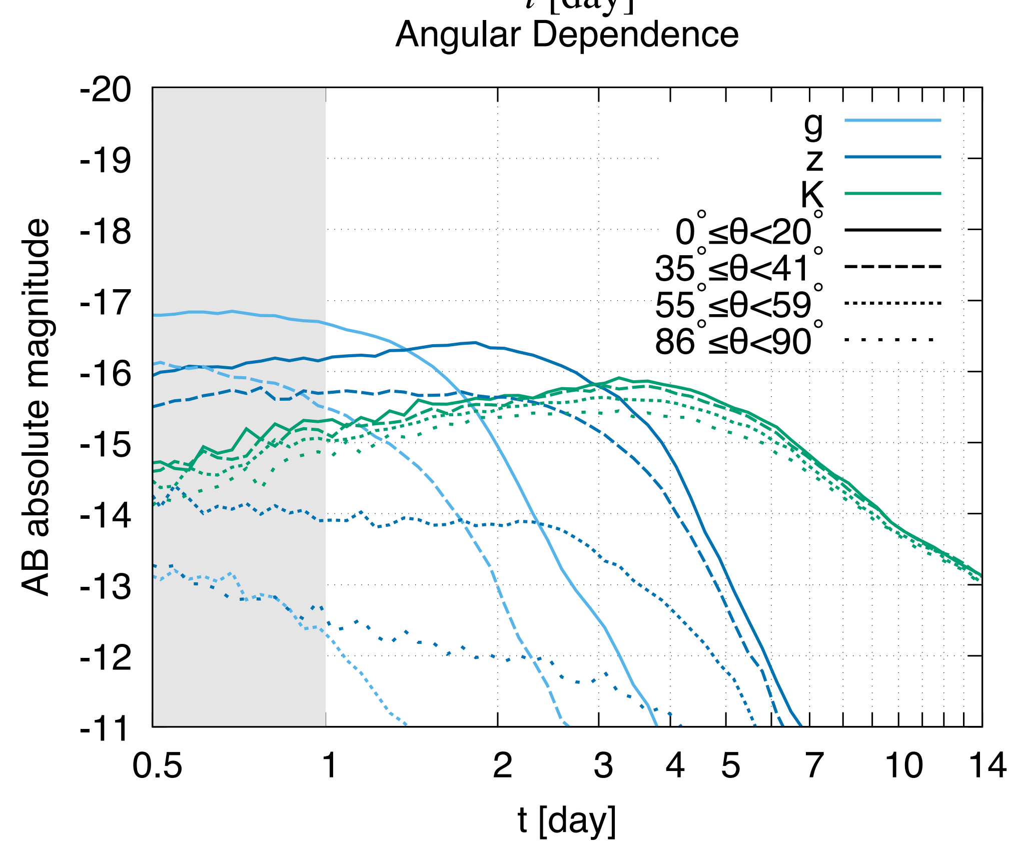

Effect of radiative transfer of photons in multiple ejecta components

- **Heating up of the dynamical ejecta**

Solid: the full calculation

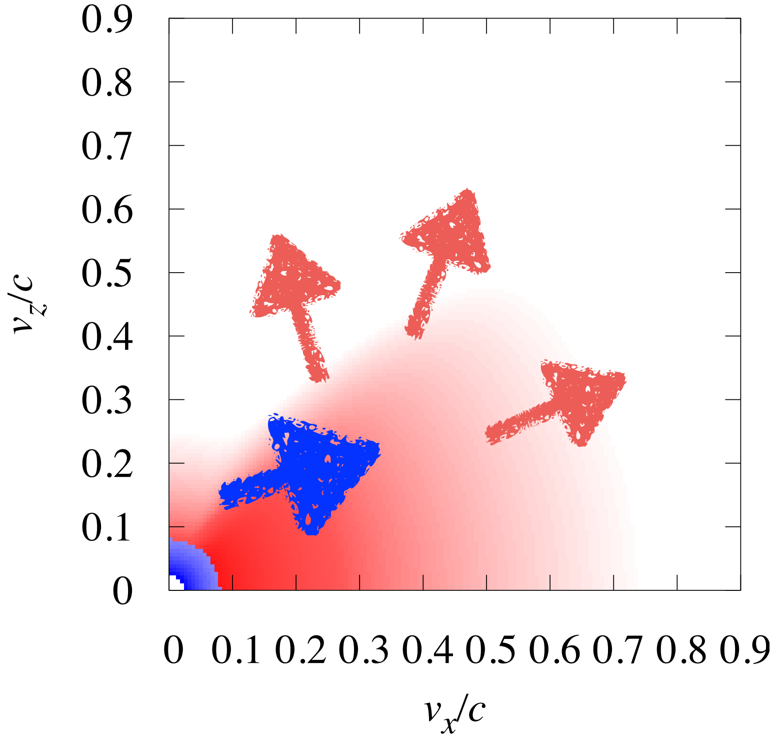

$$M_{\rm pm} = 0.03\,M_\odot,$$
$$M_{\rm d} = 0.003\,M_\odot$$

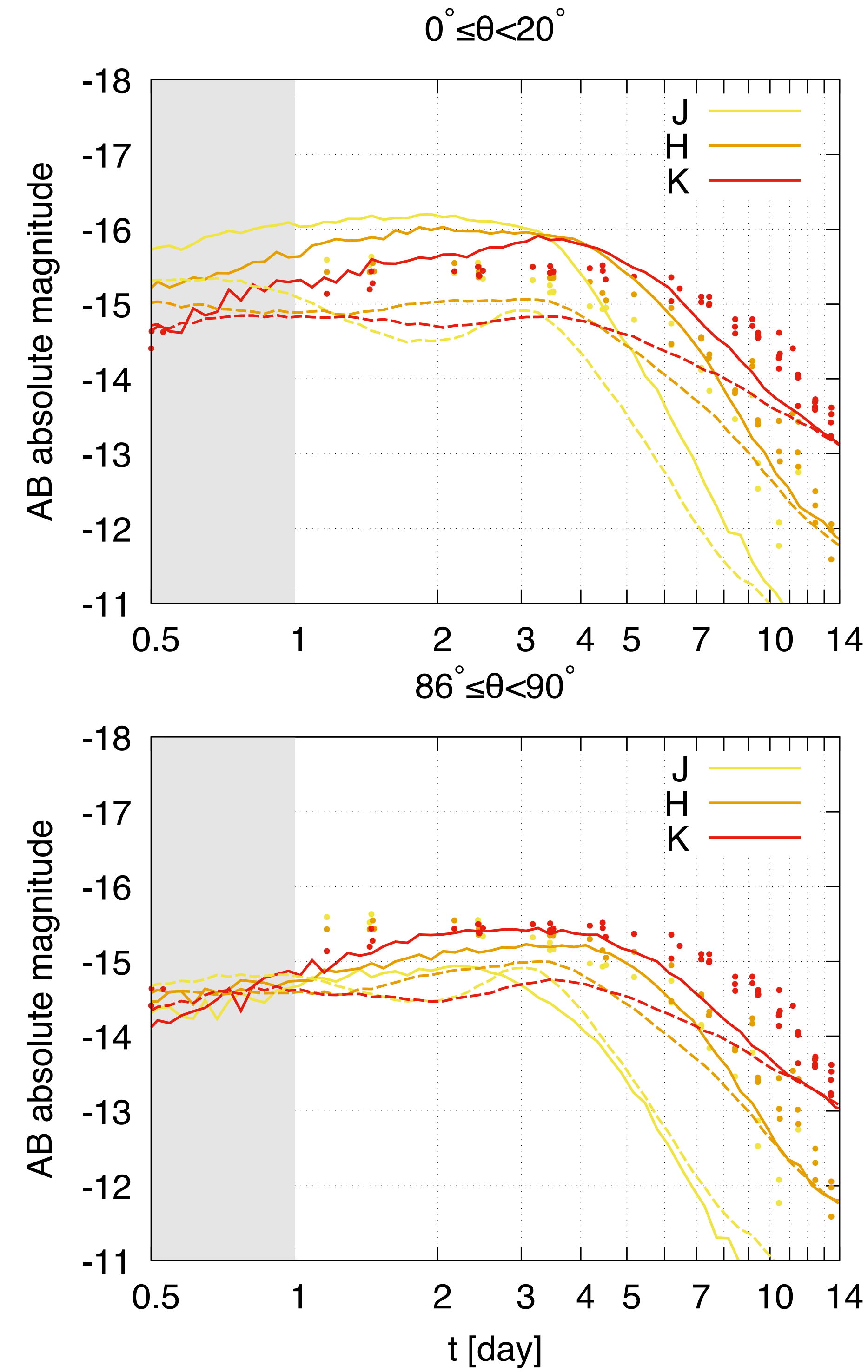

Dashed: Separately calculated and combined

Only post-merger ejecta

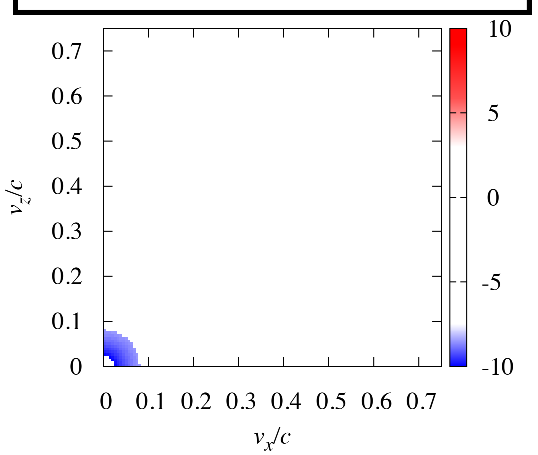

+

Only dynamical ejecta

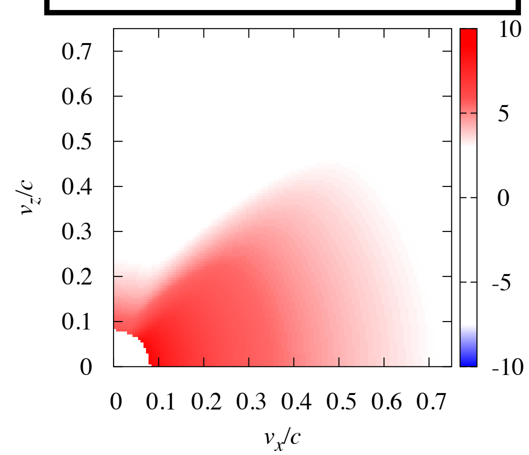

Taking the radiative transfer effect of photons in the multiple ejecta components of non-spherical morphology into account is crucial for the lightcurve prediction

GW170817

GW data analysis constraint : θ <~30°

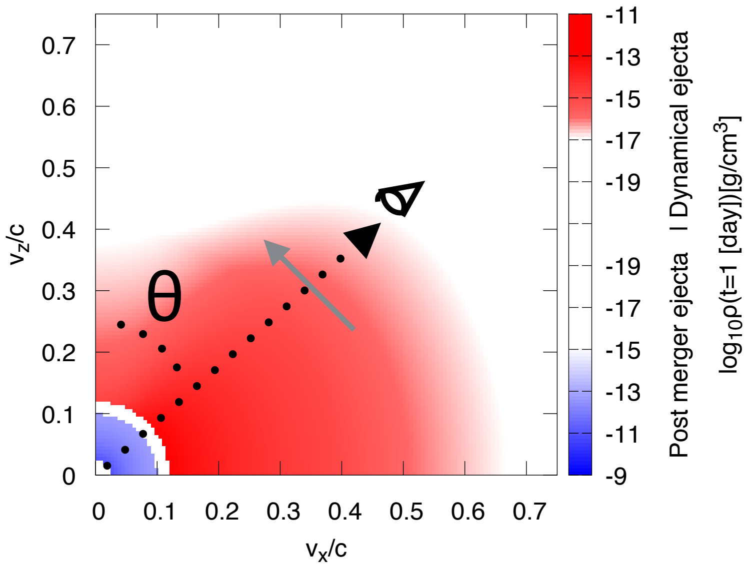

Models

GW170817-YM: Ye,pm=0.2-0.4 (Xlan~0.03), 0°<θ<21°

GW170817-YH: Ye,pm=0.3-0.4 (Xlan<<1), 21°<θ<28°

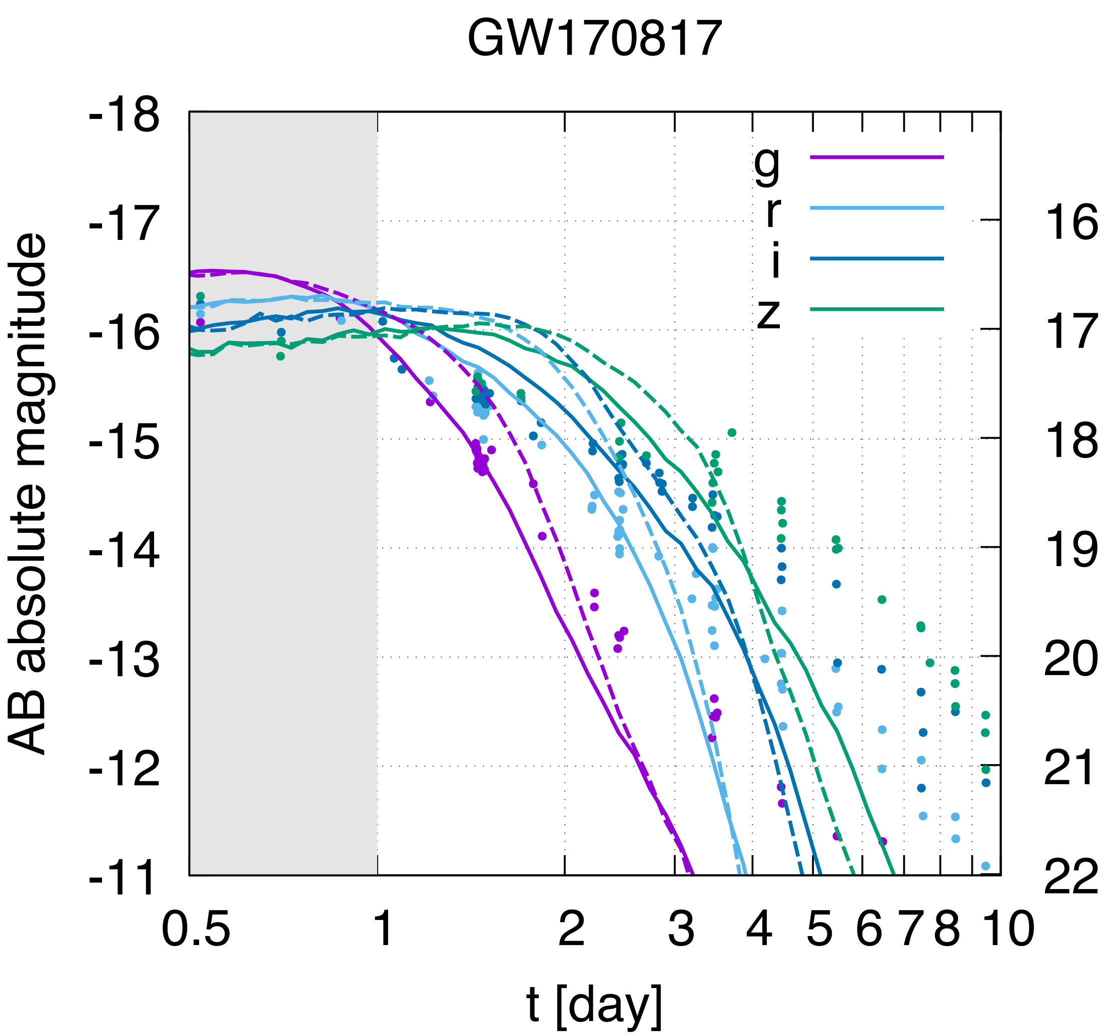

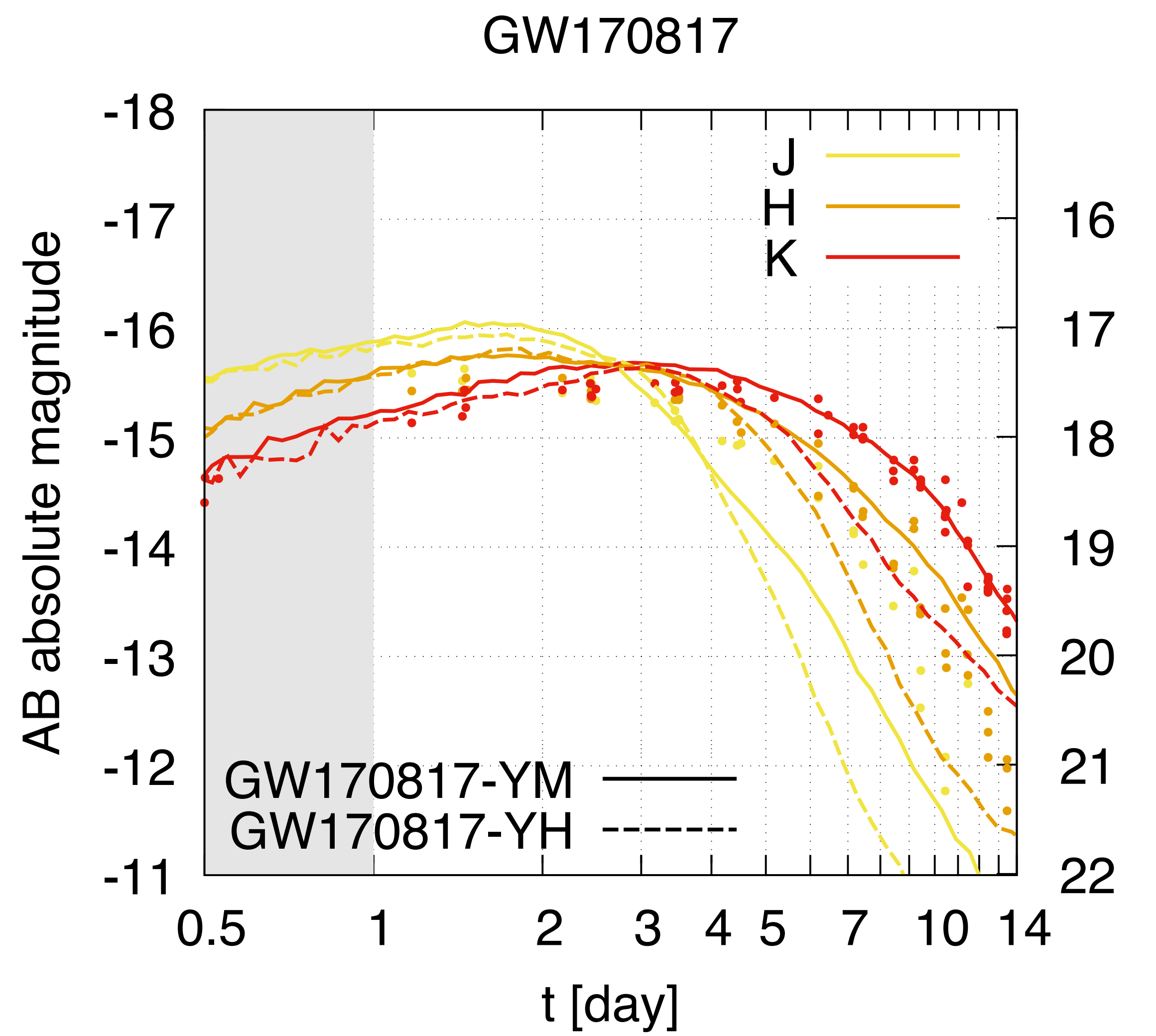

Dynamical ejecta: **0.003 Msun,** Post-merger ejecta: 0.02 Msun

Ref: KK, Shibata, Tanaka 2018, 2019

Diversity

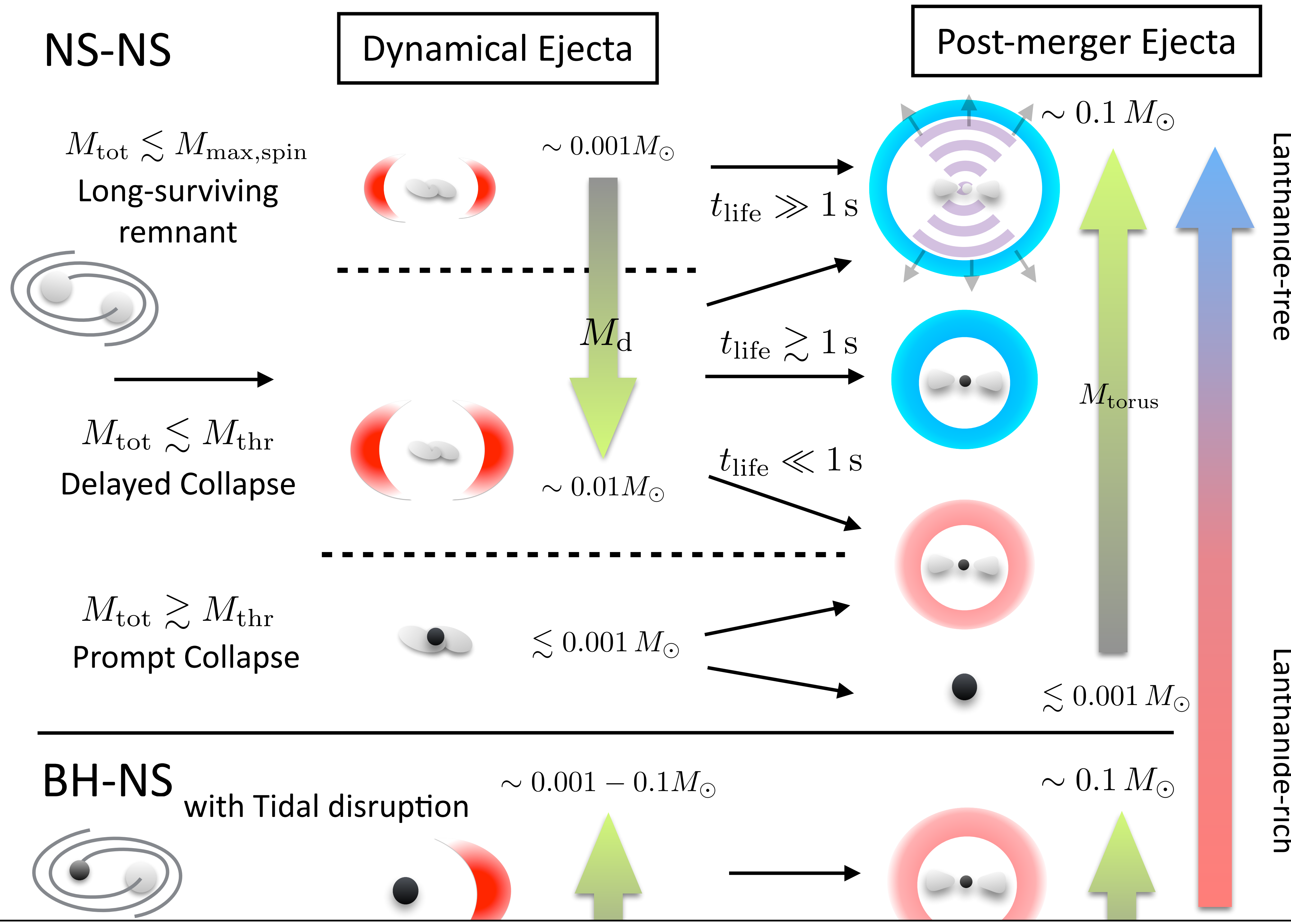

Kilonova lightcurves could show large diversity reflecting the variety in the binary parameters or the binary composition (see also e.g. Gompertz et al. 2018, Rossi et al. 2019)

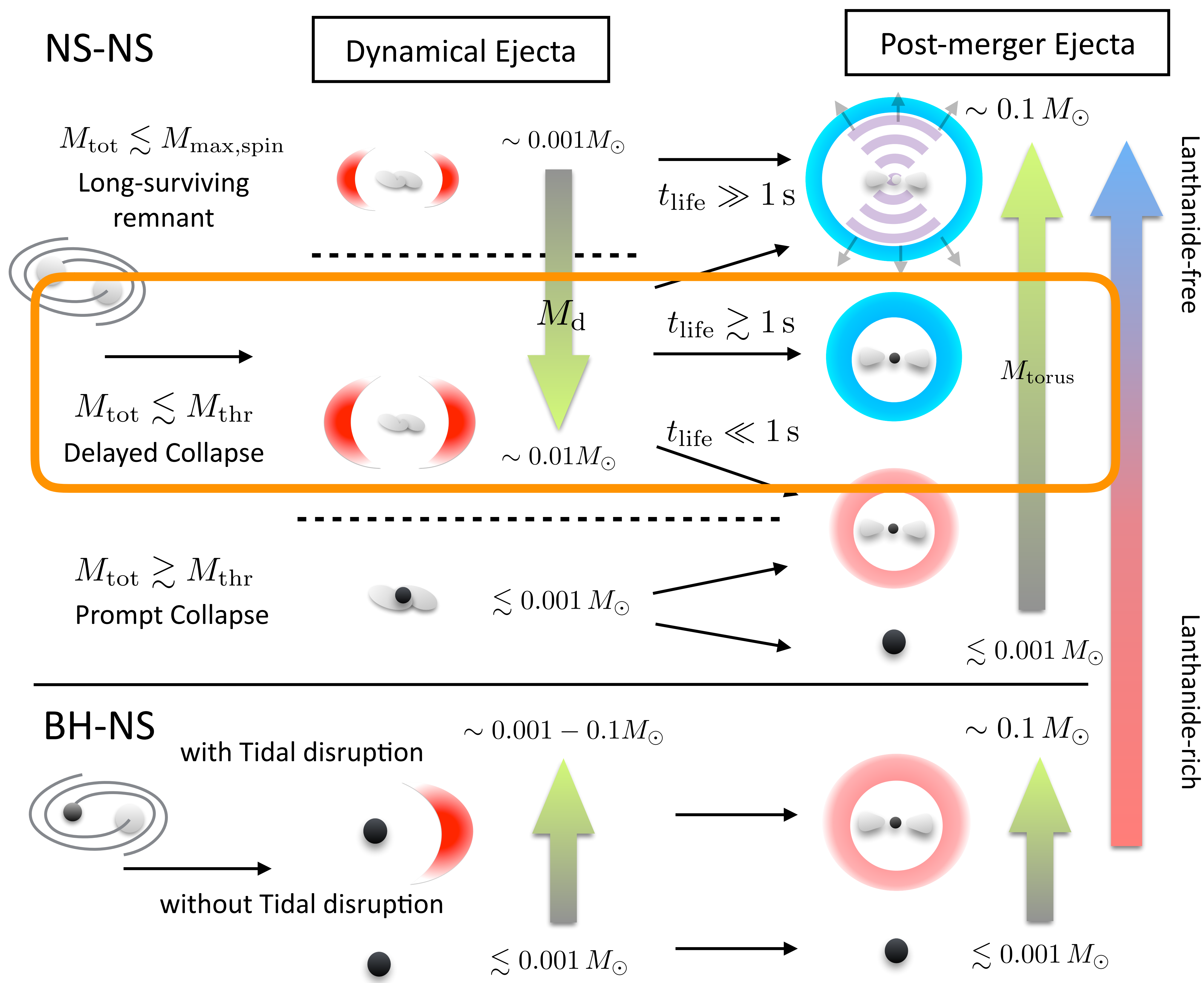
NS-NS
Dynamical Ejecta
Post-merger Ejecta
$M_{\rm tot} \lesssim M_{\rm max,spin}$
Long-surviving remnant
$\sim 0.001 M_\odot$
$t_{\rm life} \gg 1\,{\rm s}$
$\sim 0.1\,M_\odot$
$M_{\rm d}$
$t_{\rm life} \gtrsim 1\,{\rm s}$
$M_{\rm torus}$
$M_{\rm tot} \lesssim M_{\rm thr}$
Delayed Collapse
$\sim 0.01 M_\odot$
$t_{\rm life} \ll 1\,{\rm s}$
$M_{\rm tot} \gtrsim M_{\rm thr}$
Prompt Collapse
$\lesssim 0.001\,M_\odot$
$\lesssim 0.001\,M_\odot$
Lanthanide-free
Lanthanide-rich
BH-NS
with Tidal disruption
$\sim 0.001 - 0.1 M_\odot$
$\sim 0.1\,M_\odot$
without Tidal disruption
$\lesssim 0.001\,M_\odot$
$\lesssim 0.001\,M_\odot$

Remnant NS Lifetime

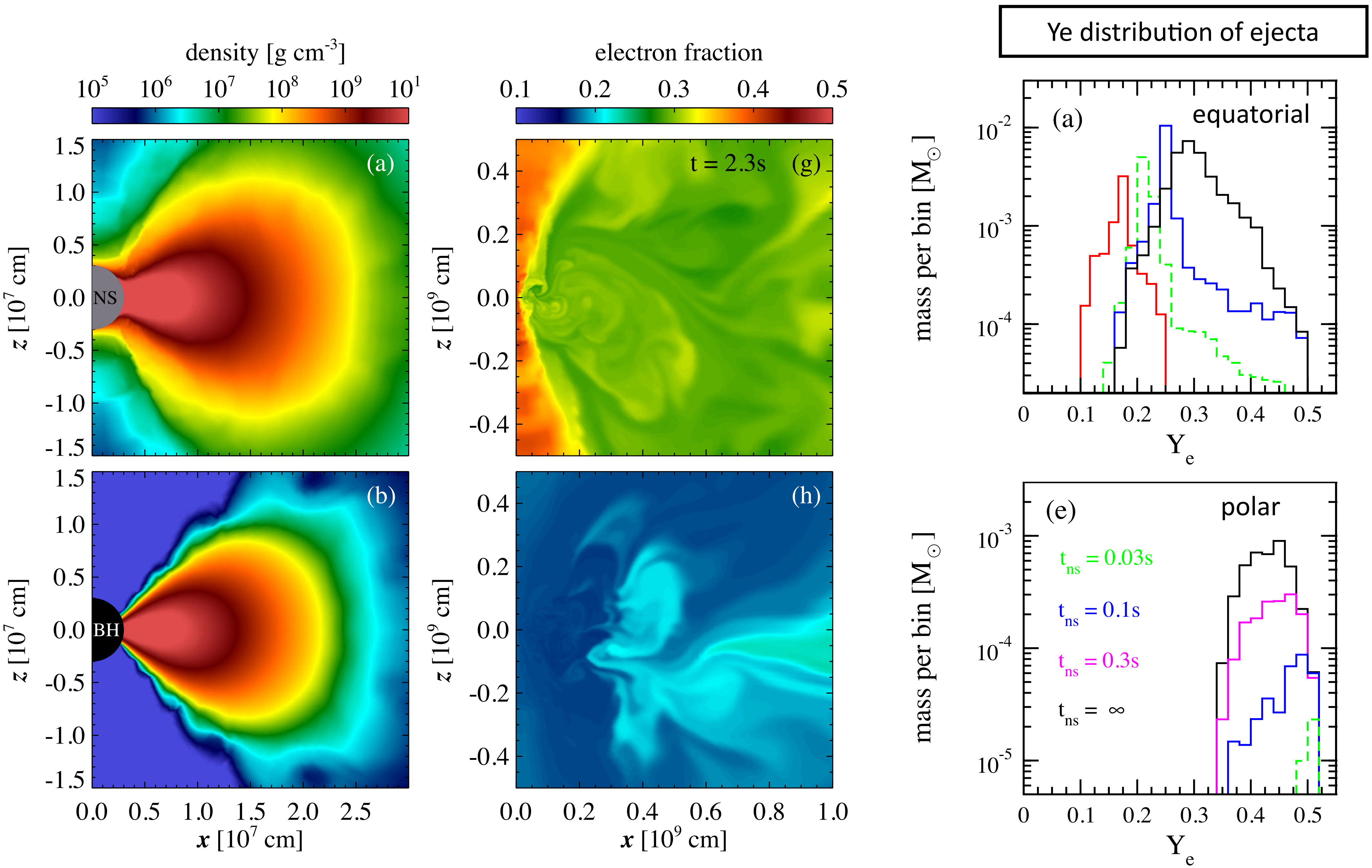

Ref: Metzger & Fernández et al. 2014

- Life time of the remnant NS has a large impact on the Ye distribution of the post merger ejecta: low (high) Ye → large (small) lanthanide fraction (See also Lippuner et al. 2017)

Ye dependence

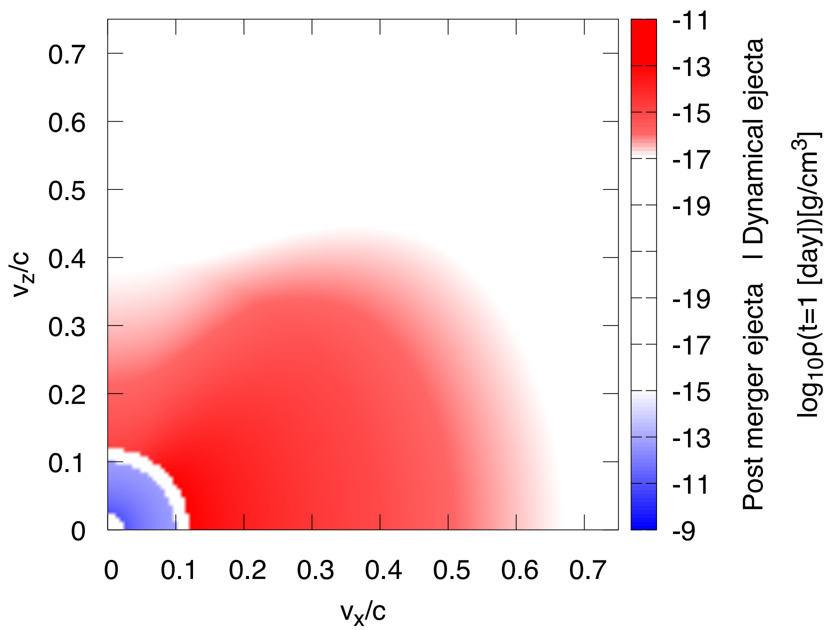

Optical/infrared EM data points observed in
GW170817 summarized by Villar et al. 2017 (D=40Mpc)

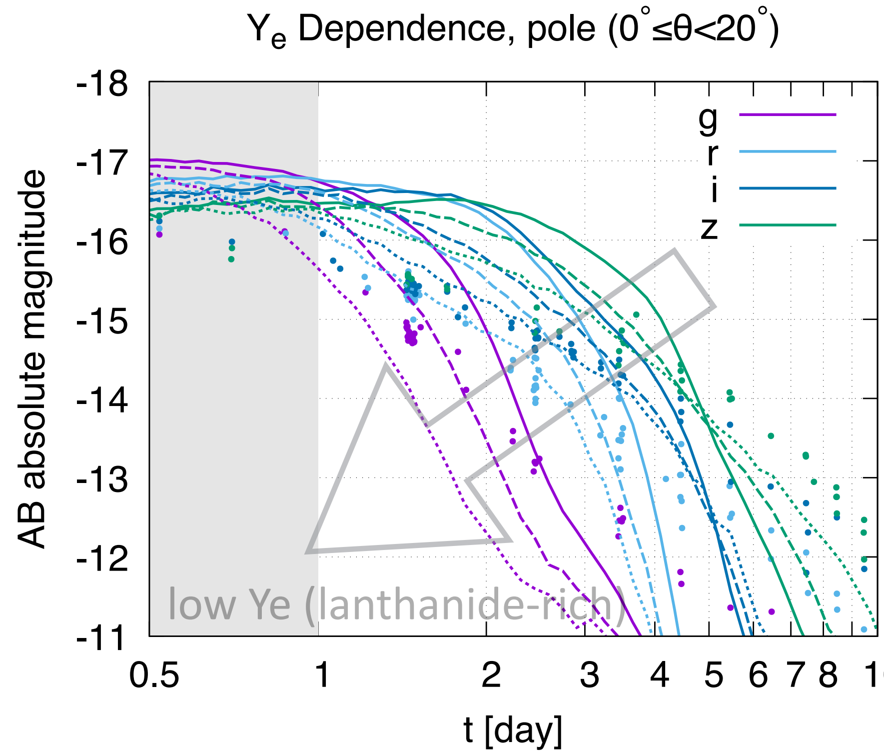

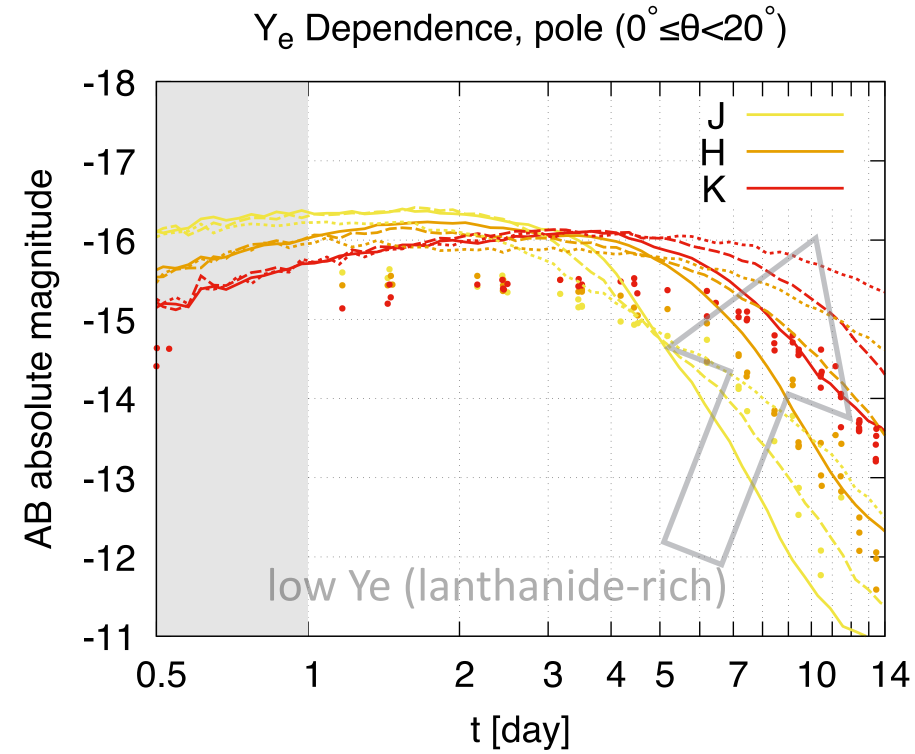

$$M_{\rm pm} = 0.03\, M_\odot,$$
$$M_{\rm d} = 0.01\, M_\odot$$

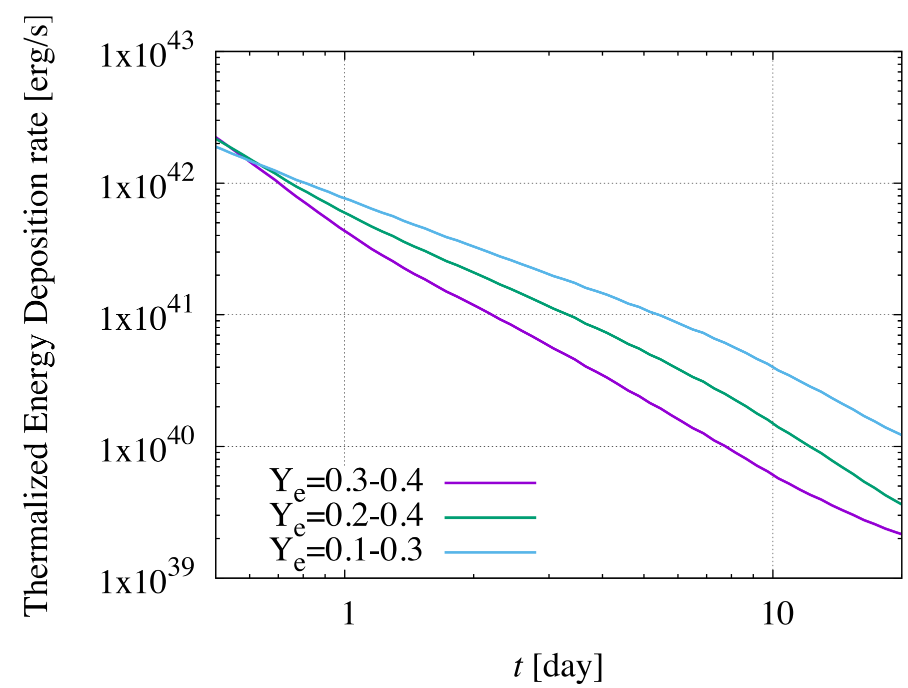

$$t_{\rm peak} \propto M_{\rm ej}^{1/2} v_{\rm ej}^{-1/2} \kappa^{1/2}$$

$$L_{\rm peak} \propto M_{\rm ej}^{1/2} v_{\rm ej}^{1/2} \kappa^{-1/2}$$

$$T_{\rm peak} \propto M_{\rm ej}^{-1/8} v_{\rm ej}^{-1/8} \kappa^{-3/8}$$

Solid:

$Y_{e,\rm pm}: 0.3 - 0.4 (X_{\rm lan} \ll 1)$

Dashed:

$Y_{e,\rm pm}: 0.2 - 0.4 (X_{\rm lan} \approx 0.025)$

Dotted:

$Y_{e,\rm pm}: 0.1 - 0.3 (X_{\rm lan} \approx 0.15)$

Ref: KK, Shibata, Tanaka 2019

Hi-Ye ejecta from BH accretion torus?

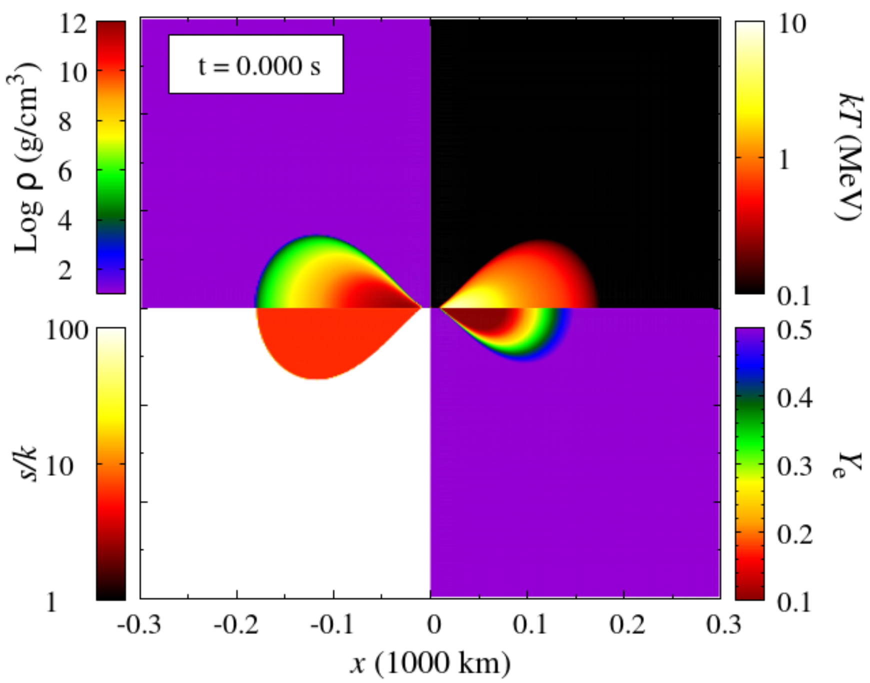

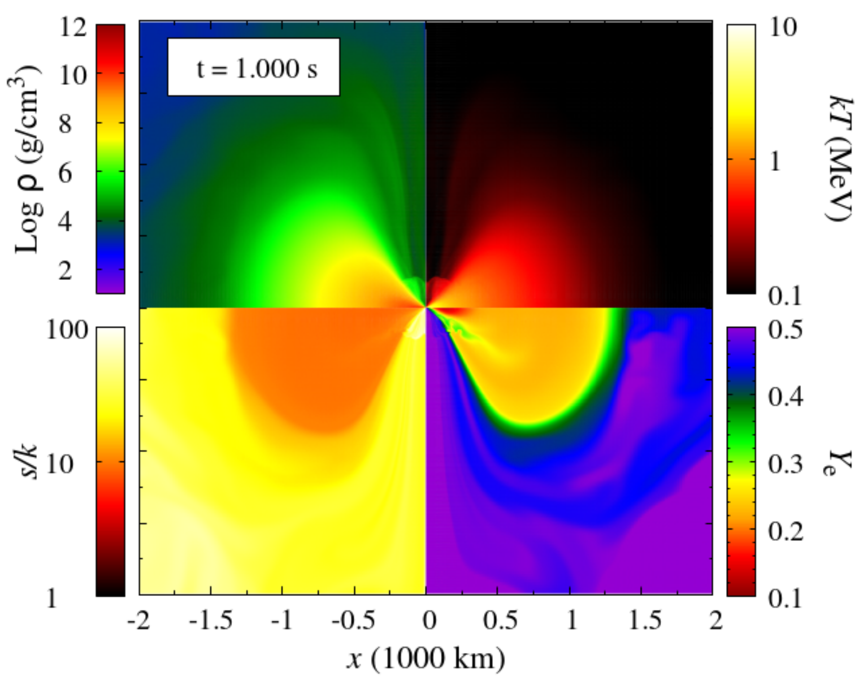

average ejecta Ye

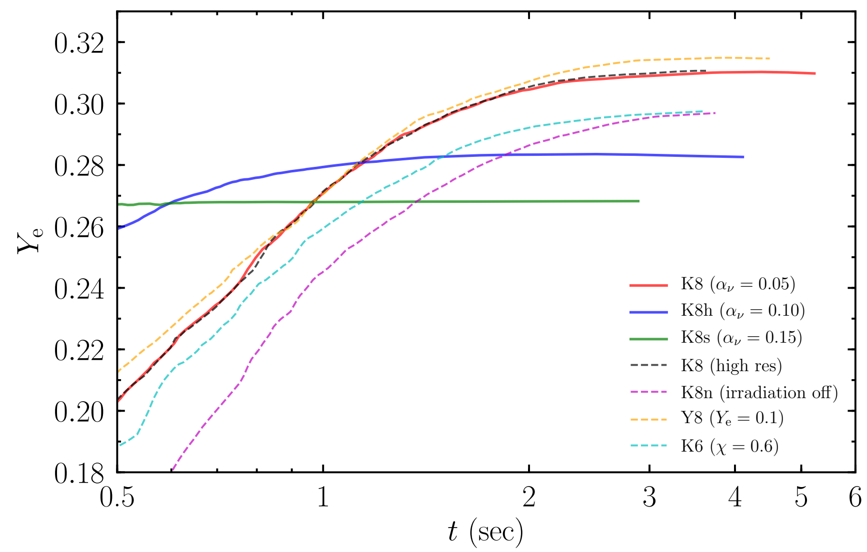

total ejected mass

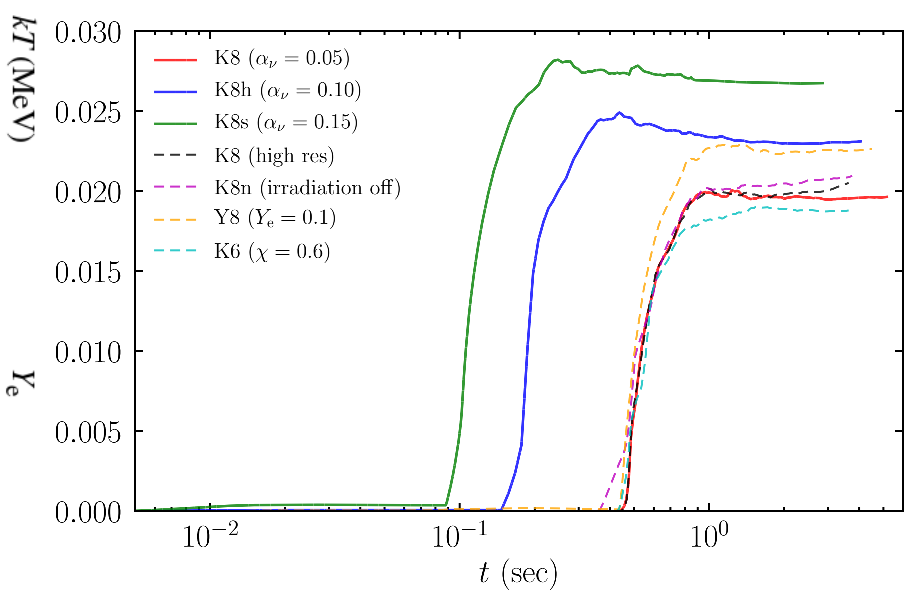

$$\mathcal{R}^{\rm f}_{\rm ec}(\rho,T,Y_{e,\rm eq})+\mathcal{R}^{\rm h}_{\rm ec}(\rho,T,Y_{e,\rm eq})$$
$$=\mathcal{R}^{\rm f}_{\rm pc}(\rho,T,Y_{e,\rm eq})+\mathcal{R}^{\rm h}_{\rm pc}(\rho,T,Y_{e,\rm eq}).$$

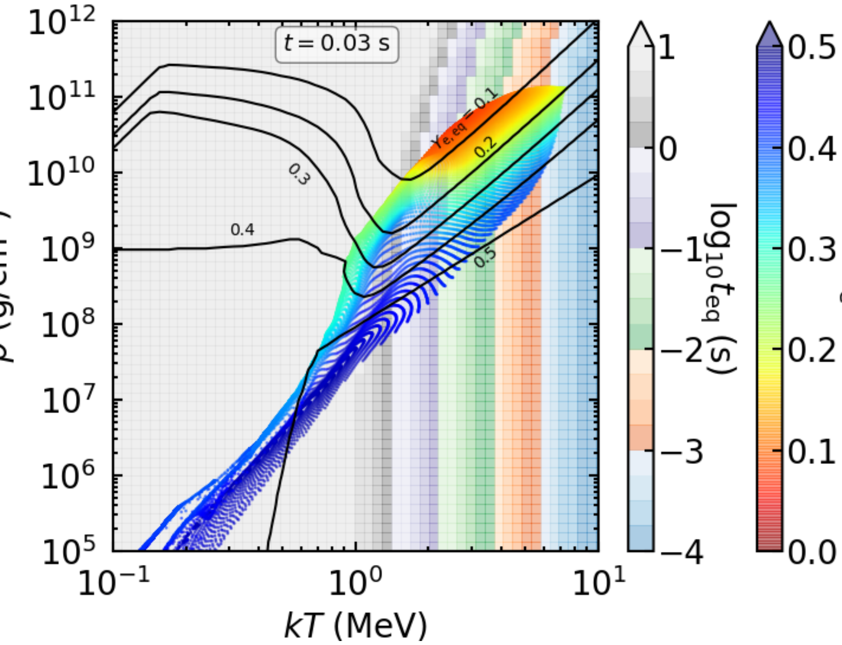

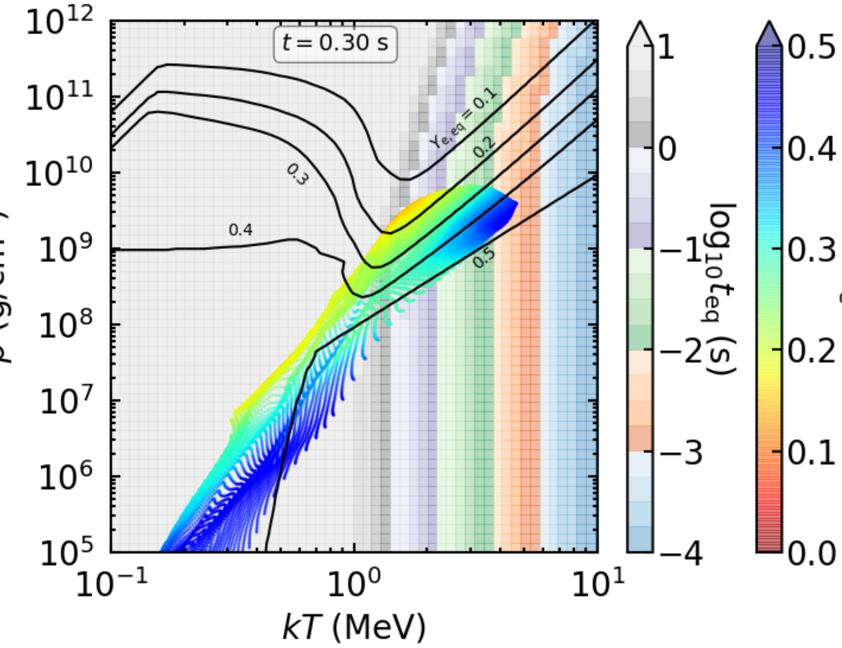

Ref: Fujibayashi et al. 2020

- Recent GR viscous RHD simulation suggests that Hi-Ye ejecta (Ye>0.3) may also be formed in the absence of remnant MNS if the ejection times scale is long (~>0.3 s)(See also Fujibayashi et al. 2020)

Comparison among various models (polar)

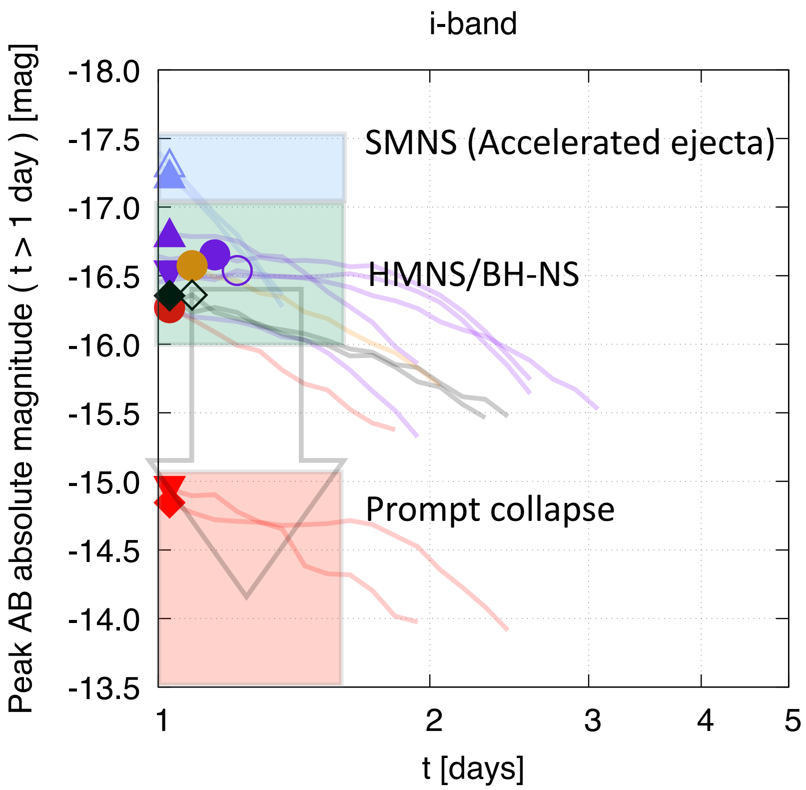

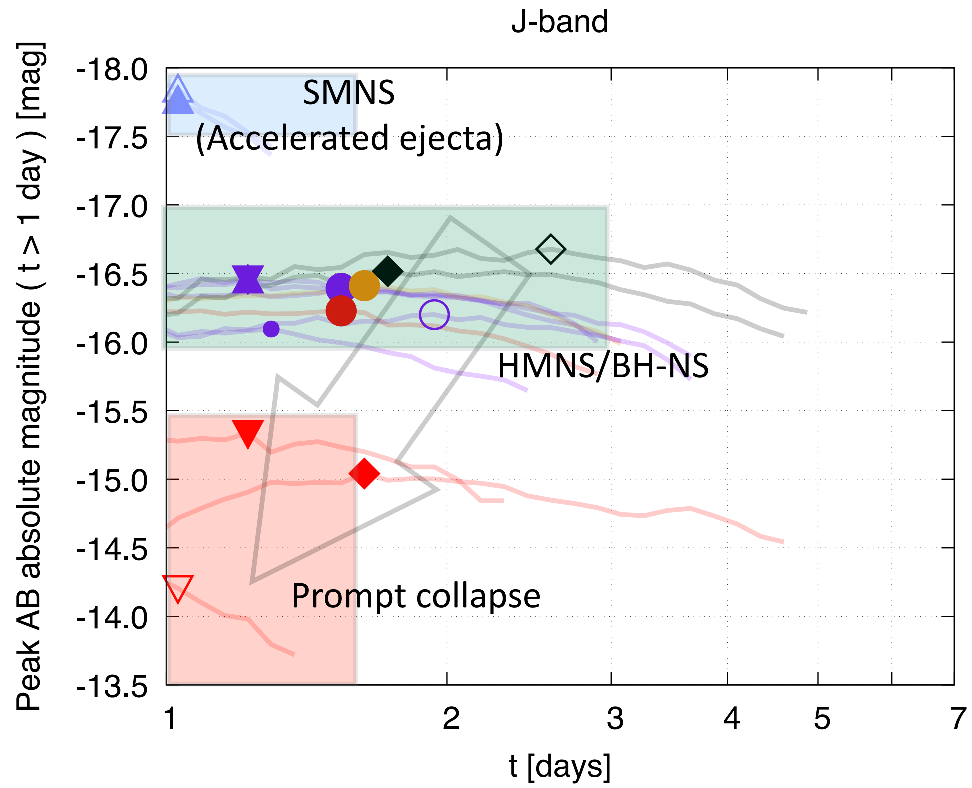

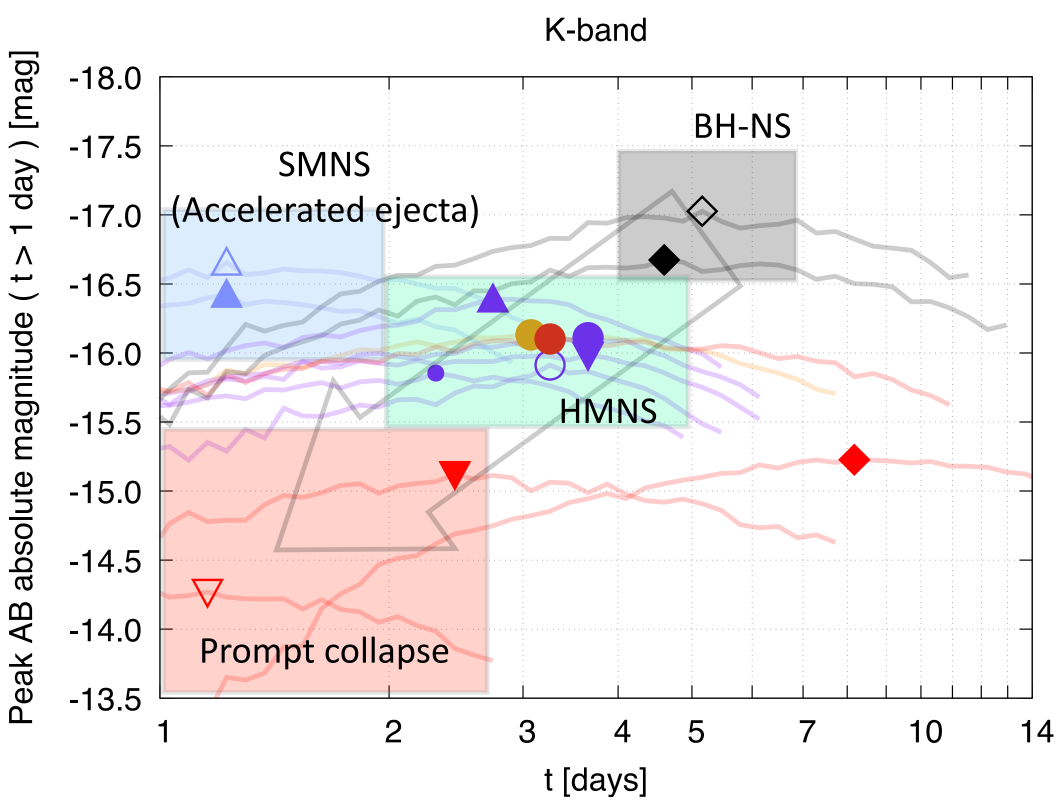

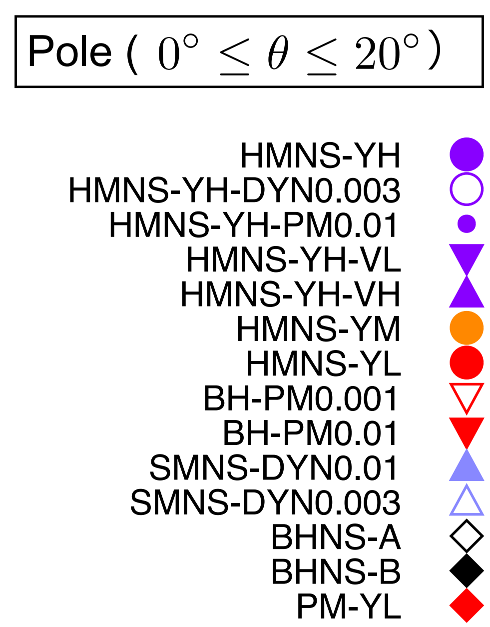

SMNS:
cases that the remnant NS survives for a long time scale (>>1 s)

HMNS:
cases that the remnant NS survives temporarily and eventually collapses to a BH

Prompt collapse:
cases that the NSs collapses to a BH immediately after the merger

- We may be able to infer the type of the central engine for kilonovae by observation of the peak brightness and time of peak in the multiple band.

*since the lightcurves for t<1day are not reliable for our calculation, we define the peak magnitude as the brightest point after t=1day.

Application to
the recent GW events

The 2nd NS-NS: GW190425

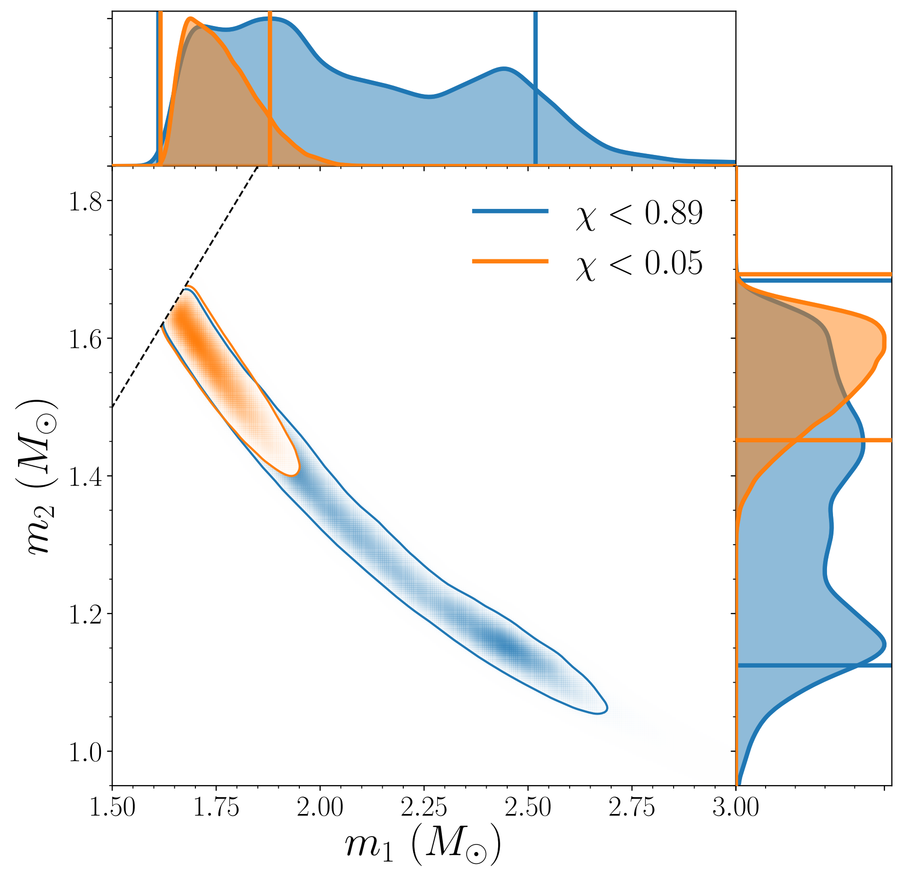

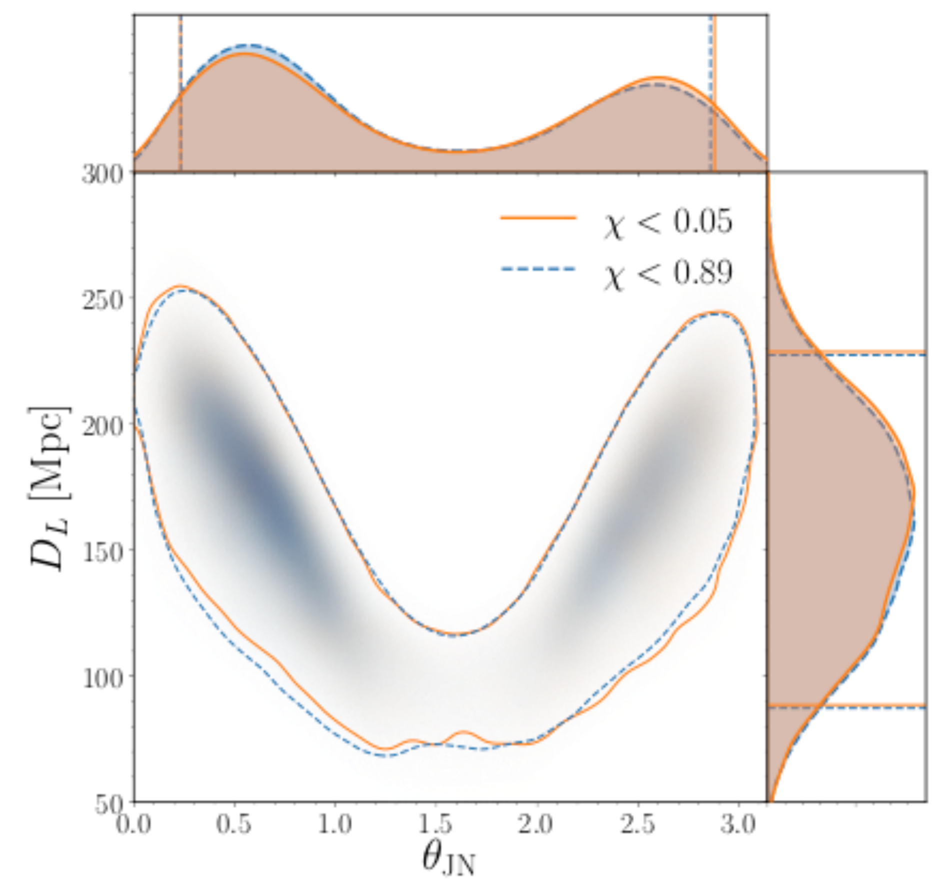

	Low-spin prior ($\chi < 0.05$)	High-spin prior ($\chi < 0.89$)
Primary mass m_1	$1.62 - 1.88\ M_\odot$	$1.61 - 2.52\ M_\odot$
Secondary mass m_2	$1.45 - 1.69\ M_\odot$	$1.12 - 1.68\ M_\odot$
Chirp mass $\mathcal{M}$	$1.44^{+0.02}_{-0.02}\ M_\odot$	$1.44^{+0.02}_{-0.02}\ M_\odot$
Detector-frame chirp mass	$1.4868^{+0.0003}_{-0.0003}\ M_\odot$	$1.4873^{+0.0008}_{-0.0006}\ M_\odot$
Mass ratio m_2/m_1	$0.8 - 1.0$	$0.4 - 1.0$
Total mass $m_{\rm tot}$	$3.3^{+0.1}_{-0.1}\ M_\odot$	$3.4^{+0.3}_{-0.1}\ M_\odot$
Effective inspiral spin parameter $\chi_{\rm eff}$	$0.013^{+0.01}_{-0.01}$	$0.058^{+0.11}_{-0.05}$
Luminosity distance $D_{\rm L}$	161^{+67}_{-73} Mpc	159^{+69}_{-71} Mpc
Combined dimensionless tidal deformability $\tilde{\Lambda}$	≤ 600	≤ 1100

Ref) Abbot et al. (2020)

EM followup

- GW190425
  - **D=156±41Mpc (Initial announce)**
  - 10,000 deg² (A:BAYESTAR)
    ->7,500 deg²(B:LALInference)
- No EM counterparts was found.
- GROWTH: Coughlin et al. 2019
  - ZTF: g & r band
    - 1st Night: ~0.1days
      ~>20.4 mag (median) (A: 36% B:19%)
    - **2nd Night: ~1days**
      ~>21 mag (median) (A: 46% B:21%)
    - 3rd Night: ~2 days
      ~>21 mag? (median) (A: 46% B:21% ?)
  - Palomar Gattini-IR: J band
    - ~> 15.5 mag (median)

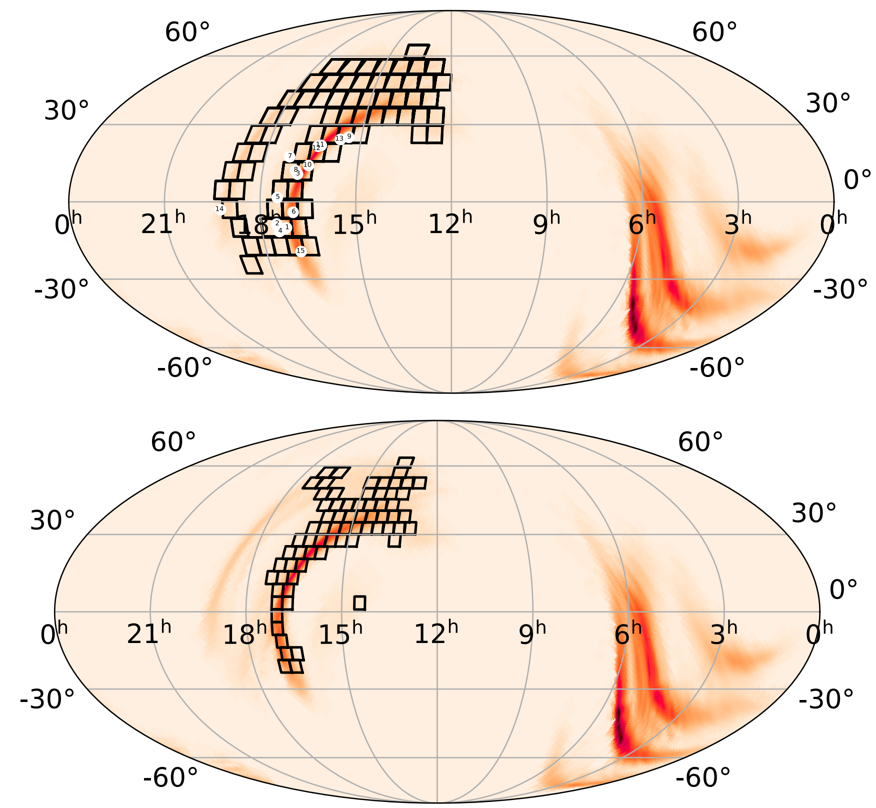

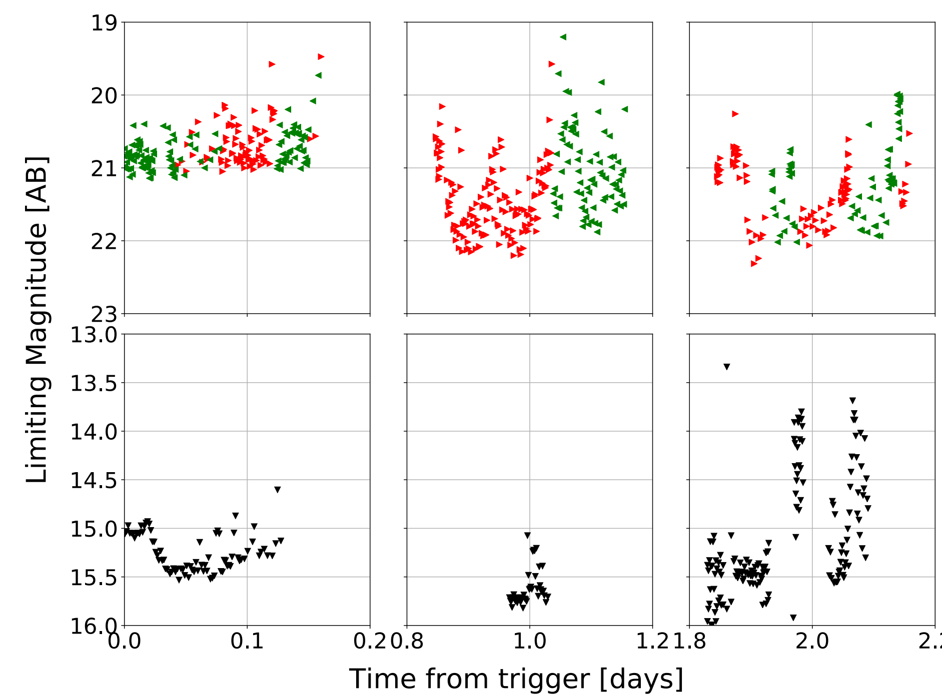

Ref) Coughlin et al. (2019)

GW190425:Merger outcome

$$M_{\rm tot} \gtrsim 3.4\, M_\odot$$

NS-NS

$q = M_1/M_2 \approx 1$

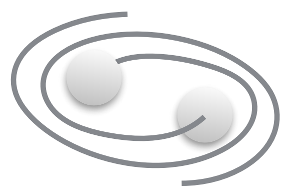

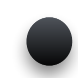

No mass ejection

$q = M_1/M_2 < 1$

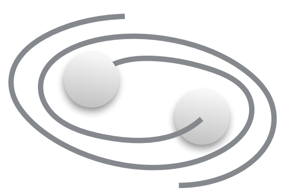

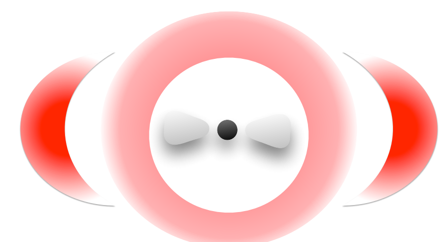

Post merge ejecta (0.01-0.03 Msun)
+ Dynamical ejecta (~>0.001 Msun)

BH-NS

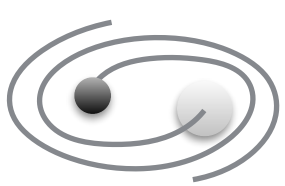

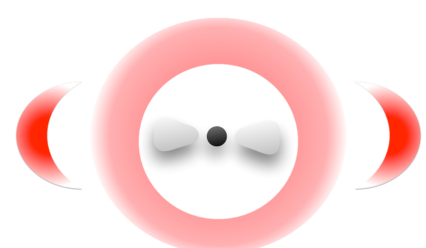

or

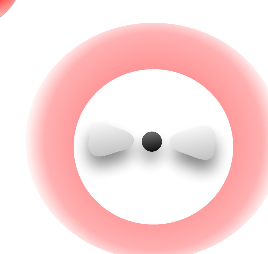

Post merge ejecta (0.01-0.03 Msun)
+ Dynamical ejecta (<0.001 Msun)

no tidal disruption
(small radius)

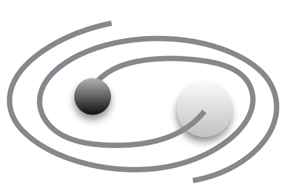

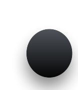

No mass ejection

Ref) Hotokezaka et al.(2013), Kyutoku et al. (2020), Hayashi et al. in prep

GW190425: Kilonova detectability

Lanthanide poor disk outflow
0.02 Msun

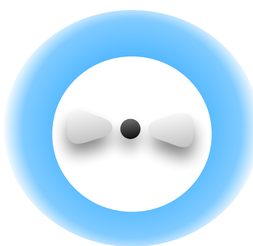

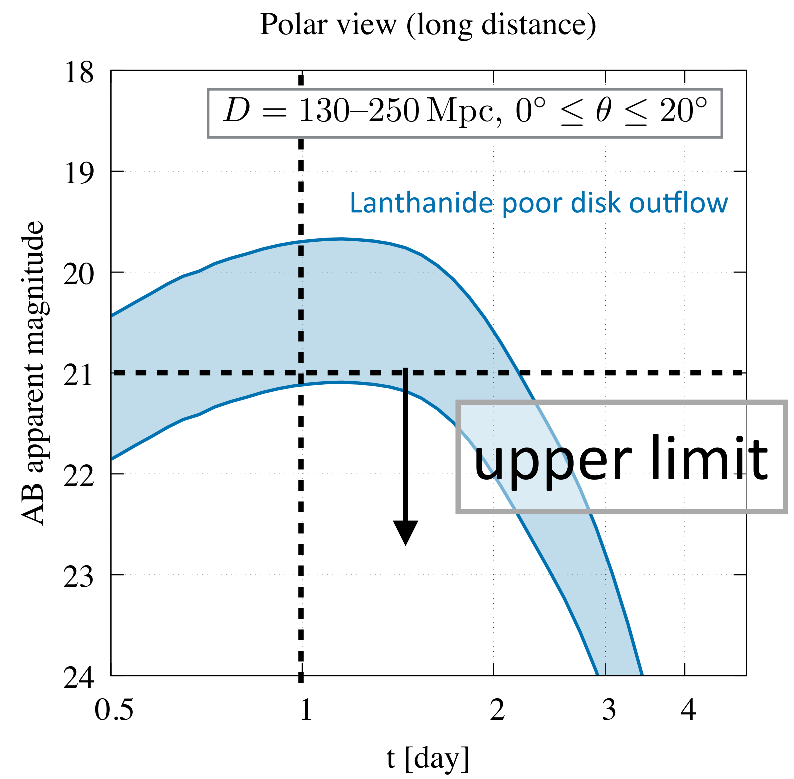

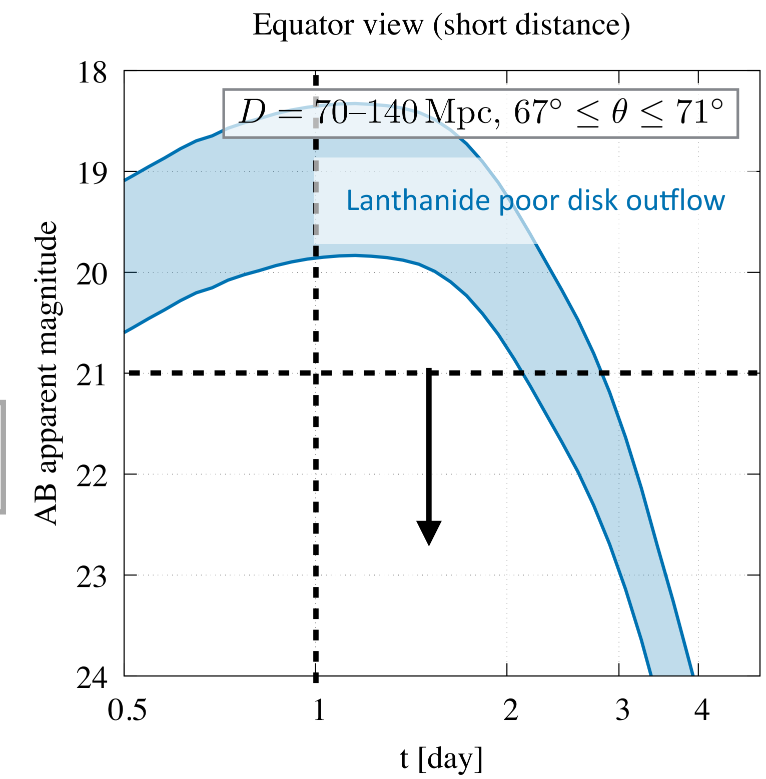

Lanthanide rich disk outflow
0.02 Msun

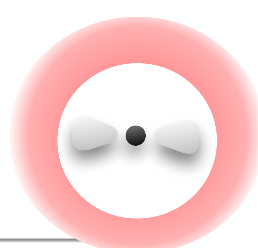

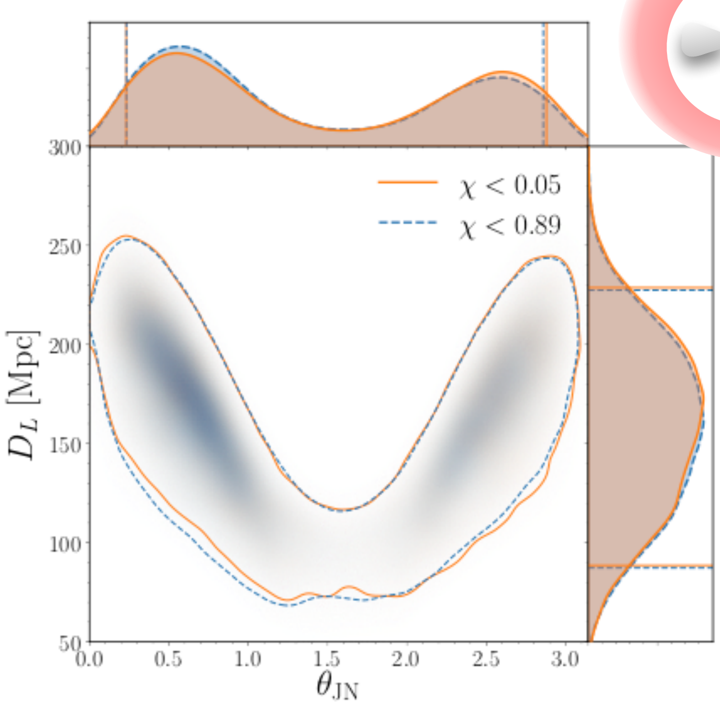

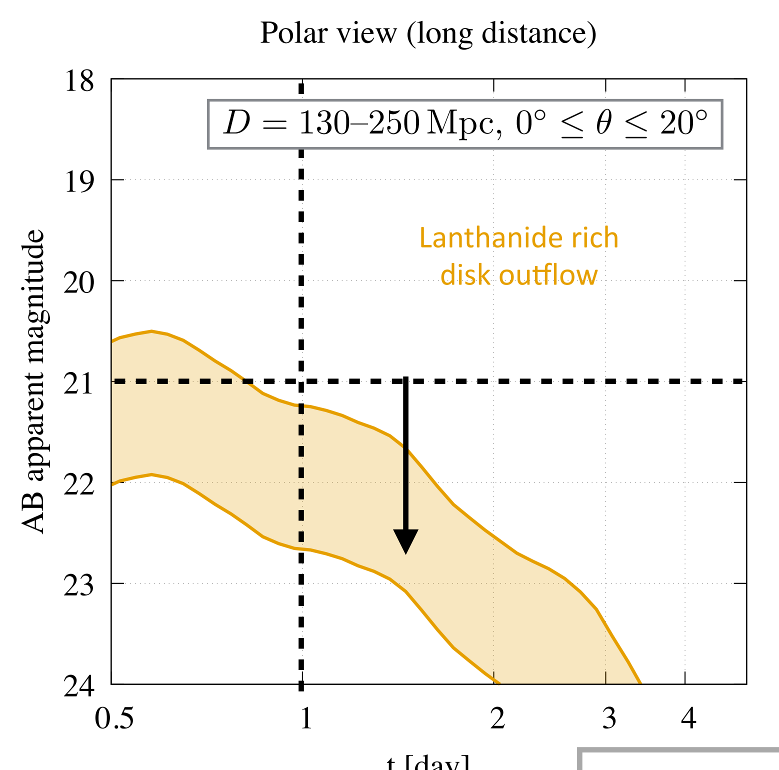

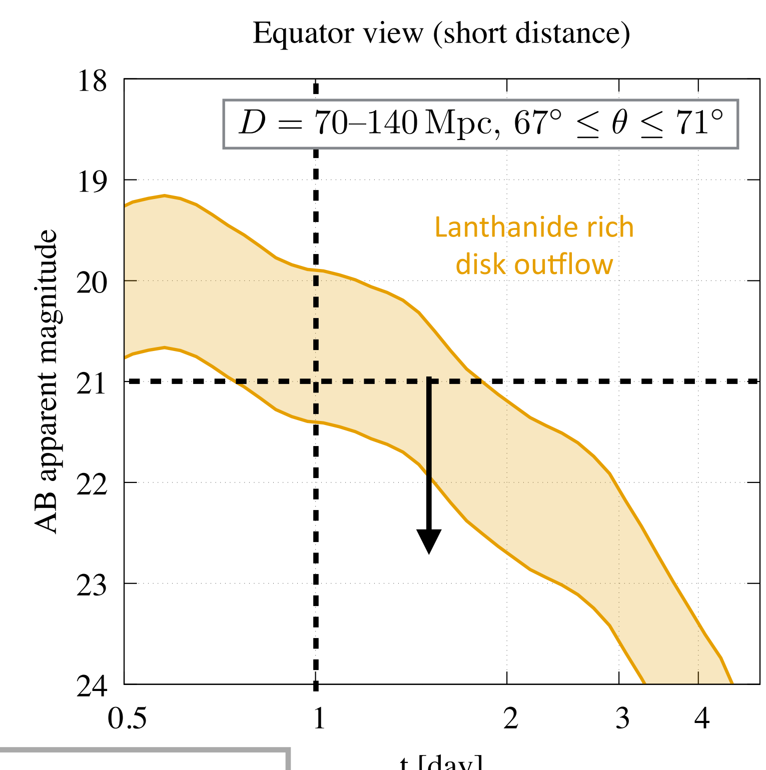

r-band lightcurve

*larger (smaller) distance is inferred for smaller (larger) viewing angle

Ref) Kyutoku et al. (2020)

GW190425: Kilonova detectability

Lanthanide poor disk outflow
0.02 Msun
+dynamical ejecta
0.0001 Msun

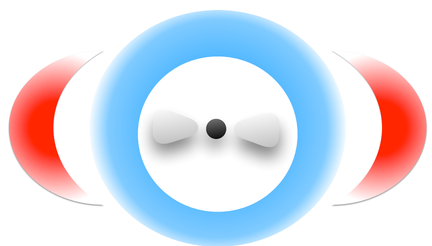

Lanthanide rich disk outflow
0.02 Msun
+dynamical ejecta
0.0001 Msun

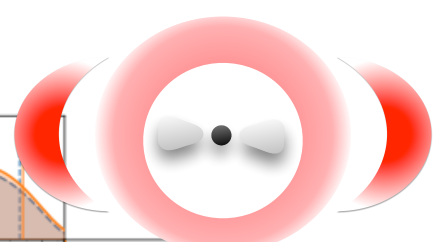

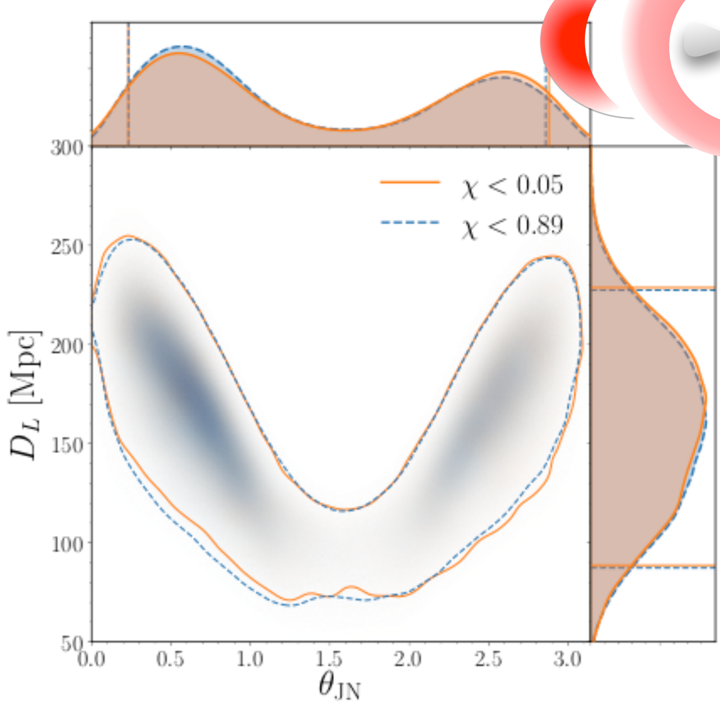

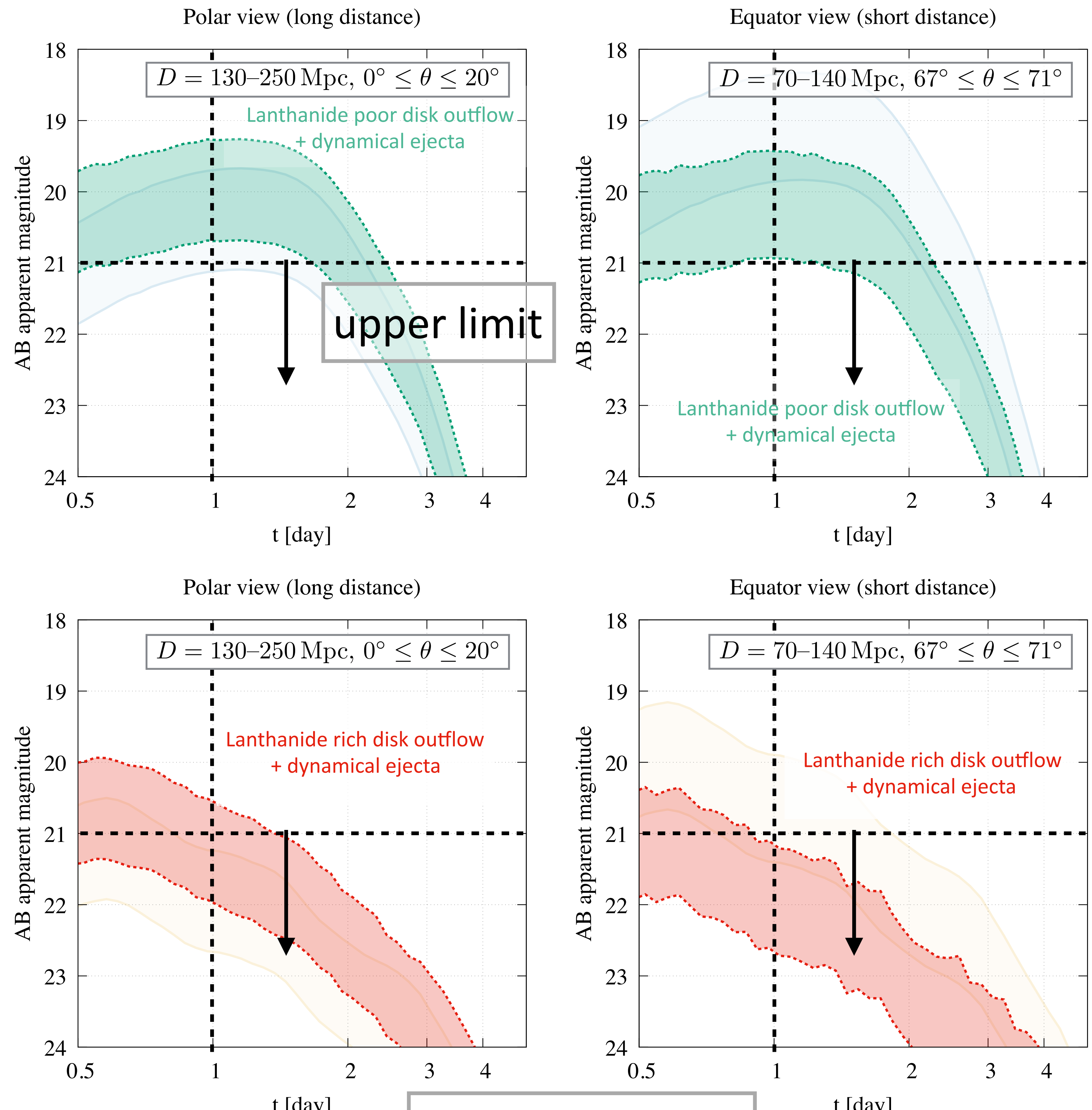

r-band lightcurve

*larger (smaller) distance is inferred for smaller (larger) viewing angle

Ref) Kyutoku et al. (2020)

Interpretation

Ref) Kyutoku et al. (2020)

Binary type[a]	Merger Outcome[b]	Detectable?[c]
low-mass BH–NS	La-poor disk	YES
	La-poor disk+La-rich dyn.	≈YES
	La-rich disk	YES if equatorial
	La-rich disk+La-rich dyn.	YES if polar
	weak/no disruption (small radius)	NO
asymmetric NS–NS	La-poor disk+La-rich dyn.	YES if polar
	La-rich disk+La-rich dyn.	YES if polar
symmetric NS–NS	massive neutron star (large maximum mass)	YES if polar
	prompt collapse	NO

- A successful detection of kilonova emission with the information of viewing angle will enable us to constrain the types of mergers for GW190425-like events.

S190814bv: a BH-NS merger candidate

- Aug. 14, 2019 21:10:39 UTC, detection of a BH-NS merger candidates has been reported
- False alarm rate:~ 1 / 10^{25} yrs.
- Distance: ~267±52 Mpc (c.f. GW170817: ~40 Mpc)
- Sky localization: 23 deg^2(90%)
- No electromagnetic counterpart was found
- upper limits to the optical /near infrared emission are obtained for the whole sky region.

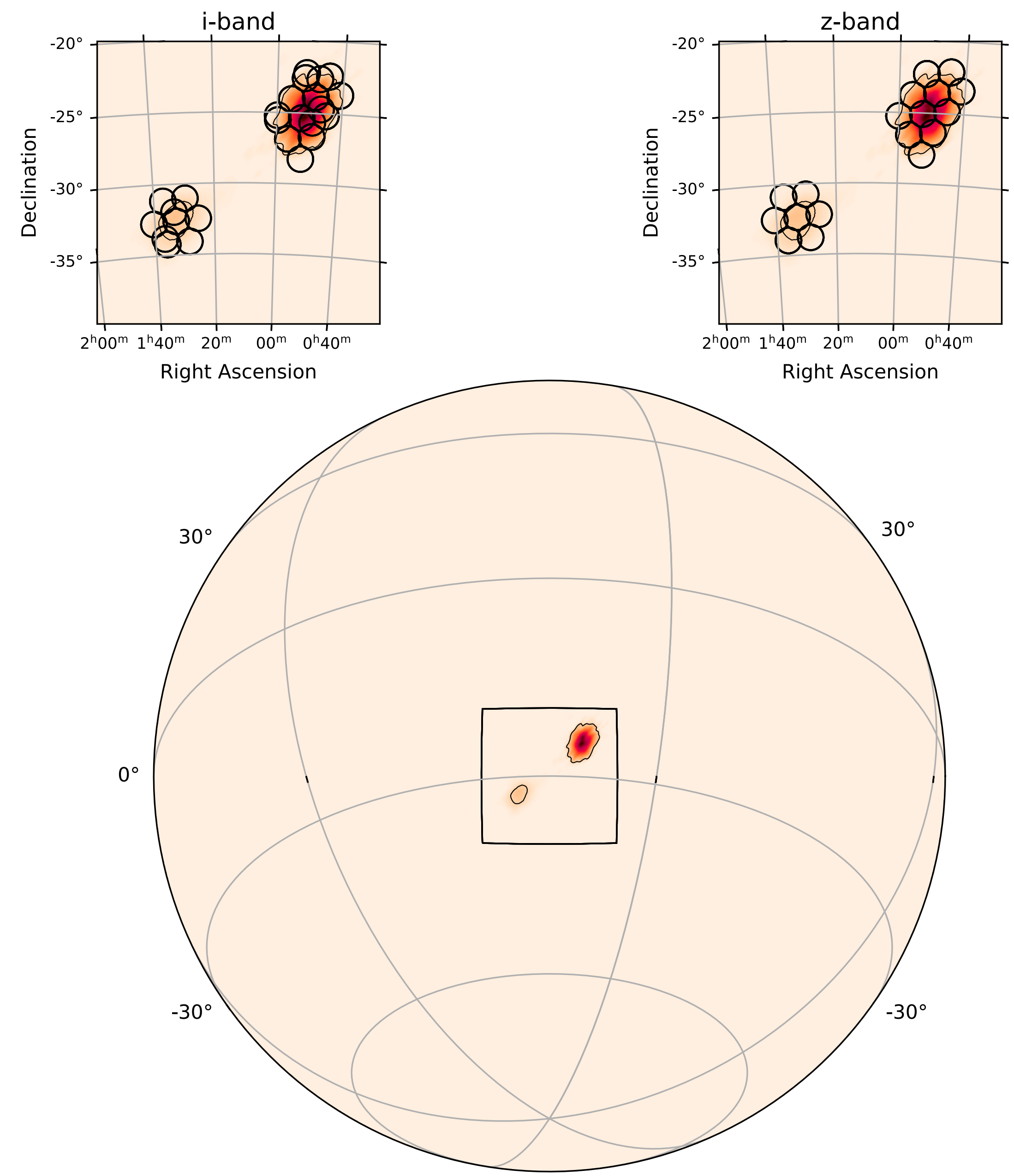

Ref) Andreoni et al. (2019)

Can we constrain the binary parameters from EM upper limits?

Upper limits to optical / near infrared emission

$$M_{\rm pm} = 0.02\,M_\odot \quad M_{\rm d} = 0.02\,M_\odot$$

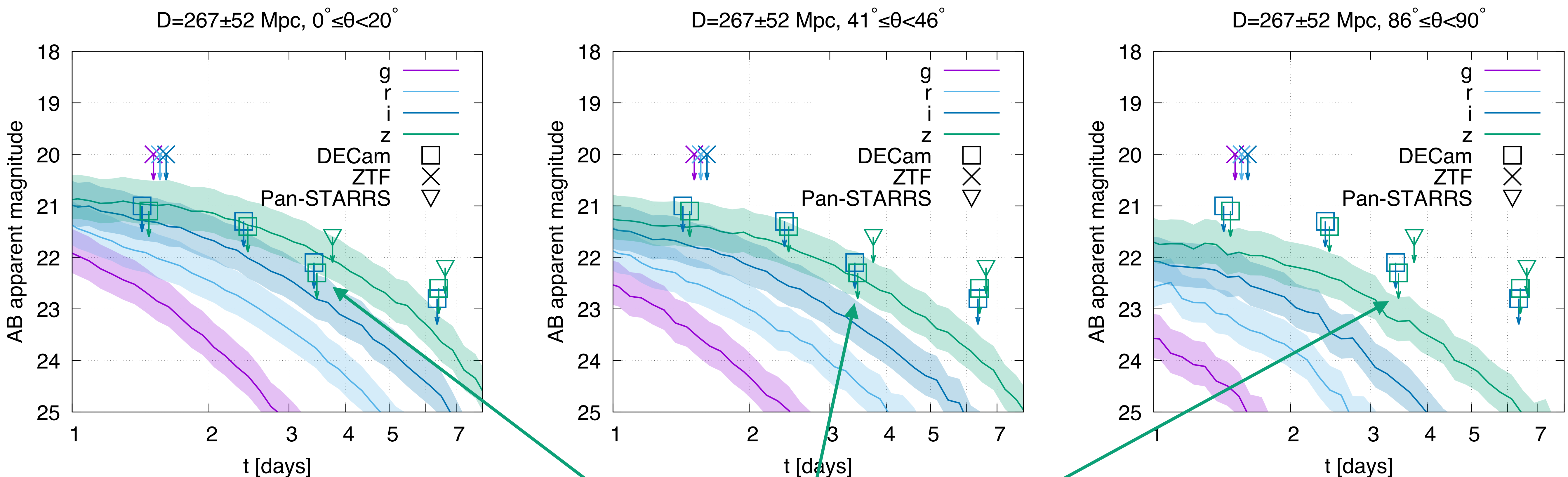

Shaded regions denote the uncertainty due to the error bar in the distance measurement

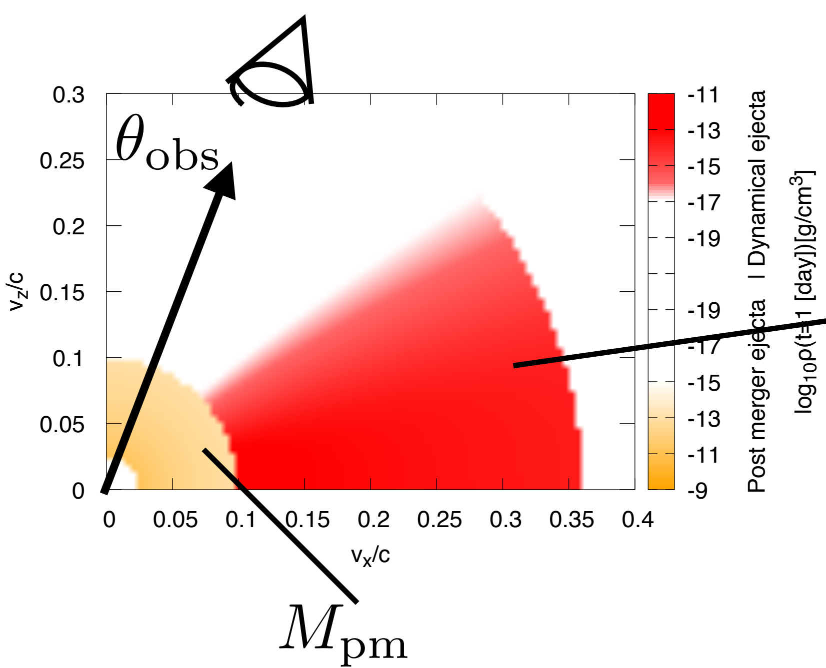

The upper limit z=22.3 @ t=3.43 d gives the strongest constraint on the lightcurve (Andreoni et al. 2019)

Ref) Andreoni et al. 2019, Singer et al. 2019 ,Smartt et al. 2019, Kawaguchi et al. (2020)

Constraint on the total ejecta mass

Ref) Kawaguchi et al. (2020)

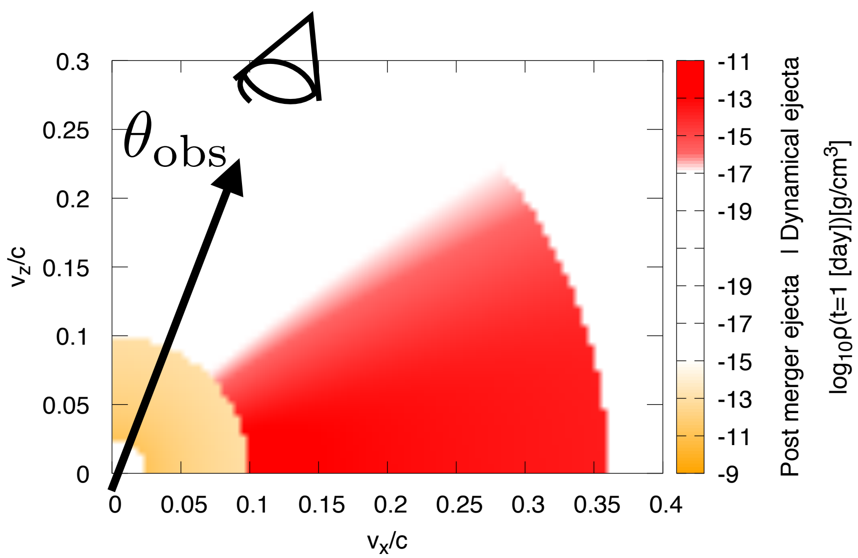

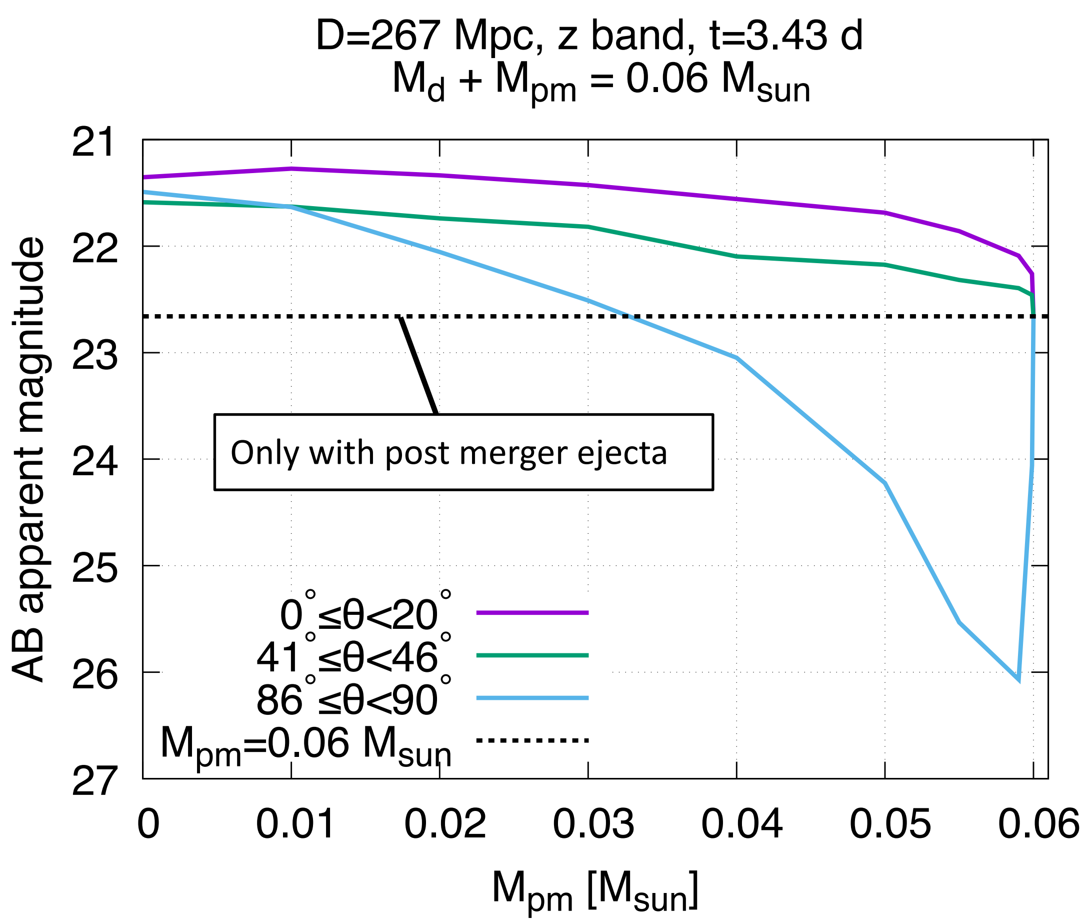

The upper limit z=22.3 @ t=3.43 d gives the strongest constraint on the lightcurve (Andreoni et al. 2019)

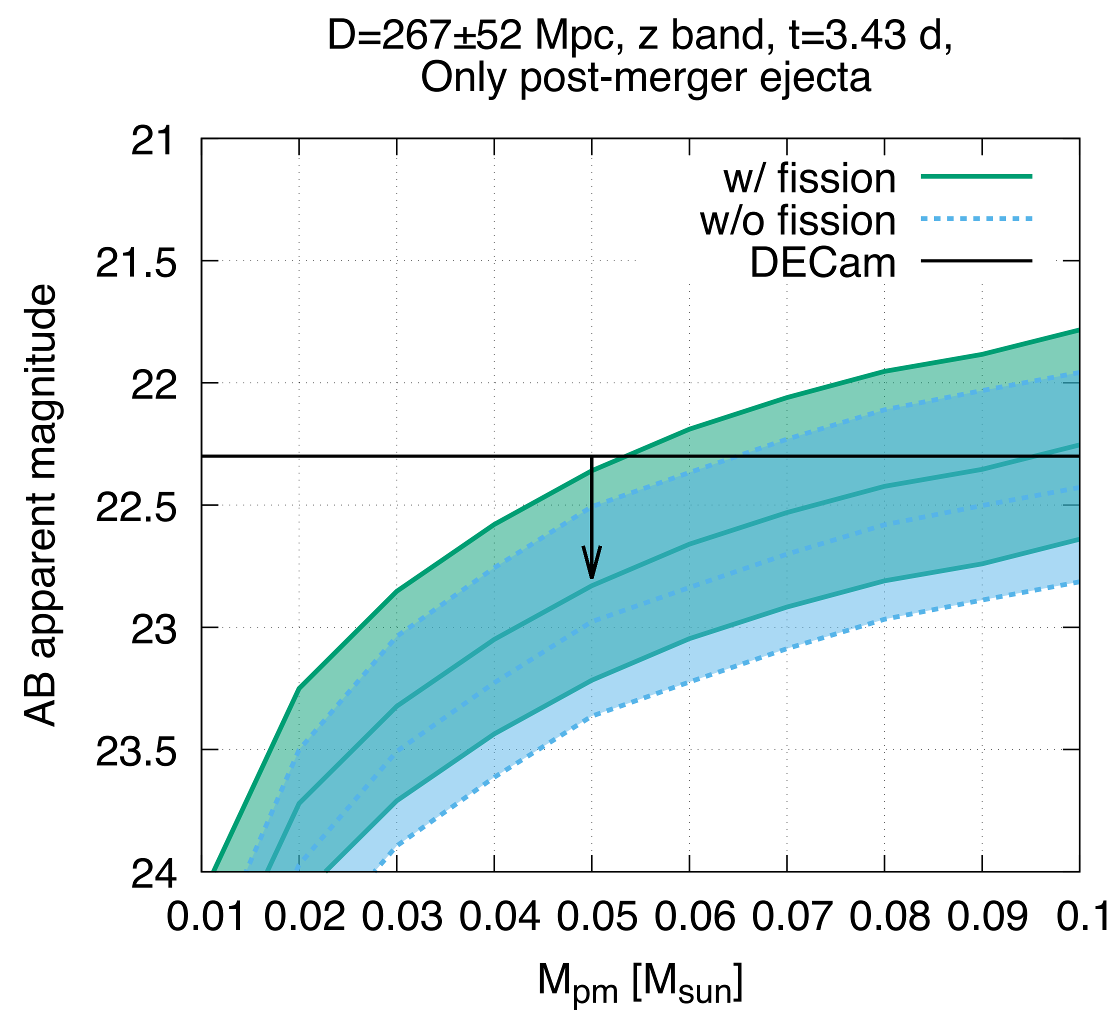

$$M_{\rm tot} \lesssim 0.1\,(0.07)\,M_\odot$$

$$\text{for } D = 267\,(215)\,\mathrm{Mpc},\ \theta_{\rm obs} \leq 45^\circ$$

Constraint on the dynamical ejecta mass

Ref) Kawaguchi et al. (2020)

$M_d \leqq M_{pm}$ is assumed
since the remnant torus mass is typically much larger than the dynamical ejecta mass
(see e.g., Kyutoku et al. 2015)

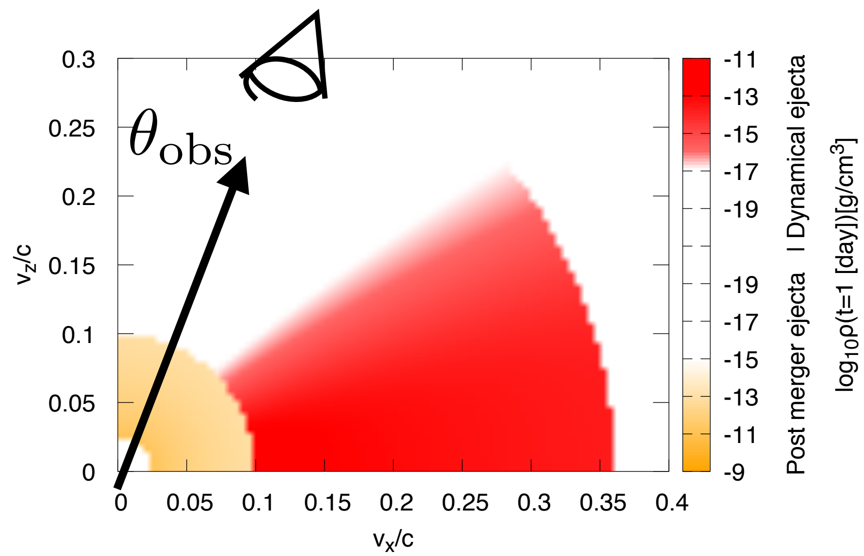

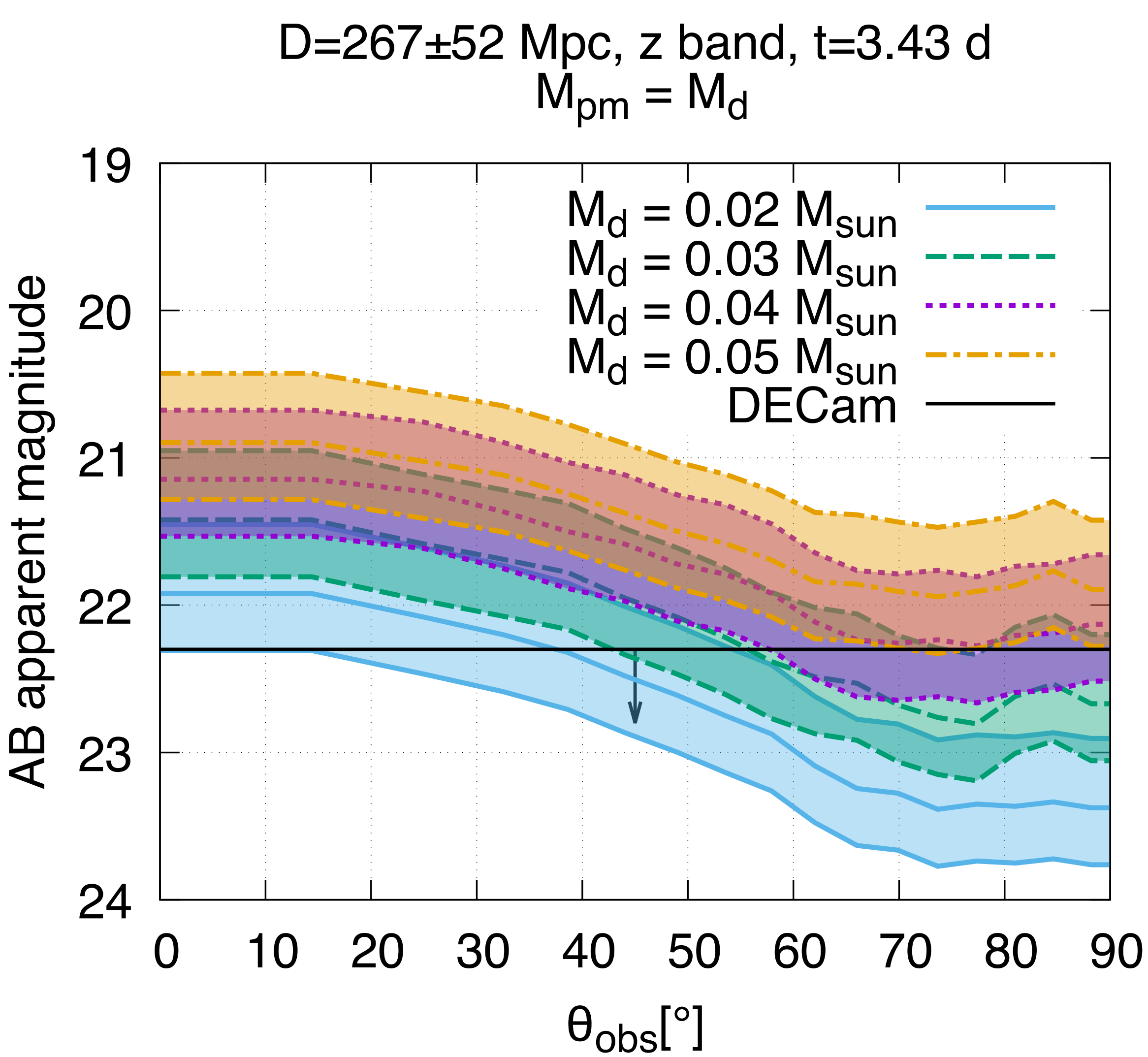

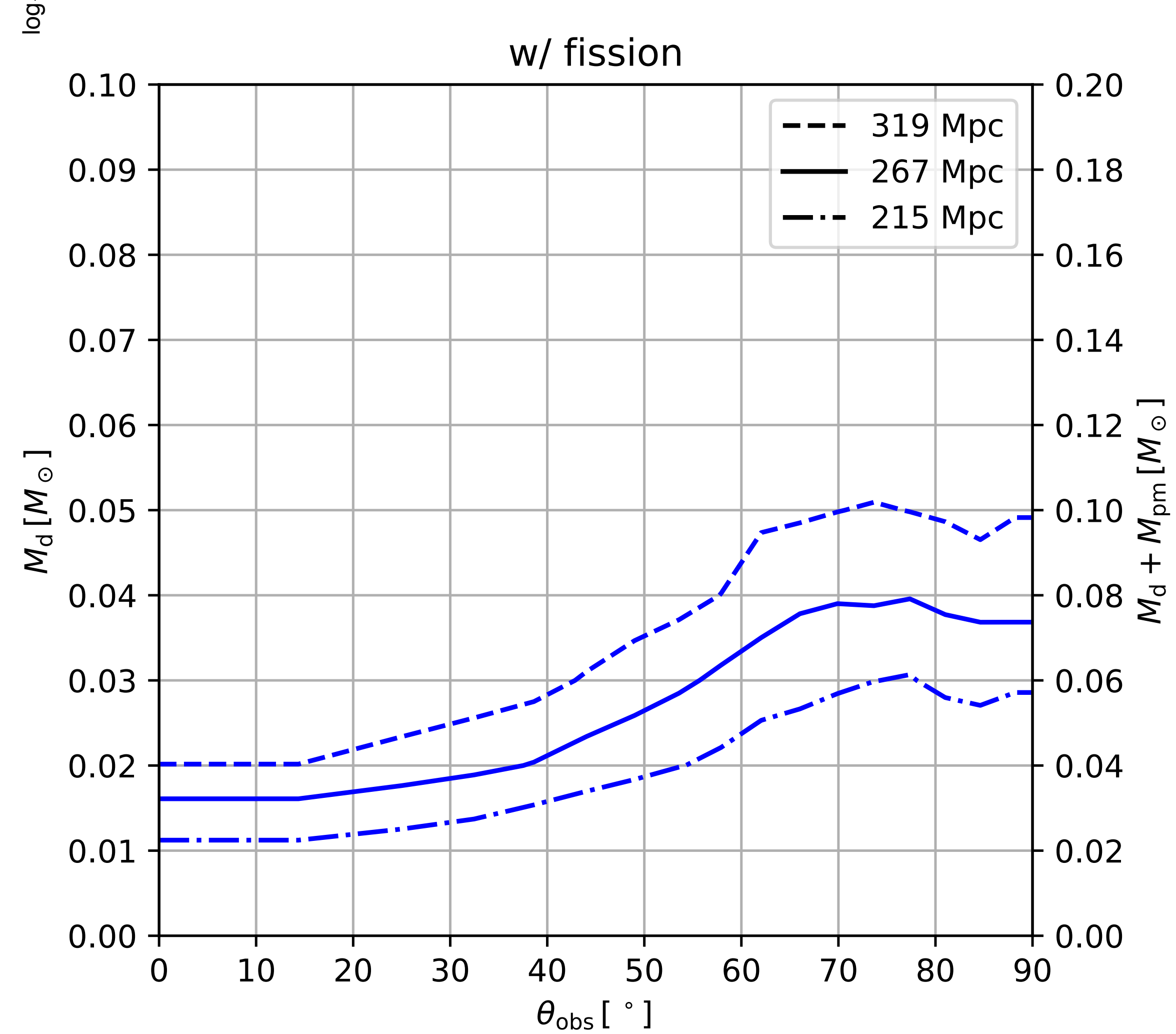

Md<0.02 Msun, 0.03 Msun, and 0.05 Msun
for the viewing angle ≤ 20°, ≤ 45°, and for ≤ 90°

Constraint on binary parameters

$$\mathcal{M}_c = \frac{m_{NS}^{3/5} m_{BH}^{3/5}}{(m_{NS} + m_{BH})^{1/5}}$$

$$\chi_{eff} = \frac{m_{BH}}{m_{NS} + m_{BH}} \chi_{BH}$$

Ref) Kawaguchi et al. (2020)

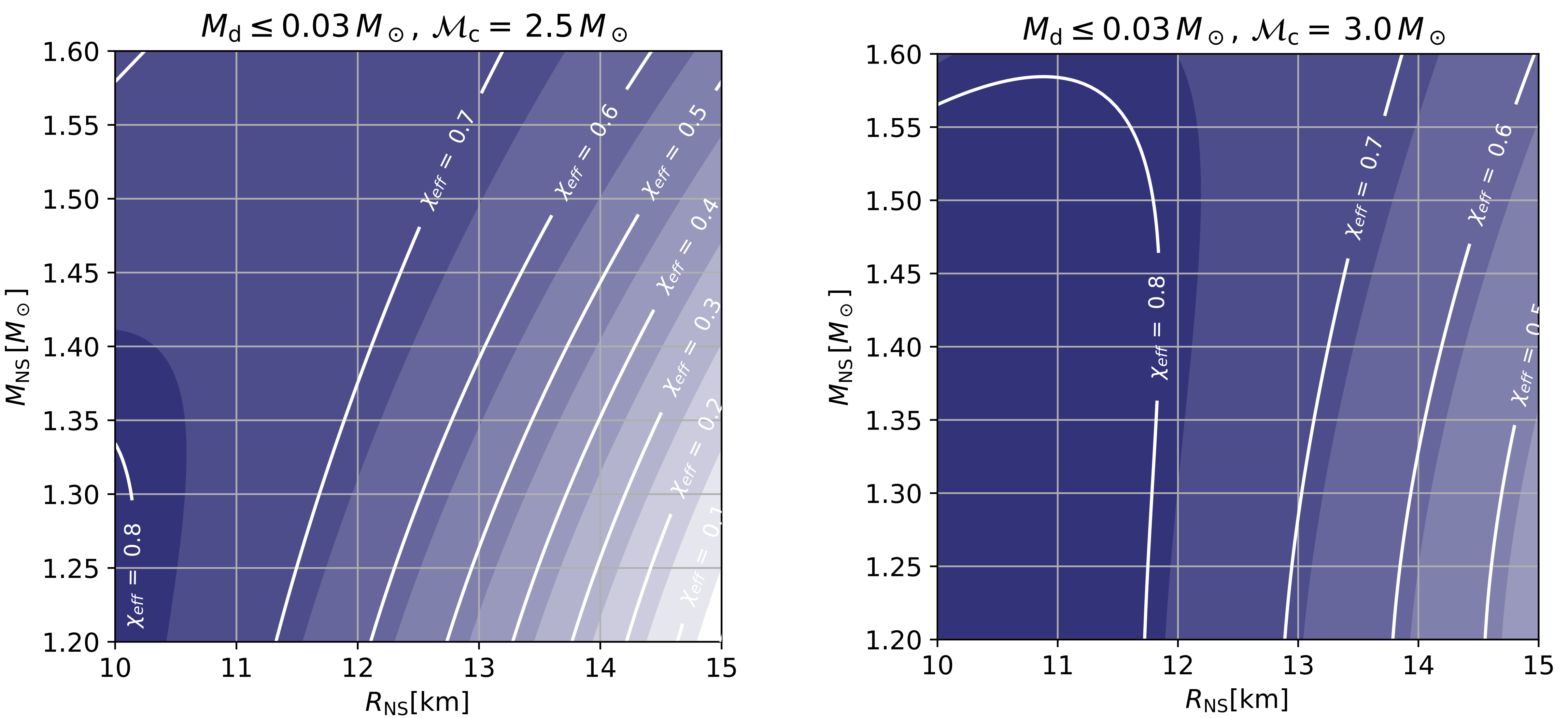

- A strong constraint on the NS mass-radius relation can be obtained from the upper limit to the dynamical ejecta mass (~0.03 Msun) for a BH-NS event with the chirp mass smaller than 3 Msun and effective spin larger than 0.5

Update in observations

Ref) ENGRAVE (2002.01950, 2020)

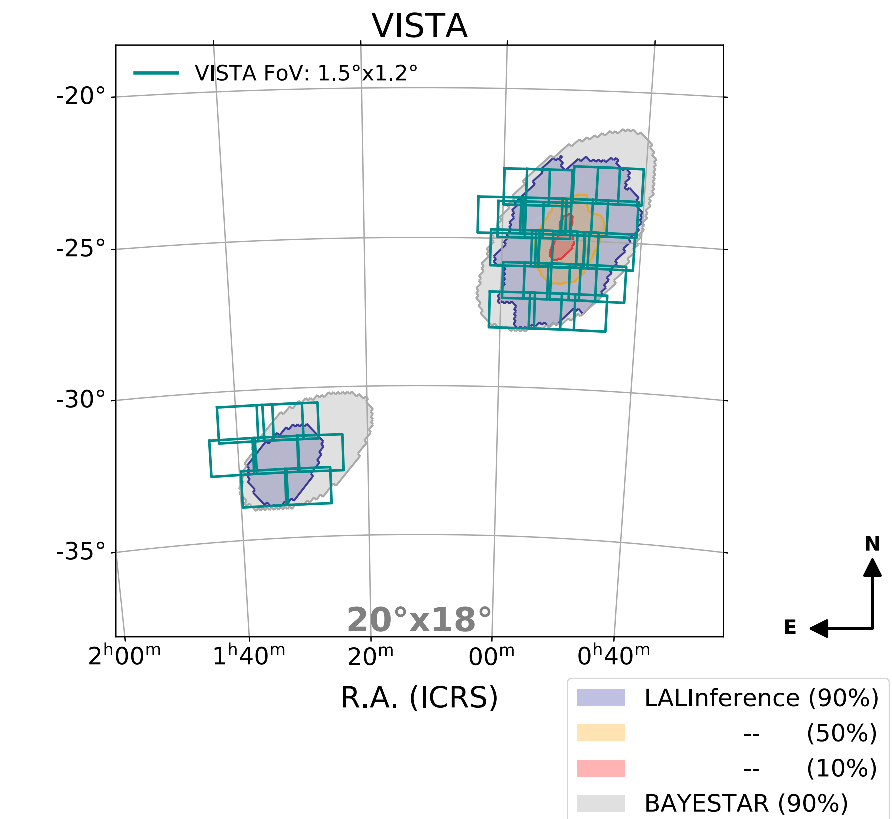

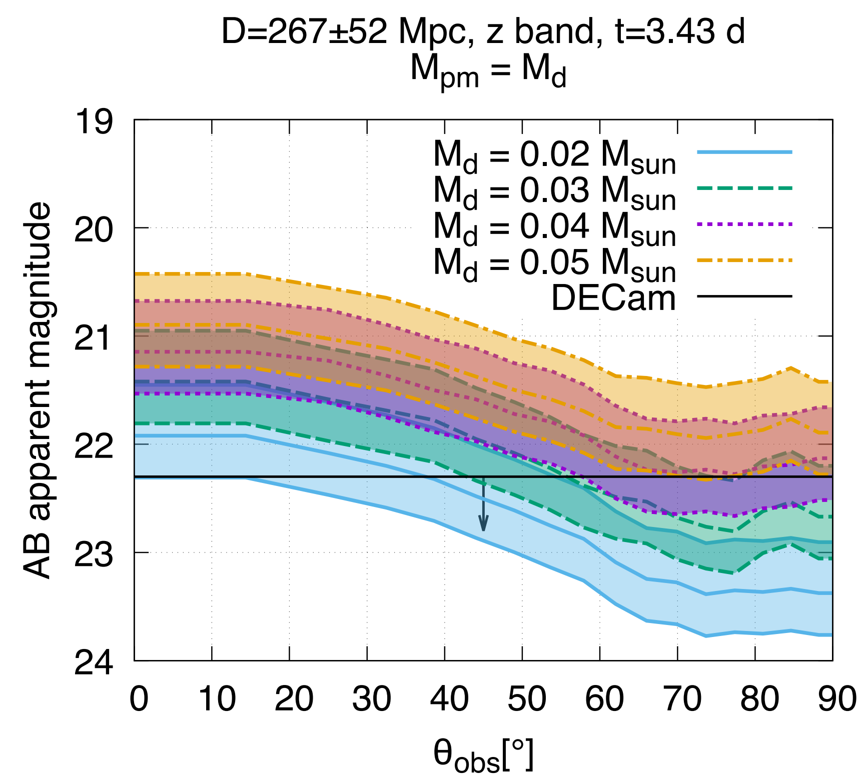

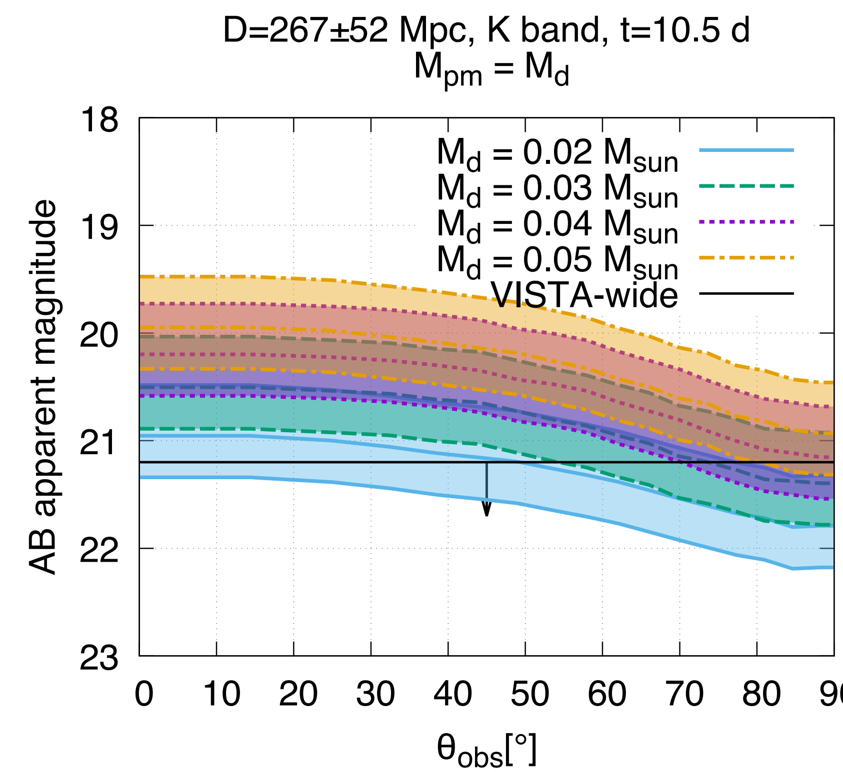

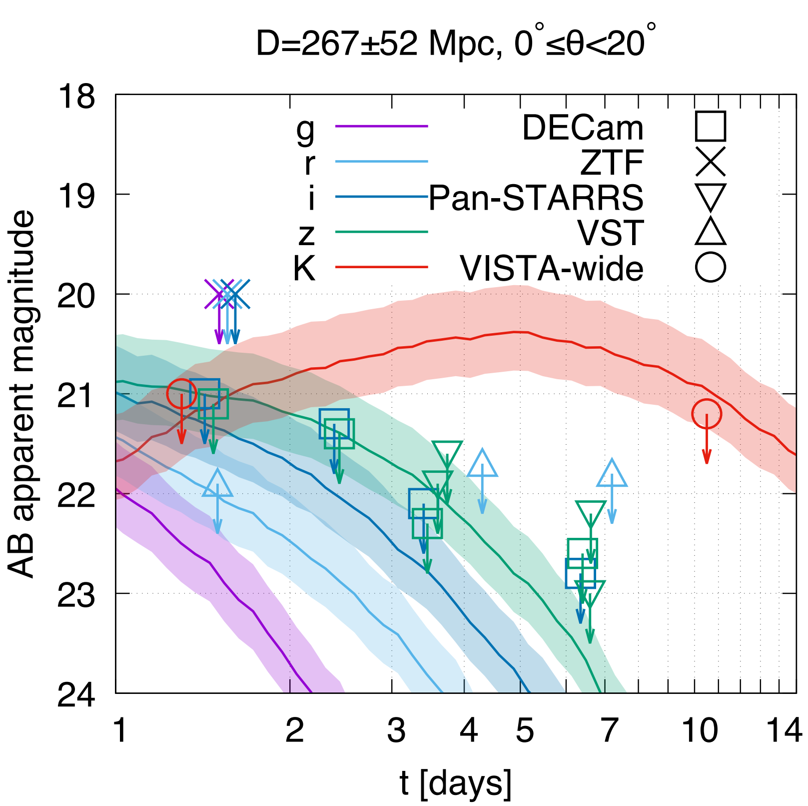

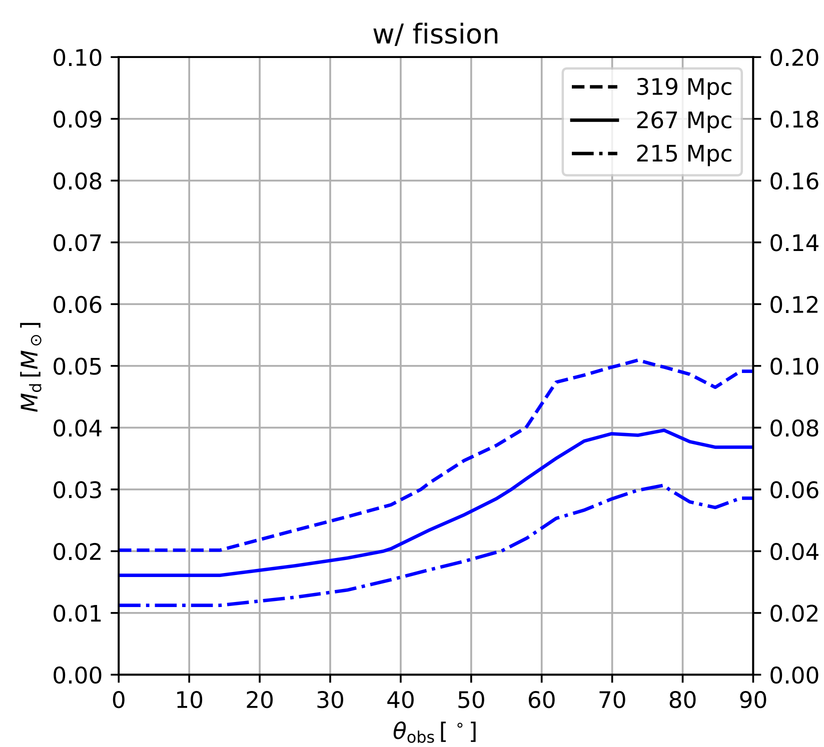

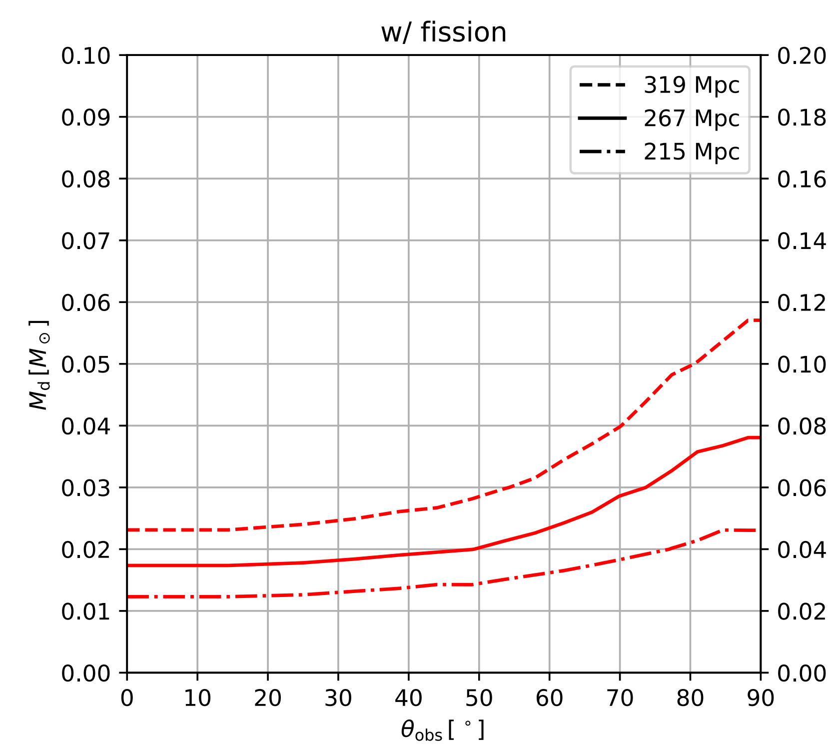

Summary

- **The radiative transfer effect between the multiple ejecta components with non-spherical geometry** are crucial for the quantitative prediction of the kilonova lightcurves.
- We perform radiative transfer simulations for kilonova lightcurves **in various situations** employing ejecta profiles predicted by **numerical-relativity simulations.**
  We demonstrate that kilonova lightcurves could show **large diversity** reflecting the variety in the binary parameters or the binary composition.
  - We show that we may be able to **infer the type of the central engine for kilonovae** by the observation of the peak in the multiple band lightcurves.
- We applied our theoretical prediction of mass ejection and kilonova models to the upper limits obtained by the EM follow up for the recent GW events.
  - We show that **some types of central engine can be ruled out** for GW190425 **if the event is within the area of observation**. We also show that a successful detection of kilonova emission with the information of viewing angle will enable us to constrain the types of mergers for GW190425-like events.
  - We constrain **the total ejecta mass** to be less than **0.1 Msun** for **the face-on observation** at the distance of **267 Mpc** for S190814bv.
  - We show that the dynamical ejecta mass for S190814bv should be less than **0.02 Msun, 0.03 Msun, and 0.05 Msun** for the viewing angle **≤ 20°, ≤ 45°, and for ≤ 90°,** respectively.

Current work

- Comprehensive modeling of KN lightcurve based on NR simulations
- -> need to evolve the ejecta profile until the homologous expansion phase
- GRHD code (fixed metric):

  Sedov-Taylor: OK
  BH-torus: OK

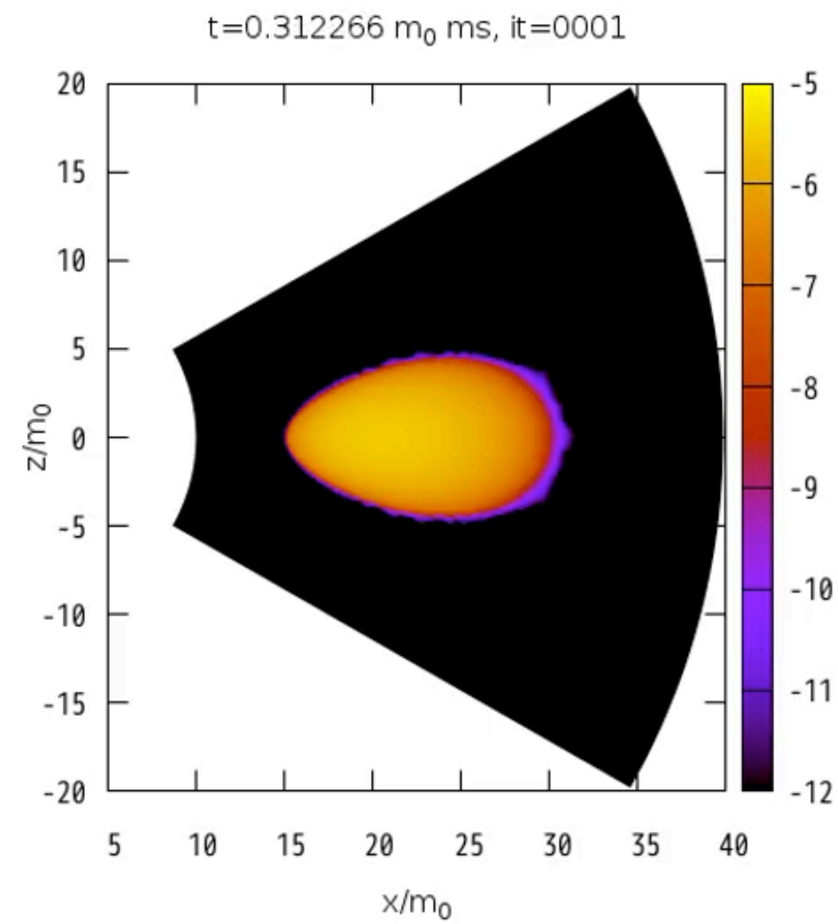

BH torus

Outflow test

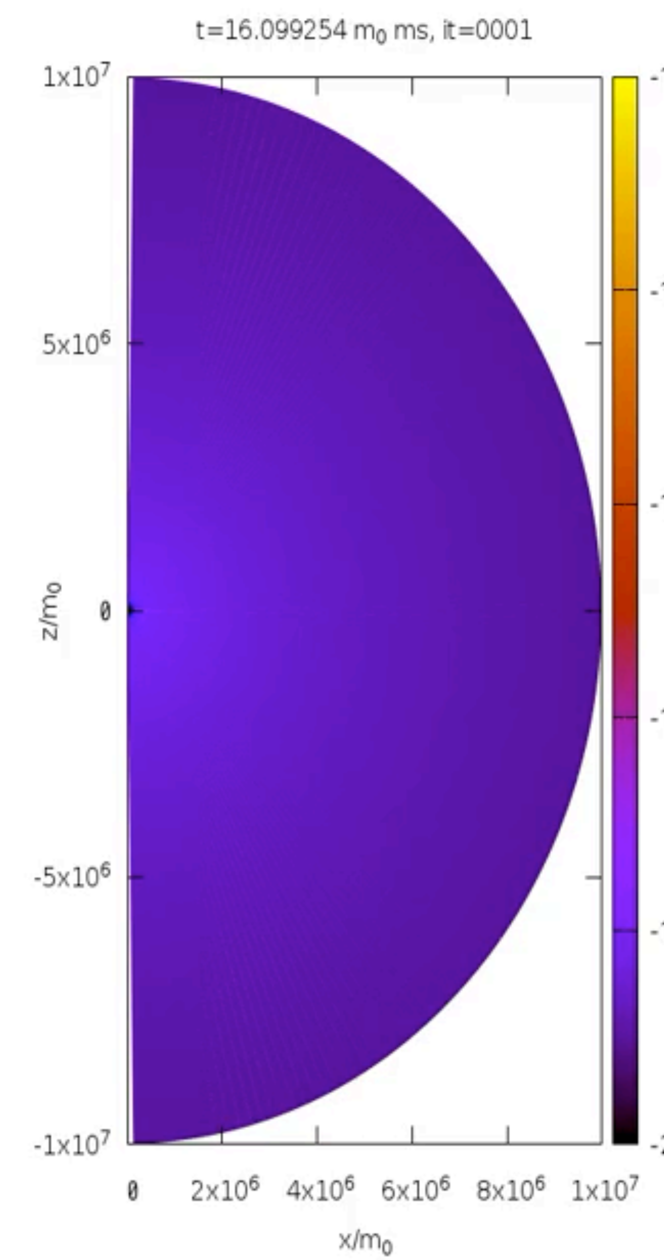

Properties of kilonovae / macronovae

Order Estimation

ref) Li & Paczyński 1998

$$t_{\rm peak} \approx 3.3\,{\rm days} \times \left(\frac{M}{0.03M_\odot}\right)^{1/2} \left(\frac{v}{0.2c}\right)^{-1/2} \left(\frac{\kappa}{1\,{\rm cm^2/g}}\right)^{1/2}$$

$$L_{\rm peak} \approx 2.0 \times 10^{41}\,{\rm ergs/s} \times \left(\frac{f}{10^{-6}}\right) \left(\frac{M}{0.03M_\odot}\right)^{1/2} \left(\frac{v}{0.2c}\right)^{1/2} \left(\frac{\kappa}{1\,{\rm cm^2/g}}\right)^{-1/2}$$

$$T_{\rm peak} \approx 3.1 \times 10^{3}\,{\rm K} \times \left(\frac{f}{10^{-6}}\right)^{1/4} \left(\frac{M}{0.03M_\odot}\right)^{-1/8} \left(\frac{v}{0.2c}\right)^{-1/8} \left(\frac{\kappa}{1\,{\rm cm^2/g}}\right)^{-3/8}$$

$M_{\rm eje}$:ejecta mass

$v_{\rm eje}$:expanding velocity

κ :opacity

f : energy conversion rate

- The emission is expected to be bright in **the optical and infrared wavelength**.
- **The mass, velocity, morphology, and <u>the composition(electron fraction)</u>** of the ejecta characterize the lightcurve of the kilonova/macronova.